Untersuchungen zu den neurophysiologischen Grundlagen
der funktionellen Kernspintomographie
(fMRI)

Examinations about the neurophysiological
basis of
functional MRI

Dissertation
zur Erlangung des akademischen Grades
doctor rerum naturalium
(Dr. rer. nat.)

genehmigt durch die Fakultät für Naturwissenschaften der
Otto-von-Guericke-Universität Magdeburg

von Dipl.-Biologin Elena Kammerer
geboren am 07.05.1976 in Alma Ata

Contents

Chapter 1

Introduction

Today blood oxygenation level-dependent (BOLD) fMRI is a customarily used tool for clinical application and research. Its popularity arises from the fact that it does not require radioactive tracers and allows non-invasive examinations, what makes it a tool of choice especially for experiments on humans. However, despite the intense use of BOLD mediated fMRI the physiological mechanisms behind the contrast could not be cleared until now. This lack of a proper explanation prevents an adequate interpretation of all these outcomes.

Neurovascular coupling

The BOLD contrast is used as an indirect indicator of neural activity. Neuronal activation increases the local cerebral metabolic rate of oxygen ($CMRO_2$) and glycose consumption. In result, cerebral blood flow (CBF) increases to compensate for the elevated demand. The increased supply outweighs the actual consumption, more oxygen is transported into the activated region than can be used. I.e., the proportion of oxygenated hemoglobin (Hb) increases. Hemoglobin can be used as intrinsic contrast agent. Increases in the ratio of deoxygenated hemoglobin results in a MR signal loss, while increases in the proportion of oxygenated Hb improves the MR signal [94].
The linkage between neural activation and local $CBF/CMRO_2$ change is called the neurovascular coupling, or functional hyperemia.
A multitude of models has been developed and improved during the recent years describing the dynamics of CBF and CBV in response to changed neural activity [12, 23, 80, 85]. Although these models become more and more realistic and predictive, they provide so far no explanation for the mechanism linking neural activity and vascular responses.

Neurovascular or neurometabolic coupling

An intense discussion is going on about the basis of neurovascular coupling. Two approaches for explanation are prevalent in that discussion. The metabolic pathway assumes BOLD generation to be directly coupled to the local cerebral metabolic rate of oxygen consumption ($CMRO_2$) reflecting local energy demand. According to this, the aerobic metabolism would result in vasodilatory metabolites as CO_2 and H^+ affecting CBF and CBV [33, 54]. Other authors favour the transmitter pathway, not presuming O_2 consumption necessarily to precede the chain of events leading to BOLD generation [10, 44]. Here BOLD contrast changes are assumed to be coupled in first line to transmitter release at the synapse triggering a release of vasodilatory mediators. In that case several mediators could be candidates involved

in BOLD production, acting on different sites. These mediators will be addressed later in the text.

The different approaches find themselves expressed in the distinctive use of the terms neurovascular and neurometabolic coupling. 'Neurometabolic coupling' is used to accentuate the linkage between neural activity and its oxygen consumption, while 'Neurovascular coupling' only refers to the general conjunction between neuronal activity and CBF changes and is sometimes used equivalent with the first called term. The reason may be that both terms can hardly be regarded separately.

Possible mechanisms behind BOLD generation

A discussion about neurovascular coupling and BOLD generation is complicated by the fact that experimental results vary considerably dependent on the observed brain region or examined species. It is most likely that more then one single pathway answers for BOLD generation. In the following section several mechanisms and mediators in question will be introduced.

The largest part of the energy consumed during neuronal activity can be assigned to postsynaptic activity. 74% of the energy expenditure takes place in dendrites, mainly due to the re-establishment of ion gradients by Na^+/K^+ pumps and Na^+/Ca^{2+} exchangers after membrane potential changes [9–11]. This makes the postsynapse a probable site for BOLD generation.

Firing of output neurons was found to correlate to BOLD generation [51, 88, 103, 112] as well as synaptic activity, measured as LFP or EPSP [24, 76, 91, 101, 121]. In general synaptic activity provides the best correlation with BOLD responses, while a dissociation between firing and BOLD signal production can often be observed. In circuits containing many interacting excitatory and inhibitory networks even a complete dissociation between LFP, spiking and BOLD response can occur [39].

What happens during neuronal activity at the postsynapse? Transmitter, usually glutamate, is released into the extracellular space activating glutamatergic ionotropic and metabotropic receptors in the postsynaptic membrane. The membrane depolarizes, Ca^{2+} enters the cell via NMDA and voltage-dependant Ca^{2+} channels. Increase of Ca^{2+} triggers intracellular cascades producing vasodilatory molecules as nitrous oxide (NO) or arachidonic acid (AA). Postsynaptic Ca^{2+} increase can produce hyperemia, for example by activating Ca-dependent phospholipase A_2 (PLA_2), which removes AA from the membrane. Arachidonic acid can either be released into the extracellular space or provide the substrate for cyxlooxygenases (COX), a group of enzymes that was found to synthesize vasoactive prostaglandins from AA. COX-2 is mainly abundant in postsynaptic neural compartments and inhibition of the enzyme reduced blood flow increases, at least in mice [92, 98].

Postsynaptic activation can also trigger neuronal NO synthase (nNOS). nNOS was found to be physically anchored to the NMDA receptor by two postsynaptic density proteins, PSD-93 and PSD-95. It was suggested that NO production is induced via NMDA activation by glutamate [18, 19, 66, 95].

NO is assumed to signal directly to vascular smooth muscle cells, producing vasodilatation by stimulating guanylyl cyclase and by inhibiting synthesis of the vasoconstrictor hydroxyeicosatetraenoic acid (20-HETE), thereby promoting the

vasodilatory action of epoxyeicosatrienoic acids (EETs) [66]. In the cerebellum NO seems to be obligatory for a blood flow increase while in other areas it plays only a modulatory role [3, 29, 72, 100, 131, 132]. In those brain regions nitrous oxid is only one of several mediators of neurovascular coupling and its manipulation affects CBF only partially [35].

In several works presynaptic activity was related to BOLD generation. This phrasing is misleading, since usually not events taking place in excited axon terminals but rather processes following glutamate release are assumed to influence BOLD production [39, 59, 70, 71, 77, 98, 101]. Those processes can be synaptic activation of nearby neurons, but also activation of astrocytes. Nevertheless, glutamatergic action on presynaptic terminals induces Ca^{2+}-influx, Ca^{2+}-dependent signal cascades and is thus capable to change probability of glutamate release at the presynapse, provided it is presented in an appropriate pattern and concentration. However, findings about production of vasodilatory molecules in the presynapse/axonal endings are not known so far.

Furthermore it should be mentioned that also authors utilizing 2-Deoxyglucose (DG) uptake to localize energy expenditure during neuronal activation found glucose consumption mainly to be coupled to presynaptic neuronal activity [60, 93, 104, 108, 127].But these results should be interpreted critically. In fact the 2-DG stainings only showed that activation was restricted to the input layers of the examined region. A more detailed analysis is not possible with this technique, due to its limited resolution. It is very likely that the observed staining stems from activated dendrites, that is, from the postsynaptic site.

At the present, astrocyte-mediated CBF change is one of the most favoured explanations for BOLD generation. A number of astrocytic pathways is discussed therefore. Astrocytes posses a multitude of processes enveloping pre- and postsynaptic endings of neurons forming synapses on one side, while other processes ensheath parenchymal arterioles and capillaries forming so-called perivascular endfeet on the other side. This architecture is suspected for a while to play a role in the transmission of information about neural activity from synapses to the vasculature.

Activated by glutamate, astrocytes are capable of producing multiple vasoactive mediators. Activation of astrocytic AMPA and metabotropic glutamate receptors activates phospholipase C (PLC) and hence IP_3, releasing Ca from internal stores. Intracellular Ca^{2+} increases propagate into astrocytic endfeet and activate PLA_2 to cleave arachidonic acid (AA) from cell membranes. AA can then be released and converted by cytochrome P450 (CYP 4A) in vascular smooth muscle cells (SMC) to 20-HETE, a vasoconstrictor. In astrocytic endfeet AA can be metabolised via the COX-1 pathway to prostaglandin E2 (PGE_2), or by Cytochrome P450 epoxygenase (CYP 2C11) to EET, both acting vasodilatory on vascular SMCs.

Besides responding to glutamate release during neuronal communication, astrocytes do also spread the Ca^{2+} signal to neighbouring astrocytes by releasing ATP. Adenosine receptors on astrocytes transform this signal into Ca^{2+} elevations in adjacent astrocytes.

Potassium and potassium channels play as well an important role in the transmission of neuronal and astrocytic activation to the vasculature. The vascular tone

depends substantially on the membrane potential of smooth muscle cells. Hyperpolarization of vascular SMCs produces vasodilatation, depolarization vasoconstriction. Na^+/K^+-ATPases and potassium channels control the membrane potential: Kir (inwardly rectifying potassium) channels in the vascular SMC membranes and calcium-activated BK channels in SMC and membranes of astrocytic endfeet play here a major role [41, 55]. ATP-dependent (K_{ATP}) and Ca^{2+}-dependent potassium channels (BK channels being only one of them) may be responsible for vasodilatation to moderate acidosis, i.e., increased extracellular $[H^+]$.

Smooth muscle cells are connected to endothelial cells by gap junctions, endothelial cells are interconnected too. That way a hyperpolarization at one site can be forwarded some direction up and down the arteriole, a dilatation can so be conducted along this patch. During cerebral neuronal activity potassium is released, its extracellular concentration increases. An elevated $[K^+]_o$ hyperpolarizes and dilates adjacent cerebral arterioles [64]. At small elevations of extracellular $[K^+]_o$ only Na^+/K^+-ATPases in the vascular SMC membranes seem to be responsible for hyperpolarization and dilatation of SCMs. At higher concentrations Kir channels perform this task. A further increase of extracellular $[K^+]_o$ produces depolarization and vasoconstriction of the vessels [38, 55, 83]. Dreier and colleagues showed *in vivo* increasing CBF in rat cortices in response to $[K^+]$ elevation in the cerebrospinal fluid, confirming *in vitro* results of others [37, 55, 83]. However, besides the potassium increase there may be required yet an accessory mediator to change CBF [57]. Probably this is NO. At least in acidosis NO acts as mandatory modulator. Kir channels on the other side do not require NO for the induction of vasodilatation [73].

Further candidates for mediating BOLD production are interneurons with terminals in close proximity to blood vessels, containing vasoactive substances or transmitter. A variety of GABAergic axon terminals co-expressing vasoactive neuropeptides was found to abut on microvascular walls. They are termed perivascular interneurons and characterized by containing VIP, SOM, PV, NPY, CCK, or the nitrous oxid synthesizing NOS [1, 26, 28, 50, 65, 96, 119]. Of course, shear proximity is no evidence for a factual interaction between those vasoactive metabolites and the vascular bed. Though, Cauli and colleagues evoked vasodilatation in cerebral arterioles by direct activation of interneurons storing VIP and NOS, and by bath application of VIP. A NO-donor yielded the same effect. So at least VIP and NOS are capable of inducing CBF changes via interneuronal activation and this signal is mediated by the appropriate microvascular receptors [26]. Kocharyan and coworkers proved *in vivo* the participation of perivascular SOM interneurons in cortical CBF increases [65].

Moreover, stimulation of cortical inputs revealed that different sets of inhibitory interneurons, each containing different vasoactive substances, become active depending on stimulation frequency. At lower stimulation frequencies (4 Hz) GABAergic neurons containing SOM and PV could be identified, at higher frequencies (30 Hz) GABAergic neurons co-expressing VIP take over and the fraction of SOM containing interneurons increases [39]. The same study points explicitly to an involvement of SOM interneurons in neurovascular coupling.

Apart from perivascular interneurons, several transmitter-containing nerve ter-

minals were found in close association to microvasculature [27, 28, 30, 50, 67, 96]. Complementary receptors are present on parenchymal blood vessels [26, 30, 65]. Serotonergic and ACh-neurons were found to influence CBF directly [27, 28, 30].

Perivascular serotonergic, norandrenergic and cholinergic terminals were found preferentially in the vicinity of capillaries, they are assumed to provide a local fine control [27, 28, 30, 96]. GABA was shown to dilate arterioles in rat hippocampal slices via $GABA_A$ receptors [40].

Approaches investigating BOLD

Different experimental approaches have been used in the past to examine BOLD generation in humans and laboratory animals. In the beginning main focus was put on simple functional mapping [17, 62, 110, 111]. But soon experiments aimed to correlate physiological parameters and hemodynamic response by performing experiments mainly on rat, mouse, ape and cat. For that CBF or BOLD responses were evoked by applying visual, acoustic, olfactory and somatosensory stimulation protocols. Visual and somatosensory stimulation emerged meanwhile to be the most prefered tools of choice [6,22,25,48,52,56,61,63,75,81,91,101,120,121,123,134]. However, a handicap of peripheral stimulation is that BOLD signals in response to the stimulus are mainly registered in the appropriate cortical regions but these regions are not activated directly. A sensory activation, registered in the cortex, was beforehand transduced via several relay stations in the brain, transforming the initially provided stimulus into a modified stimulus, and triggering local BOLD signal changes. A somatosensory stimulus is transmitted via the peripheral system and the thalamus to the primary sensory cortex. A visual stimulus transits the lateral geniculate nucleus to reach the primary visual cortex. BOLD signal changes elicited at the different transition sites do not respond to the same local input stimulus although initiated by the same external stimulation. Hence a proper correlation of local neural activity parameters (as input or output) and the according imaging signal can not be done. To address this problem, a combined approach would be required providing a direct invariable input that can be correlated to the elicited neural activity and BOLD signal obtained at the same position.

Such combined measurements were done using optical methods, measuring CBF changes and neural responses at the same time and locus. The shortcoming of the technique is that only an extremely limited spatial area can be observed [24,36,82, 90,117]. Besides, although BOLD signals depend on CBF changes, they are not equivalent with them.

Some experimentators tried to relate electrophysiological and BOLD signals by doing separate recordings [61,112,131]. In this case a correlation of neural responses and BOLD signals is difficult since the electrophysiological activity is not correlated to the imaging signals they had evoked.

First efforts to perform simultaneous recordings of neural signals (LFP, MUA) and BOLD responses in the primary visual cortex after visual stimulation are known from Logothetis [75]. The same group also applied electrical microstimulation to the V1 and obtained BOLD responses that noticeably exceeded an activation that would be produced by a passive spread of current [118].

The aim of the present study was to develop an experimental setup that allows stimulation of a direct input into a brain region with defined parameters that evoke significant BOLD response in the target area, and to determine neural responses and imaging signals in this region simultaneously. The region chosen for the experiment was the hippocampal formation.

Hippocampus as region of interest

The hippocampal formation is a compact, well delineated brain area comprising several subregions. The CA1 and CA3 form the hippocampus proper that is anatomically and functionally tightly bound to the dentate gyrus (DG), the Subicular region (Sub) and entorhinal cortex (EC). Each of these regions can be activated by a monosynaptic input originating in layer II and III of the entorhinal cortex and concentrated in a bundle of axonal fibres called the perforant pathway [126].

The hippocampus and the DG were intensely investigated during the last decades. For a long time they are objects of investigation for *in vivo* and *in vitro* experiments mainly on synaptic plasticity [15, 16]. An accurately defined laminar organization allows detailed electrophysiological recordings in all regions. Principal cells in the hippocampus are aligned in a way that cell bodies can be found in one layer, while their basal and apical dendrites form a second and third layer above and below the cell layer. Due to this architecture an activation of a cell assembly produces a homogeneous electrical field with a sink in the dendritic layer and a source in the cell body layer. Stimulation of the perforant pathway, for example, depolarizes dendrites, current from the surrounding regions flows in. Sufficient depolarization may then discharge the cells and produce a further characteristic change in current flow. Those currents can be recorded as extracellular field potentials and be analysed for details of synaptic transmission. Synaptic activity, measured as EPSPs reflect the local input, population spike amplitudes in return the excitability of a population of addressed neurons [2, 15, 16, 36].

The extracellular potentials recorded in the hippocampal formation reflect faithfully the intracellular activity in the observed cell population [7, 78, 79]. Recordings of that quality are only possible in the hippocampus. Although a layering can be found in the cortex too, it lacks a clear separation into a pure input region as it is given, for example, with the molecular layer of the DG, or a clear output region as the granule cell layer. LFPs in other brain regions are not easy to define since they comprise all sorts of neural activity, an LFP recorded in the hippocampal formation can be separated into synaptic signals (EPSPs) and population cell firing.

The present work depicts the development of a technique that allows direct electrical stimulation of a selected brain region and concurrent registration of neural activity and BOLD signal in this area. The study aims to determine the optimal parameters that produce a significant BOLD response with this technique and examines how electrical stimulation affects general neural function in the stimulated hippocampal subregion, the dentate gyrus. Further it will be examined, to what extent electrophysiological parameters (stimulation parameters as well as details of recorded neural responses) can be correlated to obtained functional MRI signals.

Chapter 2

Methods

Animals

For all experiments house breed male Wistar rats were implanted with electrodes. At the time of surgery they were between 7 and 8 weeks. After surgery they were allowed at least one week for recovery. Animals were kept in single boxes under a 12 h light/ 12 h dark cycle in a thermoregulated environment. They were fed lab chow (Ssniff, R/M-H, Soest, Germany) and given water ad libidum. All experiments were performed in accordance with the regulations of the German Federal Law on Care and Use of laboratory animals and were approved by the state animal care committee.

Electrode Implantation

For the surgical preparation animals were anaesthetized with sodium pentobarbital (Nembutal, 40 mg/kg i.p.). The head was placed into a stereotactical frame and fixed by ear bars and a biting bar. A patch of scalp between rats' ears and eyes was removed; the periosteum was scraped from the surface of the skull bones. Wound and bone were treated with 3% hydrogen peroxide to stop bleeding and to provide a clean and dry bone surface for the further preparation.
Two or three holes for nylon screws (0.80 x 0.125 mm, Plastics One Inc, Roanoke) were drilled at some distance around the later insertion points for electrodes and grounding wires for the purpose of a better fixation of the socket. Via two further drilled holes through the left parietal bone two silver wires (Ø125 μm, A-M Systems, Inc, Carlsborg, USA) each carrying a small melted silver ball and forming a hook at one side were clamped between dura and bone and fixed by tooth cement on the bone surface. They were placed several mm apart and provided a reference and grounding electrode.
For the insertion of the monopolar recording electrode into the dentate gyrus and bipolar stimulation electrode into the perforant pathway of the angular bundle two holes were drilled above the right hemisphere at -4.0 mm AP, 2.3 ML from bregma, an set 2.8 - 3.2 DV from dural surface for the former, and -7.5 mm AP, 4.1 ML from bregma, 2.0 - 2.5 DV from dural surface for the later. It was taken care that dura was removed before electrodes were lowered into the tissue. The correct placement of the electrodes was verified by giving test pulses while lowering the electrodes. When signal shape and parameters of the evoked test field potentials indicated the correct location, electrodes were fixed with tooth cement to the bone (Paladur, Heraeus Kulzer GmbH). Electrodes were house made from teflon-coated tungsten wire (Ø114 μm, A-M Systems, Inc, Carlsborg, USA), legs of the bipolar stimulation electrode were 1 mm apart. To form sockets for the connectors some

of the coating was removed from the free endings and wires were passed through two rubber pin sockets, one for stimulation, another for recording. The recording socket comprised a contact for recording and two for reference and grounding. Both sockets were fixed to the skull and incorporated into a solid sockel formed from tooth cement on the rats head.
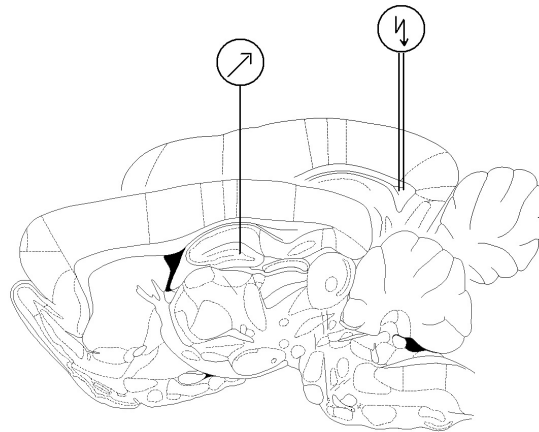

Figure 2.1: **Position of recording (front slice) and stimulation electrode (back slice).** Modified figures from [97].

Recording and Analysis of Field Potentials

For electrostimulation biphasic square pulses of 0.2 ms duration per half wave were delivered to the right side perforant pathway; evoked field potentials were recorded in the granular cell layer of the dentate gyrus of the same hippocampus side. The shape of an appropriate area dentate signal is shown below.
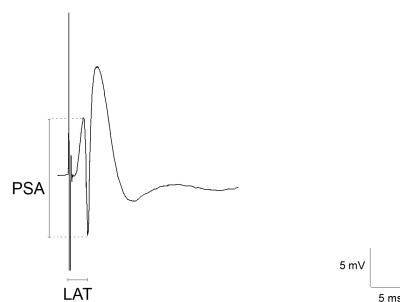

Figure 2.2: **Extracellular field potential.** Typical field potential recorded in the granular cell layer of the dentate gyrus. A positive EPSP is interrupted by the negative deflection of a population spike.

A number of parameters can be calculated from this response. The EPSP is the maximal slope of the uprising flank of the first positive deflection of the signal. It can be interpreted as a measure of incoming excitatory synaptic activity. The population spike amplitude PSA was calculated as difference between the maximum value of the first positive deflection and the minimum of the following first negative deflection. The population spike is known as summed spiking activity produced by the granular cells. Latency (LAT) is calculated as time interval between stimulus onset and population spike maximum (see Fig 2.2).

Until recently it was common practice to calculate EPSP for the dentate gyrus from the same electrophysiological signal as PSA. However, EPSP recorded in the granular cell layer represents a mixed field potential, influenced by synaptic activity and population spikes [43]. For a reliable measurement of the synaptic activity corresponding to the population spike produced in the granular cell layer there should be a second recording electrode in the dendritic layer, the adjacent molecular layer (ibid.). A double recording of EPSP/PSA was impossible during electrostimulation along with fMRI. In contrast to recordings with one electrode and one cable, which produced only minor artefacts, an employment of two electrodes and two cables produced artefacts in the electrophysiological recordings that obviated a later analysis. In the present case one single recording electrode was positioned to record signals from the granular cell layer, in consequence only the PSA and LAT were calculated from the recorded responses.

For stimulation and recording of electrophysiological data the in-house program PWIN Intracell 1.5 (2000 Institute for Neurobiology, Magdeburg) was used. It controls the analogue digital converter power CED 1401 (Science Products GmbH) producing stimulus pulses and can be used for simple signal trace analysis (single pulse recordings). For analysis of train responses Excel 2002 and Matlab R2006a were applied. Recorded signals were filtered between 1 Hz and 5 kHz and amplified (differential amplifier, INH, 156 Science Products, Hochheim, Germany) and saved on a hard-disc for later offline analysis. Recording rate was 4 kHz for 2.5 Hz stimulation, 6.024 kHz for 5 Hz stimulation, 5 kHz for 10, 20 and 100 Hz stimulation. The different recording rates were due to limitations of the recording program.

fMRI and Electrophysiological Recordings

For a combined fMRI/electrophysiology experiment rats were anaesthetized with isoflurane. The head was fixed with a bite bar and mounted into a head cone retractable into the transmission/recording coil. Perpetuation of anaesthesia was enabled by supply of inhalant into the head cone. Isoflurane 1.0-1.5 % was provided mixed with $N_2O:O_2$ (50:50, v:v). Contacts for electrostimulation and recording were plugged into the respective rubber pin sockets, cables were led out the scanner in line with the z-axis (Fig 2.3).

Anatomical and functional MRI was performed on a 4.7 T scanner (Bruker Biospec 47/20) with a free bore of 20 cm and a 200 mT/m gradient system (BGA 12). RF excitation and signal collection was performed by a 50 mm Litzcage, a birdcage-like small animal imaging system from DotyScientific Inc (Columbus, SC, USA).

Anatomical images were obtained with fast spin-echo sequence providing T_2-weighted images (RARE): TR = 4 s, TE = 15 ms, 256 x 256 matrix, RARE-factor 8, 4 av-
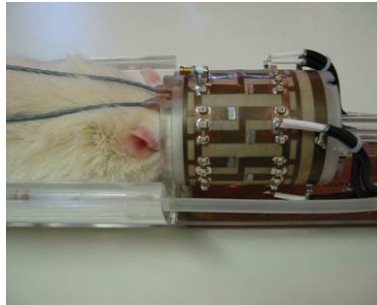
Figure 2.3: **Rat head positioned in an animal coil.** Head fixed in the head cone inside the coil, contacts for stimulation and recording plugged into the sockel and led out the coil.

erages. For functional imaging an echo planar imaging (EPI) sequence was chosen: TR = 2 s, TE = 24 ms, 64 x 64 matrix. An alternative functional imaging sequence (FLASH) was rejected for a longer acquisition time, and because better results could be achieved with EPI. Field of view (FOV) was 4 cm x 4 cm during anatomical and functional imaging, slice thickness (1mm) and number of slices 8, in horizontal orientation. That resulted in anisometric voxel with a resolution of 156 x 156 x 1000 μm for anatomical images and 625 x 625 x 1000 μm for functional images.

For a combined recording of fMRI and electrophysiological data the problem of the different time scales of these two techniques had to be resolved. Electrophysiological processes are fast and take place on a scale of milliseconds, thus electrophysiological experiments and stimulation protocols are designed to be applied for relatively short time intervals. Meanwhile multi-slice fMRI measurements require up to several seconds per frame, in the present experiments this was 2 s. A stimulation protocol had to be found that would be feasible to be applied to a rat for a time long enough to allow sufficient functional signal collection without harming the animal. For that electrophysiological protocols already known from neural plasticity research were modified.

The first electrostimulation protocols tested were utilizing low frequencies: 0.2, 2.5, 5, 10 and 20 Hz. Stimulation was delivered in blocks, one block containing an 8 s continuous stimulation train followed by a 52 s interval of rest. These low frequency experiments consisted of 7 stimulation blocks. Only the 0.2 Hz experiments consisted of 8 stimulation blocks of 60 s length, 40 s of this being stimulation. fMRI measurements started one minute before stimulation onset, recording a BOLD signal baseline, and finished after the last resting term (Fig 2.4). Electrophysiological responses were only recorded during the 8 s of stimulation. Later a longer lasting experiment applying 10 Hz for 15 stimulation blocks was conducted to check if a longer lasting stimulation would weaken the BOLD response produced during later stimulation blocks.

BOLD signal recording

electrostimulation & electrophysiological recordings

| | | | | | | |
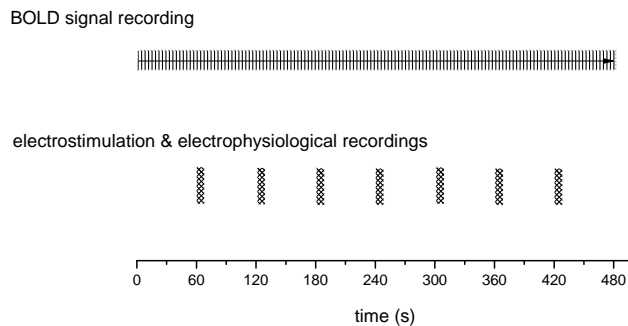0   60   120 180 240 300 360 420 480

time (s)

Figure 2.4: **Stimulation blocks and fMRI imaging schedule.** Time courses of parallel electrostimulation and BOLD signal recording. 8 min of continuous fMRI recording at 30 frames per min. Below, seven blocks of electrostimulation each delivered for 8 s, followed by a 52 s break.

In two additional experiments the influence of stimulation train length (stimulation duration) and stimulation intensity on BOLD signal production was tested. A 20 Hz stimulation protocol was chosen because it was already shown to produce a reliable BOLD response.

To test the role of stimulation duration, stimulation trains within a block were reduced to 4 seconds (56 s rest). To test the role of stimulation intensity, length of stimulation trains was kept at 8 s but they were delivered only with threshold stimulation intensity. Threshold stimulation intensity is defined as current producing barely a population spike to single test stimuli.

Viable stimulation intensity for experiments was determined in anaesthetized animals 30 min before an experiment started by recording input-output relations (I/O) between stimulation intensity and evoked response (PSA) produced in the granular cell layer of the dentate gyrus. For the determination of the sensitivity of the observed cell population current of rising intensities was applied to the perforant pathway in steps of 100, 200, 400, 600, 800 μA in intervals of 2 and 5 min (2, 2, 5, 5, 5 min). The resulting curve has a sigmoid shape (see Fig 2.5). The quantity of current producing 50 % of the PSA-maximum was used for stimulation.

In the initial experiments the determination of proper stimulation intensity (50 % PSA_{max}) was neglected in the interest of a sufficiently high population spike. Since it was unknown how much stimulation was necessary to produce a clear BOLD response, in the initial experiments a stimulation intensity was chosen that produced population spike amplitudes of at least 2 mV. With rising experimental experience recording of Input-Output relation as described above became a customary tool for determination of stimulation intensity.
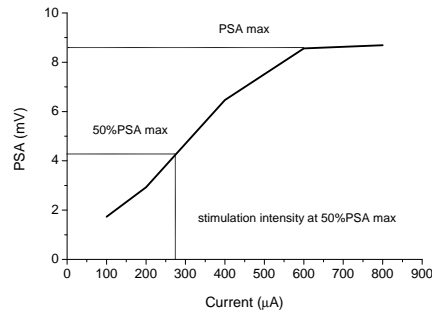
Figure 2.5: **Determination of stimulation intensity.** Example of an I/O curve and 50 % max value estimation, recorded in the granule cell layer of the dentate gyrus.

For high frequency experiments another type of stimulation protocol utilizing 100 Hz and 200 Hz was designed. Stimulation trains took again 8 seconds but stimulation was not continuous as in low frequency stimulation. Here a stimulation train comprised 8 bursts of 10 or 20 stimuli applied at the beginning of each second (see Fig 2.6). High frequency protocols were applied for 15 minutes, i.e., 15 blocks.
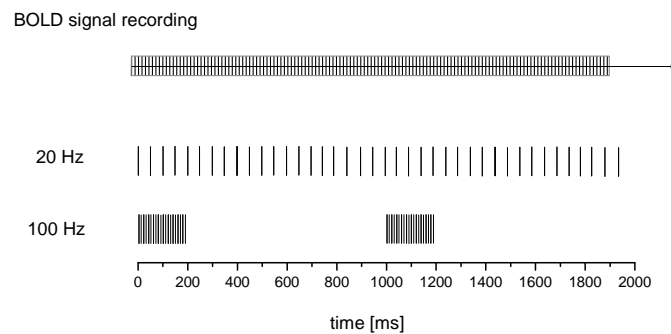
Figure 2.6: **Continuous vs. burst stimulation.** Two seconds of continuous 20 Hz stimulation compared with two seconds of 100 Hz burst stimulation. Both apply 20 stimuli per s. Above, ongoing functional imaging.

100 Hz and 200 Hz stimulation bursts usually did not produce more than one population spike per burst in the dentate gyrus, i.e. all responses following the first stimulus were inhibited. So for the analysis of the spiking activity only the first population spike was evaluated.

Control 1: Lesion and Misplacement of Stimulation Electrode
Two variants of controls were prepared to prove that nothing else than stimulation of the perforant pathway triggered events that caused the observed production of

BOLD response in the hippocampus. First, the perforant pathway was cut after electrode preparation was finished as usual. This would prevent an active transfer of excitation evoked at the stimulation site. Second, recording electrodes were misplaced by implanting them into a region that provides no direct input to the DG, in that case into the inferior colliculus.

Control 2: Effect of Stimulation Protocols on DG Signaling

Two series of control experiments were done to examine the long term effect of the stimulation protocols on signal production in the dentate gyrus. They were both conducted outside the scanner.

The first set consisted of baseline and control recordings in ISO- anaesthetized rats before and after application of stimulation protocols typically used in fMRI experiments. Before the actual control experiment started, an I/O curve was recorded on the anaesthetized animal to determine the adequate stimulation intensity (50% PSA_{max}). Moreover the proper functioning of inhibition was tested by a paired pulse protocol. Paired pulses were applied in intervals of three minutes and were each spaced 10, 20, 50 and 100 ms. Stimulation intensity was I = 50% PSA_{max} (see Fig 2.5). At this intensity the PSA of the second pulse following the conditioning pulse should be suppressed at intervals below 80 ms and increased at a paired pulse interval of 100 ms [122]. Animals that did not fulfill this condition were excluded. Controls were recorded outside the MR scanner but using the same cradle containing the rat recording coil and anaesthetization cone that was used for fMRI experiments. Ventral heating was used to keep rats' body temperature constant. Body temperature was recorded over the whole experiment and during all experiments with anaesthetized animals.

For the baseline recording one data point was recorded every 5 minutes for 30 minutes. The single data point was an average of responses to five test pulses spaced 10 s. This spacing is known to exert no effects on following responses. After baseline recording an fMRI stimulation protocol was applied for 7 minutes (low frequency) or 15 minutes (high frequency). Recording of the control baseline started immediately after the end of the stimulation term. For the following 30 minutes control baseline was recorded in intervals of 5 minutes. For the last two hours test pulses were applied in intervals of 15 minutes.

When the recording of 2.5 h control baseline was finished an I/O curve was recorded again. Control experiments were performed for 2.5 Hz, 5 Hz, 10 Hz and 100 Hz.

A similar second set of baseline recordings was done on unanaesthetized animals. It should serve for a comparison with ISO-anaesthetized animals and examine the effect of anaesthetization on the production of electrophysiological signals. For that purpose, animals were placed into recording chambers on the eve of the experiment to get used to the surrounding. Recording chambers were 50 cm x 50 cm boxes, 100 cm high; with three intransparent sides and one side made of Plexiglas through which animals could be observed. Contacts for stimulation and recording were plugged into the socket and connected to a freely revolving swivel above the boxes allowing the animals to move unhampered during the recording. Cables were light and flexible to prevent an annoyance of the animals.
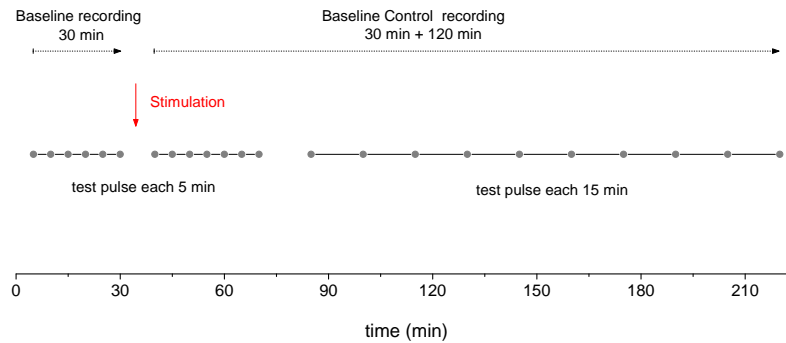
Figure 2.7:   **Scheme for control recordings.** Control for Isoflurane - anaesthetized animals. 30 min of baseline recording, interrupted by electrostimulation typically used in fMRI experiments, followed by a control baseline recording continued for 150 min. Data points of the baselines represent responses to single test pulses, successive responses do not interact.
Control recordings for unanaesthetized animals follow a similar sequence but they are slightly longer. Baseline was recorded for one hour and control baseline for four hours. Responses to test pulse were registered each 5 min during baseline and first hour of control.

For the determination of appropriate stimulation intensity an I/O curve was recorded before each control experiment also for unanaesthetized animals. Inhibition was checked the same way as described in ISO controls. This was done 2 hours before the baseline/control experiment started.

For the baseline recording one data point was recorded every 5 minutes for 60 minutes. A single data point was an average of responses to five test pulses spaced 10 s as in anaesthetized animals. After baseline recording an fMRI stimulation protocol was applied for 7 minutes (low frequency) or 15 minutes (high frequency). Recording of the control baseline started immediately after the end of the stimulation term. For the first 60 minutes, a control baseline was recorded in intervals of 5 minutes. For the following three hours, test pulses were applied in intervals of 15 minutes (Fig 2.7).

When the recording of 4 h control baseline was finished an I/O curve was recorded again. Control experiments were performed for 2.5 Hz, 5 Hz, 10 Hz and 100 Hz. In non-anaesthetized animals behavioural protocols were registered, when animals responded to stimulation with behavioural changes.

Data analysis and Statistics

fMRI-Analysis
For analysis of functional MRI data BrainVoyager QX software package Version 1.8 (Brain Innovation, Maastricht, The Netherlands) was employed. Anatomical and functional raw data were uploaded and transformed from the scanner format into BrainVoyager format. The following pre-processing comprised 3D motion correction and temporal smoothing only. Pre-processing was kept simple to prevent an excessive smoothing of the original data.
3D Motion correction consisted in a trilinear interpolation. For temporal smoothing a Gauss filter (3 points) was applied. A linear trend removal and temporal high-

pass filter (3 cycles per time course) were applied to eliminate low frequency drifts from voxel time courses caused by technical (scanner-related) noise.

To identify brain regions displaying increased or decreased BOLD-signal a voxel-wise univariate statistical analysis was executed. A correlation analysis compared a predicted reference function with the real BOLD signal time course. A two gamma HRF function served as reference function representing a model of the expected hemodynamic response function. A correlation coefficient close to -1 or +1 indicates high correlation between predicted and real BOLD time course. A following t-test determined the probability for a high correlation. The delivered statistical t-values provided an activation map after being set to a certain threshold level ($6 \leq t \leq 8$). For visualisation and better orientation functional data were overlaid with the corresponding anatomical images.

All statistical analyses were done on pre-processed BOLD time courses.

Statistics for fMRI and electrophysiological data

Spatial extent of BOLD activated area was determined by counting significantly activated voxel in the both hippocampi and subicular/ enthorhinal cortex areas (threshold: statistic value $6 \leq t \leq 8$). A non-parametric Mann-Whitney-U-test was used to compare the activated area of different frequencies.

For a quantification of signal increase, the area under the curve for a time interval of 30 s or 15 frames following stimulation onset was calculated for each stimulation block (Fig 2.8). Since baseline shifts could often be observed after the first stimulation train, the increments for all following blocks had to be determined in comparison with the baseline section preceding each new stimulation block (see Fig 2.8). Comparison with individual baselines made sure that the proper signal increment for each individual stimulation train was determined. Values ≤ 100 % were set zero.

For a statistical comparison of BOLD baseline shifts individual baselines (green intervals) were compared to the first, initial baseline (red interval). Linear models for the signal time courses were calculated and t-tests were conducted on the outcomes of these regression models (i.e. calculation of contrasts). This approach accounted for the dependent character of baselines data in one experiment. All subsequent baselines are not independent from initial.

For a statistical evaluation of the effect of electrostimulation protocols on neural signal production, linear models were applied again. Two kinds of change in signal production were expected due to electrostimulation, and tested for. First, longer lasting changes of population spike production could occur in response to the stimulation. That is, response to single stimulus pulses would be different before and after electrostimulation. Second, population spike production during stimulation could be changed as immediate response to stimulation trains. To answer the first question electrophysiological baselines were recorded before electrostimulation and compared with control baselines recorded afterwards. Two test the second question, spiking occurring during electrostimulation was compared to the same baseline. Changes in response to stimulation trains during stimulation could give evidence about processes happening due to stimulation itself, such as short term plasticity effects.
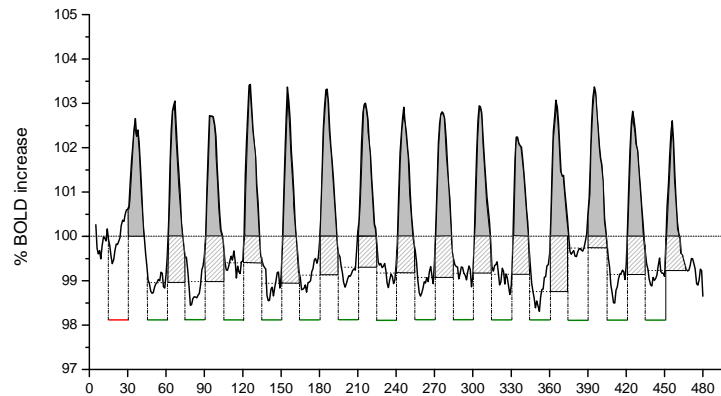
Figure 2.8: **Determination of BOLD signal increment and baseline shift.**
First, red interval symbolizes initial baseline, following green intervals individual baselines.
Individual baselines comprise values measured during 15 frames or the time interval of 30
s ahead of stimulation onset. Bold signal increment is the sum under the curve for the
remaining 30 s following stimulation onset. In the displayed plot BOLD signal increment
(gray) is calculated in relation to the initial baseline (continuous horizontal line). For
comparison: difference in BOLD signal increment when related to individual baselines
(hatched).

According to that regression models were calculated for functions comprising base-
line and control baseline and for functions comprising baseline and response during
stimulation. Each control experiment/animal was assumed to form one function.
T-tests were conducted on the outcomes of these regression models (calculation of
contrasts). This approach accounted for the dependent character of all responses
following baseline recording, since control baselines and responses during stimula-
tion can not be assumed to be independent from baselines.

Chapter 3

Results

First the technical feasibility of conjoint fMRI and electrophysiological measurements was tested. For the functional imaging a FLASH sequence or an EPI sequence were considered. To produce a comparable image quality a FLASH sequence would demand 4-6 s per picture/frame and a slice thickness of 1.5 mm, whereas an EPI sequence only required 2 s per frame and a slice thickness of 1 mm. So, the EPI sequence was chosen for the functional imaging.

114 μm tungsten electrodes produced artefacts in MRI and fMRI images as can be seen in Figs 3.1. In EPI images artefacts came in form of voxel extinction: 2-6 voxel in plane for recording electrodes, and 12 voxels for two-shank stimulation electrodes. Besides that images showed no strong distortions produced by electrodes, brain subregions as the hippocampus could still be distinguished properly.
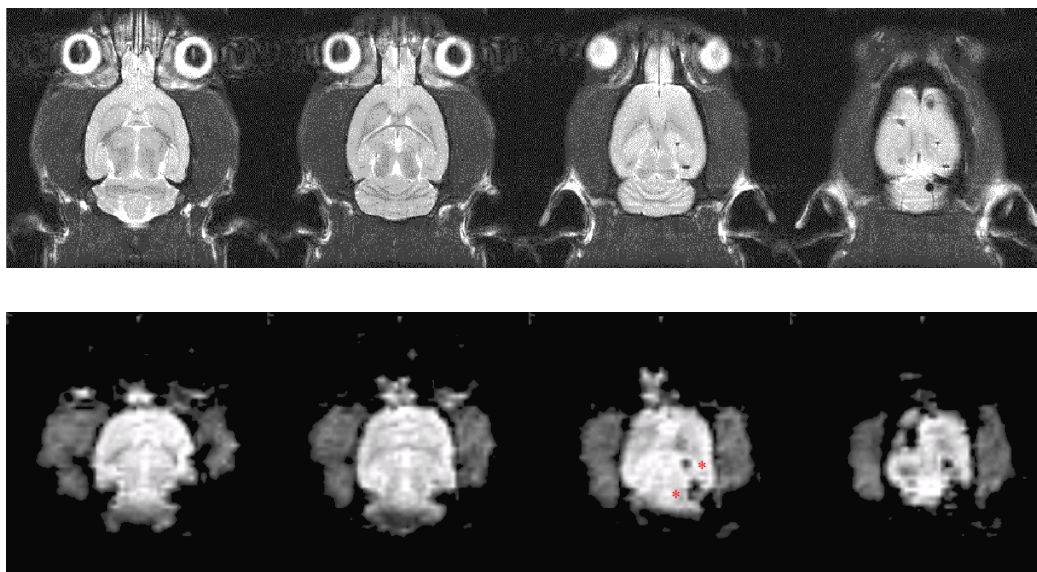

Figure 3.1: **Typical artefacts produced by electrodes in MR images.**
Upper row displays the anatomical images of the upper four layers of a scanned rat brain. Red stars mark the pircings produced by the recording and stimulation electrodes. The Two-shank stimulation electrode leaves a wider artefact.
Lower row displays the complementary EPI images of the upper four layers. Brain subregions appear clearly discernible. Voxel size is 0.625 mm in plane, 1 mm thick.

Drastic image distortion could occur with wrong orientation of wires for electrostimulation/recording in relation to the head coil. When these thin cables were

led out of the scanner along the coil, image quality was impaired. By putting the cable along the opposite direction and leading them out on the other side of the scanner distortions could be avoided. Electrostimulation itself did not impair image quality.

Electrophysiological recording could be conducted without problems during fMRI as long as only one recording electrode was utilized (see trace in upper Fig 3.2). With a second recording electrode large artefacts appeared in the electrophysiological recording during fMRI/ electrostimulation (lower Fig 3.2). The disturbance made it impossible to record electrophysiological signals bipolarly.
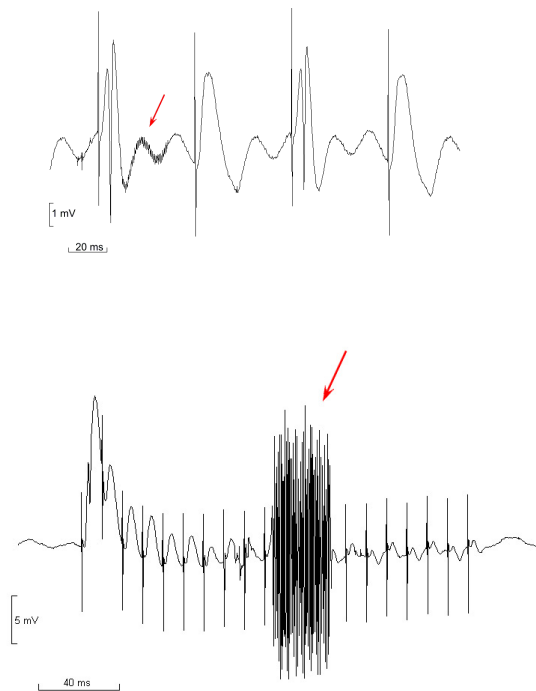
Figure 3.2: **Artefacts in electrophysiological recordings produced by the scanner. Upper trace:** Detail from a 20 Hz stimulation response recorded in the dentate gyrus. Granule cells only respond two each second stimulus pulse. Minute artefacts produced by the scanner gradient overlay the first response. These artefacts were negligible in a later signal analysis. Usually gradient artefacts were even smaller.
Lower trace: Detail from a 100 Hz stimulation response recorded in the dentate gyrus applying two close recording electrodes in the DG and molecular layer. Massive artefacts distort response traces.

Several animals were prepared as control for unspecific BOLD activation. Lesion of perforant pathway prevented stimulation of hippocampal regions and abolished there production of a BOLD response (see upper Fig 3.3). The same happened when the stimulation electrode was placed into a region close to the perforant pathway but failing to meet it (lower Fig 3.3). These controls proved that a sig-

nificant BOLD signal could only be evoked in regions connected to the perforant pathway. They proveded that a direct physical activation of the perforant pathway triggered BOLD responses particularily in the hippocampal formation. A further point against a passive spread of current is that stimulation and recording site are too far apart.
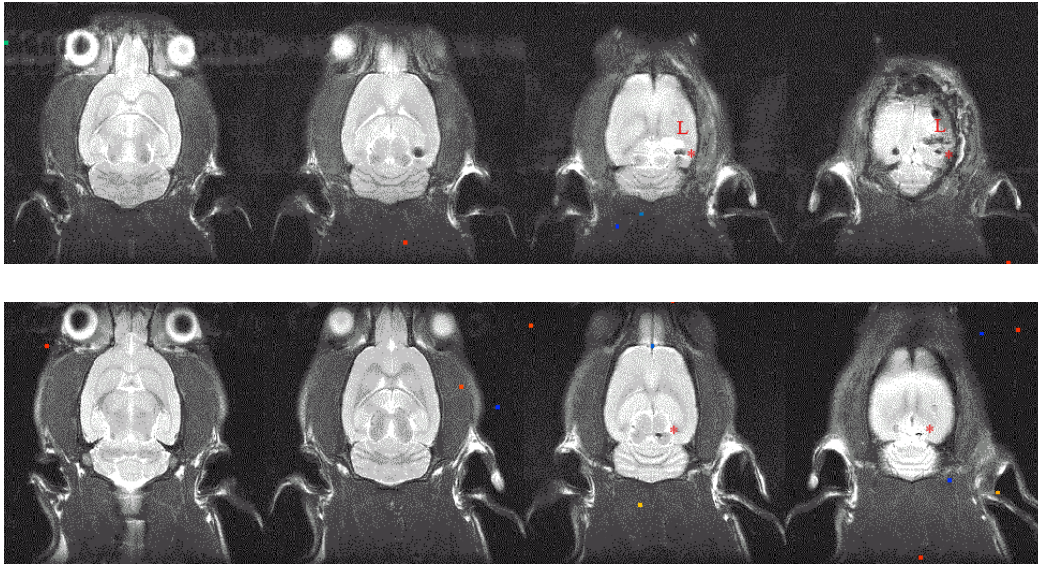
Figure 3.3: **Controls for unspecific BOLD signals.** Images display functional activation during 20 Hz stimulation mapped on anatomical images of the upper four layers.
Upper row: Lesion (L) of perforant pathway impeded activation of all downstream regions. The white patch marks the liquid-filled deeper part of the cut, the dark streak shows the tissue damage close to the brain surface.
Lower row: Misplacement of stimulation electrode (*) into the inferior colliculus produced no activation as observed in later experiments with correct electrode position (see Figs 3.11 and 3.28).

3.1   Establishment of minimal requirements for a BOLD-generating protocol

First attempts to find an appropriate stimulation protocol for BOLD generation utilized a continuous stimulation protocol of 0.2 Hz applied for 40 s in 8 blocks (stimulation intensity: 400 μA). This could not produce a significant BOLD response. Increasing stimulation frequency to 5 stimulus pulses per s lasting for 8 s did not generate a significant BOLD signal. But when a 5 Hz stimulation was delivered for six seconds in several repeats, separated by breaks of 54 s, a significant BOLD response could be observed. Increasing stimulus pulse width from 0.1 to 0.2 ms further improved the BOLD response (stimulation intensity: 400 μA).
The following block-design protocols were derived from these initial experiments. 'Low frequency protocols' employed electrostimulation with frequencies between 2.5 and 20 Hz. In those stimulation protocols 2.5, 5, 10 or 20 stimuli per second were delivered continuously for 8 s, followed by a 52 s break. One experiment comprised seven stimulation blocks (see Fig 2.4 in Methods). The corresponding fMRI measurements started one minute before electrostimulation to provide a baseline for the evoked BOLD responses. So, one low frequency stimulation experiment took 8 minutes. Before the actual fMRI experiment started an anatomical data set was obtained for each animal.

'High frequency protocols' utilized stimulation frequencies between 50 and 200 Hz. Since continuous stimulation with higher frequencies was supposed to have damaging effects on the animals, burst stimulation was chosen for those frequencies. Burst stimulation protocols comprised an amount of stimulus pulses equivalent to 10 and 20 Hz continuous protocols. In a burst protocol 10 or 20 stimuli were delivered in the beginning of each second for 8 s (see Fig 2.6 in Methods). Each set of 10 or 20 stimuli is called a burst. An 8 s stimulation block was again followed by a 52 s break (Fig 3.5).
The equivalent number of stimuli in low and high frequency stimulation experiments allowed examining the question if frequency or simply number of delivered pulses were responsible for different outcomes in BOLD production.

3.2   Low frequency protocols - fMRI

For low stimulation frequencies the probability of BOLD generation increased with increasing frequency (Tab 3.1). At 2.5 Hz generation of a BOLD response was very unlikely. A significant BOLD activation could be observed in only one of six animals. This was probably due to an exceptionally low level of anaesthetization. Fluctuation during the BOLD signal time course was large in this case and the result could never be reproduced.

5 Hz stimulation produced significant BOLD responses in the dorsal hippocampus in half of the animals. Activated area varied considerably from animal to animal, but maximal signal increment due to stimulation was ~3% in all experiments, compared to initial baseline. Activation followed stimulation immediately in train 1 and occurred on a similar level during the following trains. There was a tendency
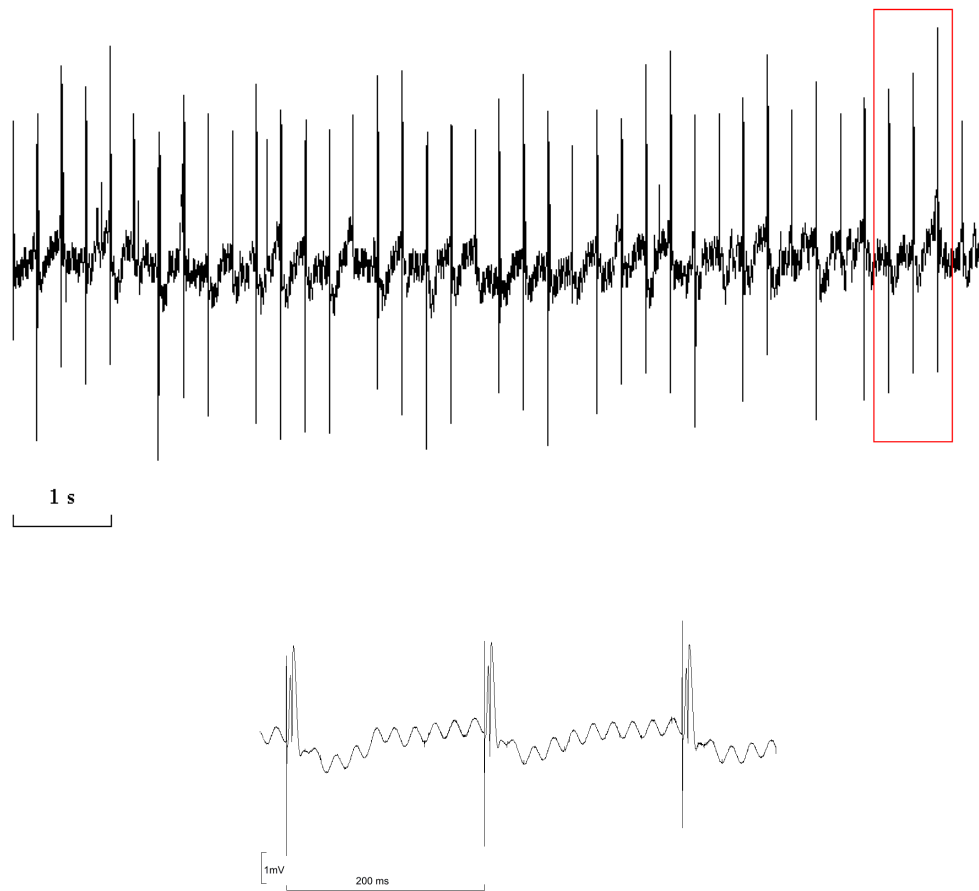
Figure 3.4: **Upper trace:** Response to continuous stimulation. Example of recorded responses to a continuous 5 Hz stimulation train, shown on a large scale.
Lower trace: Detail from trace above. Recordings were regularly overlayed by a 50 Hz alternating current.

of BOLD signal decrease in later trains (Fig 3.7, 5 Hz).
BOLD signal increase started in general during the first 2 s of stimulation. Activation increased only during electrostimulation, peaking within that interval or with its end (8 s or 4 frames after stimulation onset); sometimes with a delay of 2 s after stimulation had ceased. BOLD signal started to decrease immediately after peaking without maintaining a plateau phase.

At 10 Hz stimulation response occurred again immediately after stimulation onset. Due to the gross temporal resolution of MRI it is not possible to identify the true delay to stimulation, but it is less than 2 s, because the signal is already increased in the first frame.
In single animals increased BOLD signal intensity could be observed during the break following train 1. That was the case when electrostimulation produced after-discharges and thus neuronal activity that continued after stimulation had ceased.
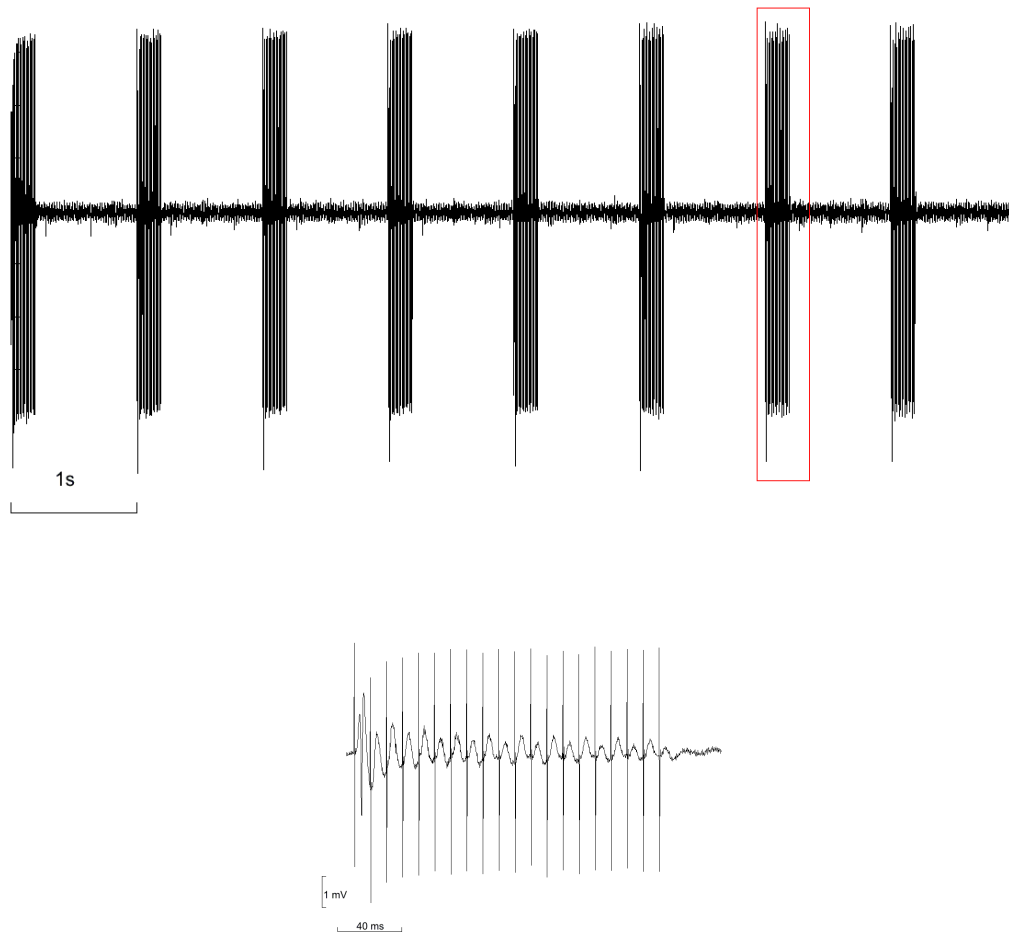
Figure 3.5:   **Upper trace:** Response to continuous stimulation. Recorded trace of responses to a 100 Hz burst stimulation train.
Lower trace: Detail from analogue trace above.

On the other side there was also a tendency to show a baseline drop after train 1. In the first experiments, applying 10 Hz trains for 7 minutes, this could not be observed as clearly as in later experiments utilizing 10 Hz protocols for 15 minutes (see part BOLD baseline shift, page 56). The reason for that different outcome of two rather equal experiments is not clear, maybe anaesthetization depth plays a role.
The initial increase after 10 Hz stimulation was ∼2.8% in train 1, followed by a slight breakdown in BOLD increase during the second train by in average 0.6%, which recovered in train 3 to 3%. During the following four trains BOLD signal increased constantly to ∼4% (Fig 3.7, 10 Hz).

20 Hz stimulation produced a BOLD response pattern very similar to 10 Hz. Increases in BOLD activation exceeding stimulation duration could be observed more often in consequence to afterdischarges following train 1 that were more likely to

happen with 20 Hz stimulation. With 20 Hz the baseline drop became obvious. The lower chart in Fig 3.7 displays a strong signal fluctuation between train 1 and 2, visible as broad shadow of standard deviations. These were produced by animals experiencing extended BOLD signal increase on the one side and animals with a baseline drop on the other. In train 2 BOLD signal increase stopped slightly below the former level at ∼2%. Only in train 3 BOLD increase started rising again to ∼3% and increased further until ∼4.5% in train 7. These were increments compared to initial baseline. When baseline shift is considered and BOLD increases were determined in comparison to individual baselines, i.e., baseline preceding BOLD responses, increments were considerably higher (plus up to 1%). More about baseline shifts will be discussed in the part 3.7 Figure 3.7.

Table 3.1: **Efficiency of several low frequency protocols for BOLD generation.**

Applied frequency	Probability of sig. BOLD response (animals)	Ø No. of activated voxels in case of sig. BOLD response (ipsilateral hippocampus)	Sampling size N
2.5 Hz	0% (17%*)	0 (3*)	N=6
5 Hz	50%	8.5 ±6.8	N=12
10 Hz	78%	15.4 ±7.8	N=9
20 Hz	100%	19.9 ±10.0	N=8

* One animal, never repeated

10 Hz appeared to be an optimal frequency for further experiments, since it produced BOLD responses almost with certainty and it offered less risk to cause additional discharges compared with 20 Hz. Thus, a second experiment was conducted applying a 10 Hz protocol for 15 instead of 7 minutes. A longer experiment should test if BOLD signal generation would be exhausted by longer lasting stimulation. This was not the case, BOLD signal increases remained on a constant level as long as stimulation trains were delivered, that is, until train 15. Only a minor decrease in amplitude could be observed during the last four trains, when ΔBOLD was still about 2 - 3% (Fig 3.7). As mentioned above, a significant baseline shift could often be observed after the first stimulation train in long lasting 10 Hz experiments. The baseline remained then on a lowered level during the rest of the experiment (see Fig 3.8 and part 3.7 Figure 3.7). That shift could be observed after train 1 despite the afterdischarges because those ended 15 s after stimulation termination at the latest. This is within the time, the BOLD signal was assumed to require to return to baseline (i.e. 30 s following stimulation onset). During the remaining 30 s the baseline could drop considerably. The big standard deviations after train 1, displayed in the averaged BOLD signal time course (Fig 3.8), originates from the large differences between the outcomes of single animals. While some showed no baseline shift, others showed a decrease by up to 4%.

2.5 Hz   ipsilateral hippocampus   (n=5)

Figure 3.6: **BOLD signal time course displaying no response to 2.5 Hz elec-
trostimulation for 7 minutes.** One minute baseline recording before stimulation onset.
Grey bars mark stimulation intervals of 8 seconds duration (or 4 frames), white space 52
s break. Usually there is no significant BOLD activation during 2.5 Hz stimulation.
Hemodynamic reference function is displayed for comparison in dark grey. Error bars mark
standard deviation.

Figure 3.7: **BOLD signal time courses in response to frequencies generating significant activation.** Grey bars mark 8 s stimulation intervals, followed by 52 s breaks between stimulation blocks (white). Error bars mark standard deviation.

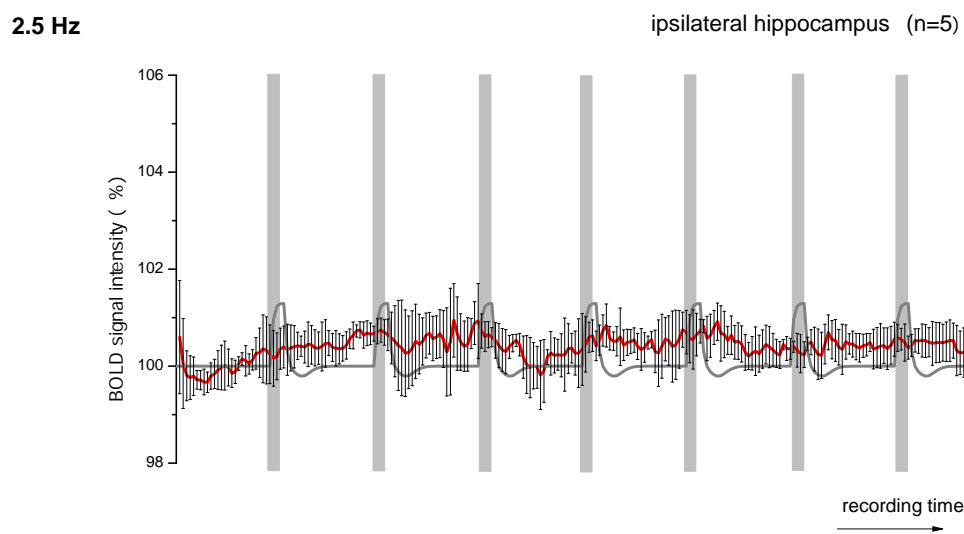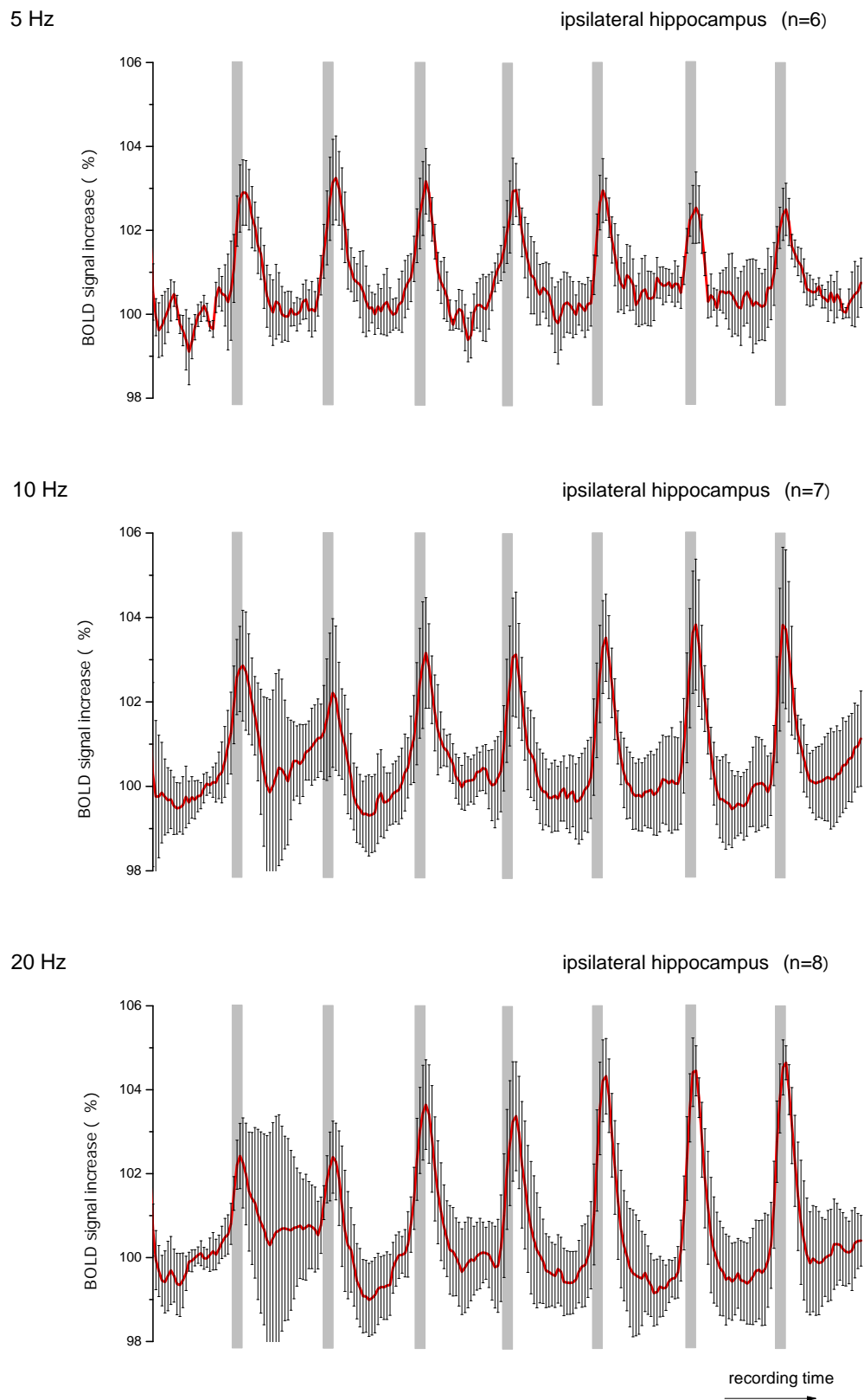100 Hz (20)   ipsilateral hippocampus   (n=6)
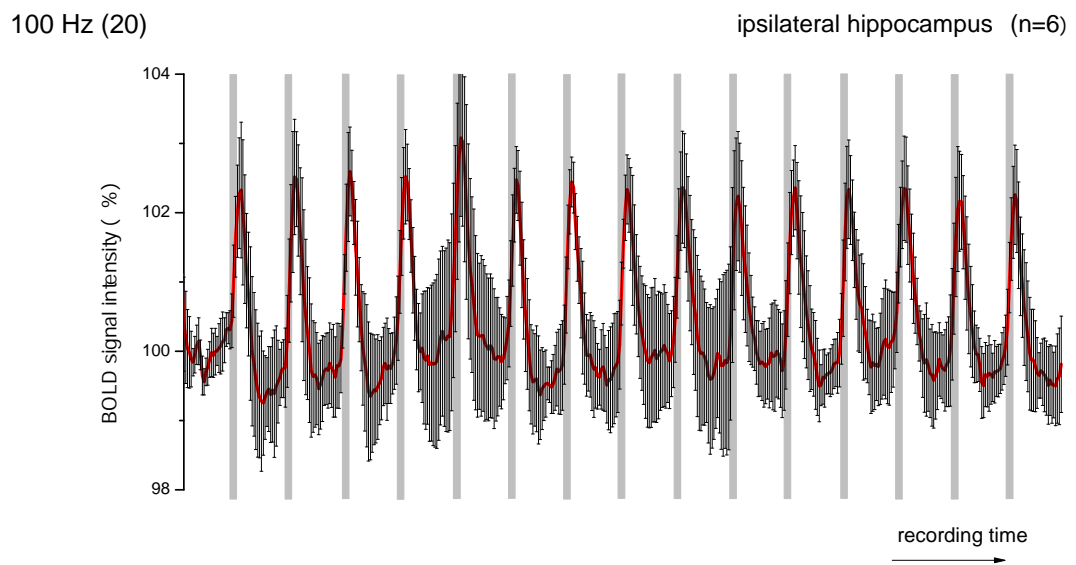
Figure 3.8: **BOLD signal time course displaying response to 10 Hz electrostimu-
lation for 15 minutes.** One minute baseline recording. Grey bars mark stimulation time
of 8 seconds (4 frames), followed by 52 s break intervals between stimulation blocks. There
is no significant decrease in amount of BOLD activation during longer lasting stimulation.
Attention should be paid to the standard deviation that is bigger in the longer lasting 10
Hz experiments compared with short 10 Hz experiments from above. The big standard
deviations arises from the intense baseline drop that can be observed more often in those
experiments. Baseline could shift by between zero and -4%. Error bars mark standard
deviation.

3.2.1 Statistical evaluation

An evaluation of activated area and amount of BOLD increase showed different correlations with stimulation frequency.

Activated area increased clearly with increasing frequency in the ipsilateral dorsal hippocampus (correlation: linearly R^2=0.96, logarithmically R^2=0.97) (left Fig 3.9). Correlation between area and frequency seemed to reach a plateau at 20 Hz, a logarithmic fitting curve matched here better than a linear. Nevertheless, differences in activated area were not significant when low frequencies were compared.

Averaged peak was maximal during 20 Hz stimulation and minimum during 5 Hz stimulation but the difference is not significant. Surprisingly the only case of activation during 2.5 Hz stimulation showed a higher activation than 5 Hz, but BOLD time course was here slightly different from other frequencies. That activation was brief: a steep rise during stimulation application and a rapid decrease to baseline after its end.

Summed signal increment, or respectively the area under the curve during the first 30 s following stimulation onset, did not differ significantly between low frequencies (compare bars in right Fig 3.9). Accordingly no correlation could be found between the summed BOLD activation and stimulation frequency.
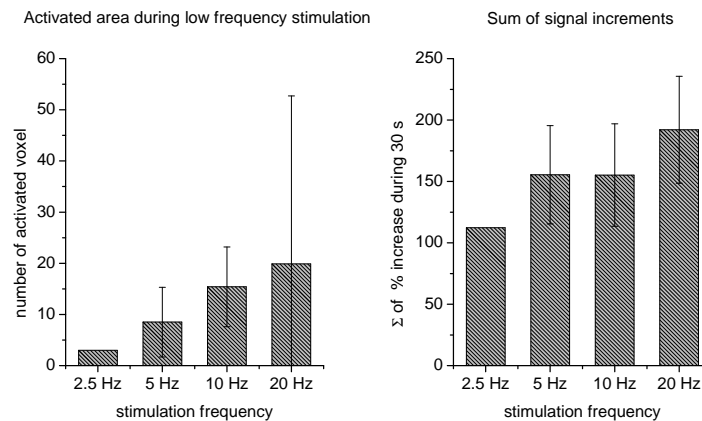
Figure 3.9: **Spacial activation and BOLD signal intensity for low frequency stimulation.**
Left chart: Activated area in the dorsal ipsilateral hippocampus. Though there is a positive correlation between activated area and applied frequency, no significant difference could be found between low frequencies in a comparison of the numbers of activated voxels.
Right chart: Sum of BOLD signal increases from baseline during 30 seconds (i.e. 15 frames) following stimulation onset, obtained during 7 stimulation blocks. The 30 s interval responds to the typical duration of a complete BOLD signal time course from its rise until return to the following baseline. Increments were calculated considering individual baselines (see Fig 2.8). Averaged values contain between 6 and 8 animals.
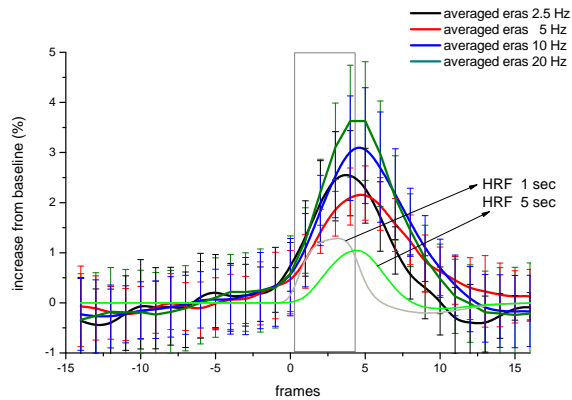
Figure 3.10: **Comparison of event related averages (ERA) for low frequency stimulation.** ERAs show that activation peak increased with stimulation frequency but not by significant amounts. Error bars represent standard deviation.
Activations in experiments applying stimulation frequencies of more than 2.5 Hz show a slower decay. For comparison two HRFs with differnt response peak times are ploted.
One ERA of one animal contains 7 averaged trains. An ERA displayed in the figure represents averages of several animals: $n_{2.5Hz} = 1$, $n_{5Hz} = 5$, $n_{10Hz} = 6$, $n_{20Hz} = 8$. Grey box marks stimulation interval.

3.2.2 Activation patterns

In several experiments BOLD activation could be observed not only in the hippocampus - as anticipated - but also in additional regions ipsi- and contralaterally from stimulation side (Figs 3.11).

5 Hz stimulation resulted in significant BOLD activations in the ipsilateral dorsal hippocampus. On the fixed significance level of t>6 no clear contralateral activation could be observed.

10 Hz stimulation evoked not only significant activation in the ipsilateral but also modest, significant BOLD signal increase in the contralateral dorsal hippocampus. Activation of the ipsilateral EC/Sub region remained mostly subthreshold, only few voxels could be observed at the chosen cut off threshold. In longer lasting 10 Hz experiments (15 trains), i.e., by averaging more trains, activation in the contralateral dorsal hippocampus became more clearly visible.

20 Hz stimulation produced significant BOLD signal increases in the ipsilateral dorsal hippocampus and ipsilateral EC/Sub region. Subicular region and entorhinal cortex can not be separated properly from the MR image at the chosen resolution. Contralateral EC/Sub region was significantly activated, contralateral hippocampus only scarcely.

Regions

5 Hz
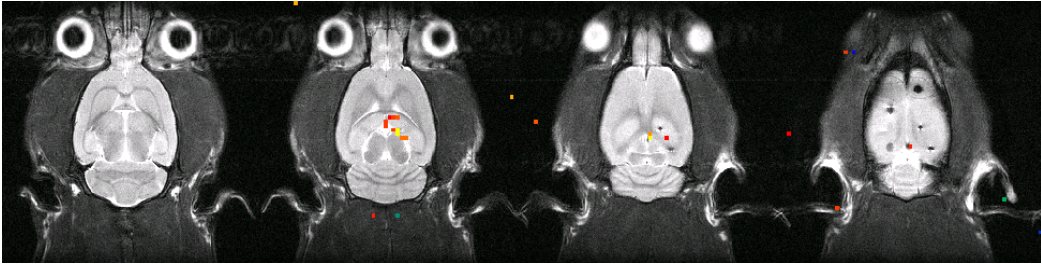
10 Hz
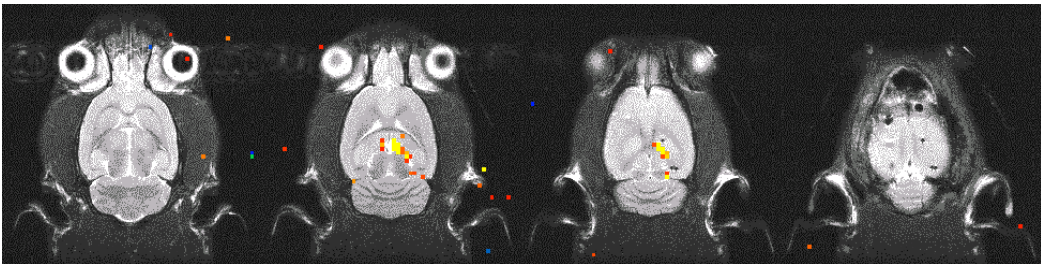
20 Hz
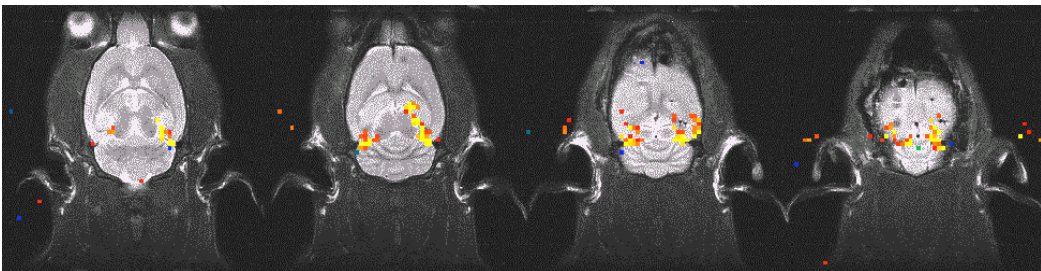
Figure 3.11: **Activation patterns during low frequency stimulation.**
Distribution of significant BOLD responses at a significance level of t: $6{\leq}t{\leq}8$ evoked
during 7 minutes of low frequency stimulation. Figures display single animals as examples
of typical activations.

3.2.3 Comparison of regional BOLD time courses

It could be observed that different patterns of BOLD signal time courses occurred in different brain regions in response to the same stimulus. That points to a disparate activation of connecting pathways in response to the same stimulation frequency. Variation of stimulation frequency produced also different activation patterns (compare BOLD time courses in the upper and lower Fig 3.12).

BOLD signal breakdown or decrease could mainly be observed after train 1 in the ipsilateral hippocampus during 10 Hz, but not as much during 20 Hz stimulation. In other activated regions signal breakdown could only be observed during 10 Hz experiments, they were not noticeable in 20 Hz experiment (compare Figs 3.12).
For a comparison of 10 and 20 Hz activations of the contralateral hippocampus and EC/Sub region, the first 7 trains of the longer lasting 10 Hz experiments were plotted here, since the first, short 10 Hz experiments did not show significant activations elsewhere than in the ipsilateral hippocampus. This approach seems to be justified given that the first 7 stimulation trains are the same in short and long lasting experiments. BOLD signal time courses showed a decrease in all regions during train 2 and 3 and recovered during train 4. From here on activation remained on a constant level until the end of experiment. Ipsi- and contralateral hippocampus activation were similar but BOLD time courses were noisier contralaterally.
Activation in the EC/ Sub region rose in tendency to higher levels than in the hippocampus, at least during the first trains.
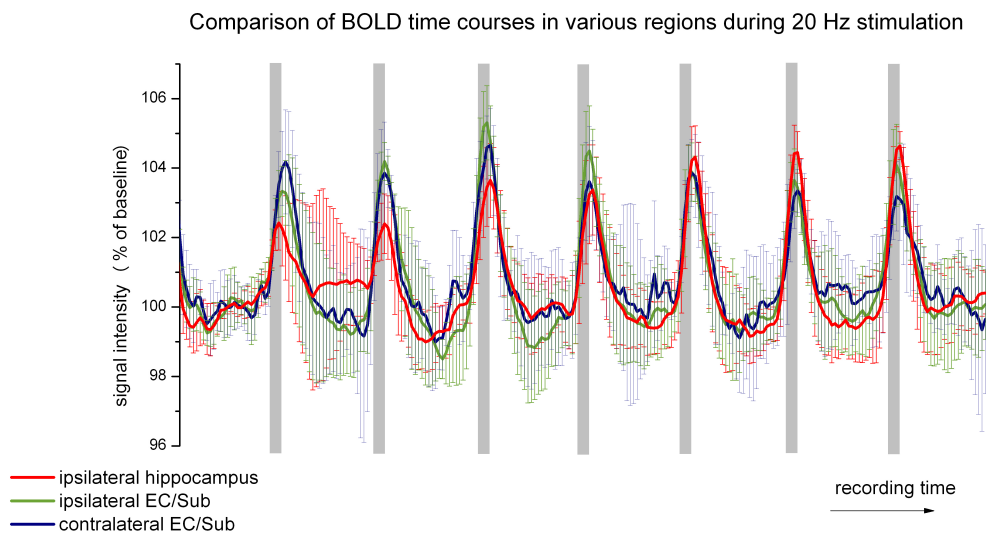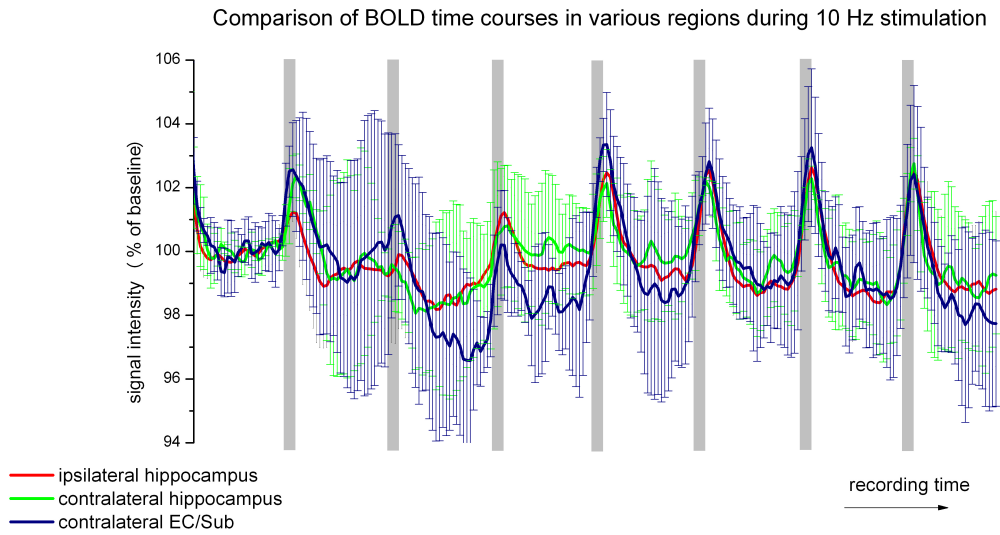
Figure 3.12: **Regional BOLD signal time courses in response to 10 and 20 Hz.** 10 and 20 Hz stimulation was capable of producing significant BOLD signals also in contralateral brain regions. BOLD signal time courses during stimulation were similar ipsi- and contralaterally except that BOLD signal increase was in tendency stronger contralaterally and in the EC/ Sub region, what became especially apparent during the first 2 - 3 trains.

3.3 Effect of stimulation parameter variation

To study how a variation of parameters apart from frequency would affect BOLD signal production a 20 Hz protocol was chosen for further experiments, since here BOLD generation was most probable. Two parameters of the standard experiment were modified: stimulation intensity and train length (stimulation duration per second).

20 Hz stimulation for 4 instead of 8 s per train produced similar BOLD signal time courses. ΔBOLD signal increased in both from $\sim$2.5% in train 1 to $\sim$5% in the end ot the experiment (Fig 3.14). A clear BOLD baseline shift could not be observed with shorter train lenght, yet individual BOLD signal time courses were noisier.

Using threshold intensity for stimulation produced again noisier BOLD signal time courses compared with standard stimulation. BOLD signal increased from the first train to $\sim$3.5 - 4% and remained on the same level during the whole experiment. No BOLD baseline shift in the intervals between stimulation trains could be observed. BOLD activation returned slower to baseline than in experiments using a higher stimulation intensity than threshold intensity (blue curves in Figs 3.13 and 3.14).
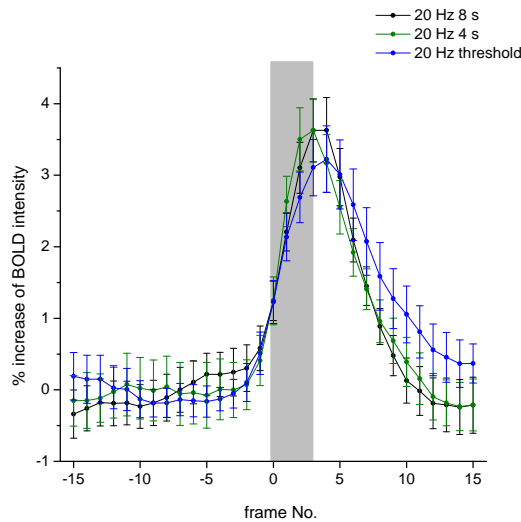
Figure 3.13: **Event related averages.** Stimulation with threshold intensity produced a slightly different activation compared with standard 20 Hz electrostimulation for 8 s and abbreviated stimulation trains of 4 s. BOLD signal returns slower at threshold intensity, showing a wider right flank. $n_{8\,s} = 8$, $n_{4\,s} = 4$, $n_{threshold} = 5$

Activated area was in contrast smaller in experiments using threshold intensity or 4 s stimulation compared with the standard 20 Hz experiment (Fig 3.11). In fact, the same regions were activated in experiments with modified parameters, but BOLD signal increase remained below the threshold of t$\geq$6. Electrostimulation for 4 s was sufficient to activate significantly ipsilateral EC/Sub region, but scarcely reached contralateral regions (Fig 3.3). Threshold intensity activated contralateral hippocampus to a comparable amount as the standard 20 Hz stimulation.

ipsilateral hippocampus
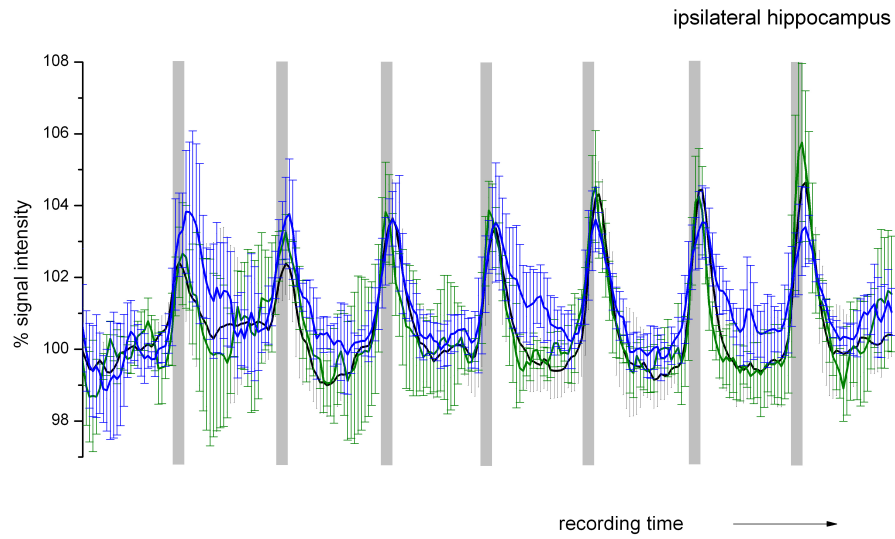
Figure 3.14: **BOLD time courses in the ipsilateral dorsal hippocampus.** Effect of parameter variation: stimulation intensity and duration. Legend as in Figs 3.13 and 3.14.
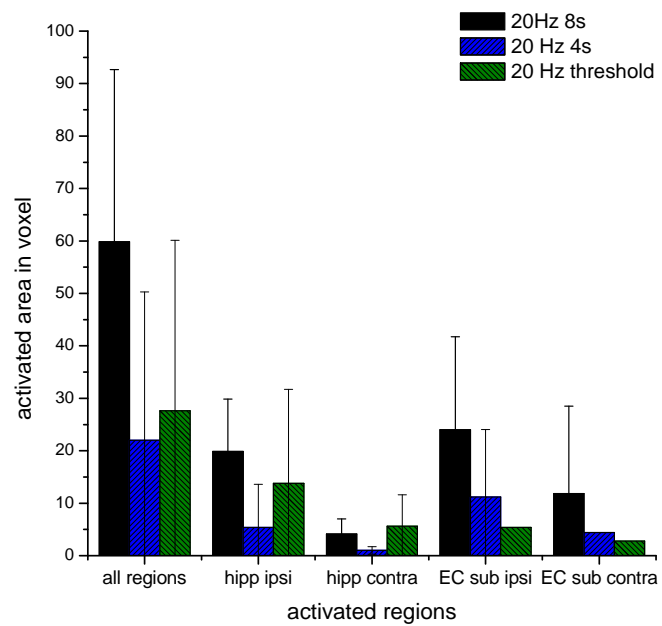
Figure 3.15: **Influence of stimulation parameters on activated area.**

Regions

20 Hz   8 s   50 % PSA max
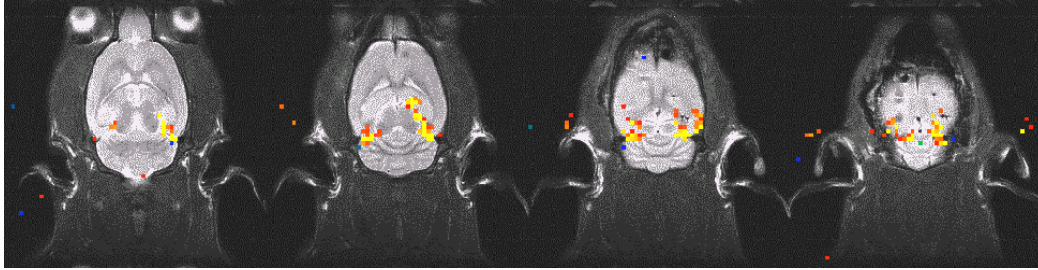
20 Hz   4 s   50 % PSA max
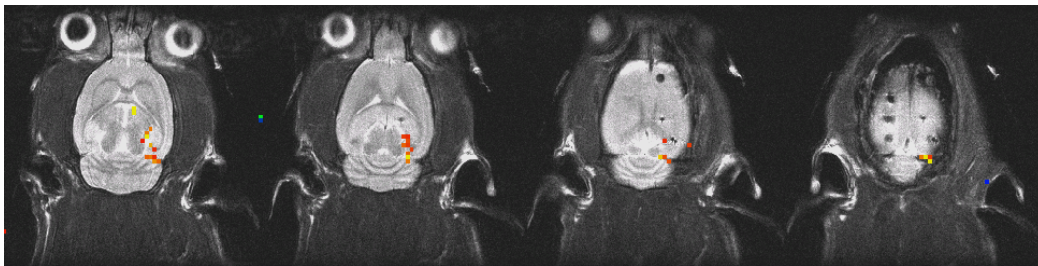
20 Hz   8 s   threshold
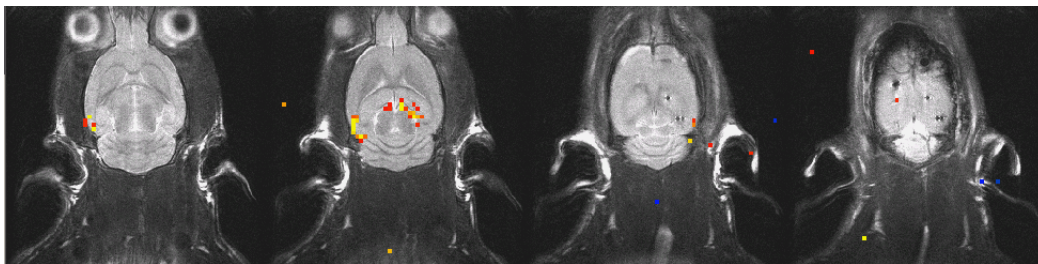
Figure 3.16: **Comparison of activation patterns with modified parameters during 20 Hz stimulation.** Distribution of significant BOLD responses at a significance level of t: $6{\leq}t{\leq}8$ evoked during 7 minutes of low frequency stimulation. Figures display single animals as examples of typical activations.

3.4   Low frequency protocols - Electrophysiology

Changes in neural activity are assumed to be the basis of BOLD generation. In the present experiments the electrophysiological measurements obtained during electrostimulation and generation of BOLD signals were analyzed in two different ways, each giving clues about another process taking place during the recording. To illustrate overall neural activity and to allow an adequate comparison with BOLD development during the experiment, spike amplitudes and latencies of population spikes were evaluated and averaged per train. A second point of interest was the course of electrophysiological signal development during stimulation.

3.4.1   Overall spiking activity

A general observation that could be made at stimulation frequencies above 2.5 Hz was a decreasing level of spiking activity during the experiment. That is, the amount of granule cell firing mirrored in population spike amplitudes decreased from train to train with ongoing stimulation.
During 2.5 Hz stimulation firing only jittered with big deviations around 100%, but no significant changes could be observed.

5 Hz stimulation produced a steady decreasing ØPSA, non regarding whether BOLD responses were produced by this stimulation or not. Pattern of ØPSA decrease curves were almost the same in BOLD positive and BOLD negative data sub sets (see Fig 3.17, 5 Hz).

10 Hz stimulation produced a profound ØPSA drop in the second train after boosting firing to ~120% in the first train. Paralleling, the BOLD signal improvement after train 2, ØPSA recovered from the breakdown, and continued firing on a much lower level compared to initial activity. From 10 Hz on, an oscillating firing pattern could often be observed, i.e., consecutive population spikes alternating rapidly between a low and a high value (for details see part 3.4.2 and Fig 3.20).

For 20 Hz no fundamental spiking breakdown could be observed in the dentate gyrus in train 2 although BOLD signal displayed a very similar pattern to 10 Hz (Fig 3.17). ØPSA took again a strong downward course. That was mainly due to the fact that only few animals responded to electrostimulation by firing during the whole experiment. Though no signal breakdown happened in train 2, other forms of firing impairment emerged in the course of 20 Hz stimulation. Signal dropouts at the end of stimulation trains occurred sometimes, complete firing dropout after two trains could be observed in two animals. This increasing failure in firing with ongoing stimulation was typically and chiefly accounted for the mentioned severely decreasing ØPSA. Oscillation of PSA values was stronger than in 10 Hz experiments, PSA alternated between a maximum value and zero (Fig 3.17, 20 Hz). Omission of actual firing had no detrimental effect on BOLD generation, i.e. BOLD response even increased during the last trains. It should be noted that synaptic activity could still be observed but not quantified even though population spike production failed.

Development of latencies showed a more consistent pattern. Latency increases due to electrostimulation could always be observed with low stimulation frequencies. Latency increased in a jump already during the first train, increasing further during the following trains. That is, population spikes occurred more and more delayed with ongoing stimulation. ØLAT increased with increasing stimulation frequency between 2.5 and 10 Hz. At 2.5 Hz the ØLAT increase by ~10 % was not significant (SD ±12 %). Already 5 Hz stimulation increased ØLAT significantly to a maximum value of 136 ±13 % in train 7. The same could be observed in 10 Hz, ØLAT increased significantly to 153 ±26 % in train 3 and remained on that level (even a slight decrease). ØLAT increase reached maximum at 10 Hz , at 20 Hz ØLAT increased only to 140 ±20 % during seven trains. The spiking delay was even less than at 5 and 10 Hz (not significant).

No correlation could be found between BOLD signal increases during the experiment and overall spiking. BOLD response increased or remained constant while spiking decreased during the experiments. Observations made in single animals even showed that population spike production could lapse entirely without affecting the perpetuation and level of a significant BOLD response (e.g. at 20 Hz).

Increasing population spike latency seemed to be closer related to BOLD generation since only in experiments with significantly increased ØLAT a significant BOLD generation could be observed. A critical point in this argumentation is that ØLAT is also significantly increased in 5 Hz experiments not generating significant BOLD response (see Fig 3.17, 5 Hz).

In summary these outcomes lead to the conclusion that a sufficiently elevated amount of inhibition (LAT) is likely to be related to BOLD production.

2.5 Hz   ØPSA per train   ØLAT per train

5 Hz   ØPSA per train   ØLAT per train

10 Hz   ØPSA per train   ØLAT per train

20 Hz   ØPSA per train   ØLAT per train
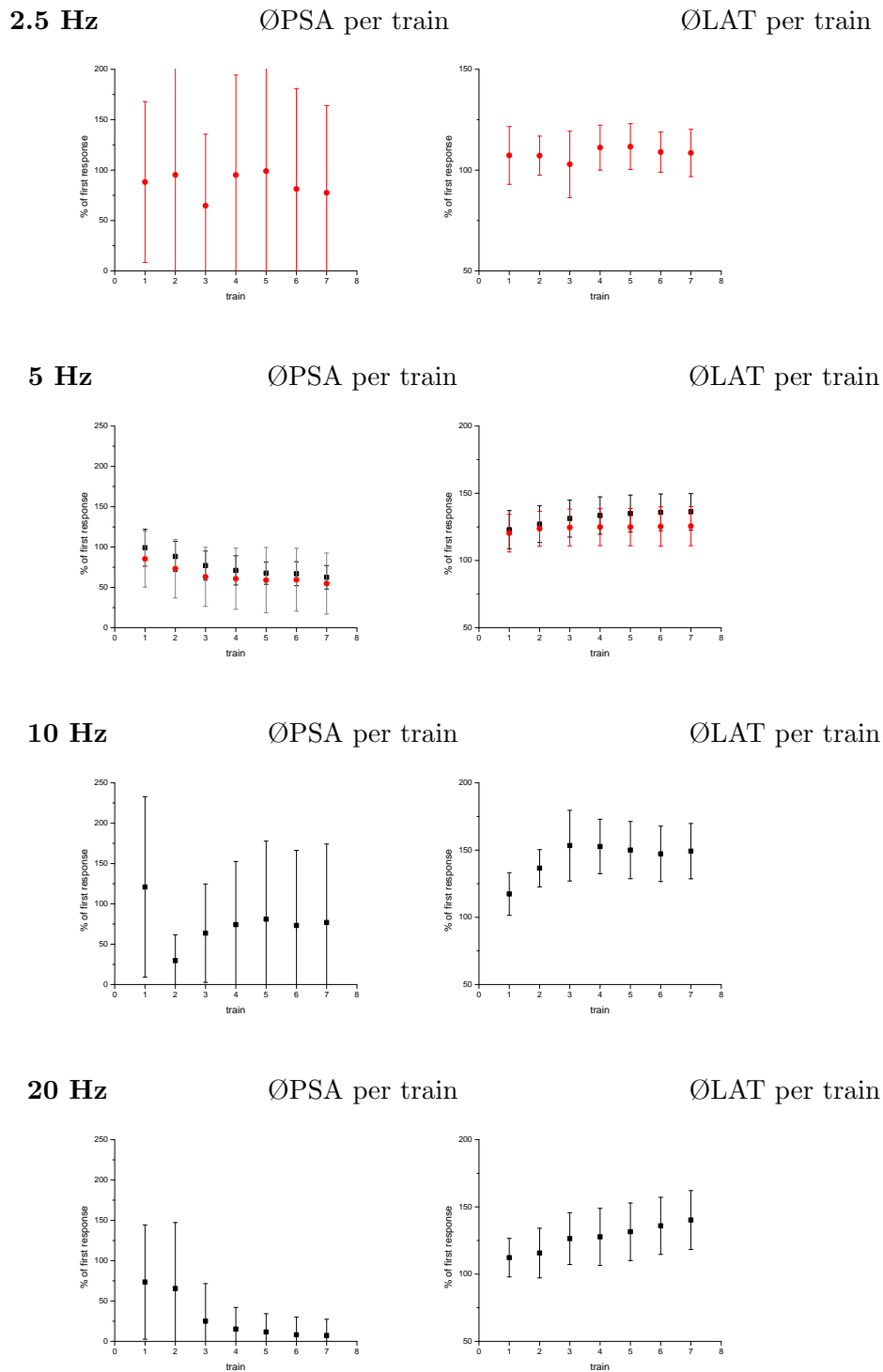
Figure 3.17: **Electrophysiological results: development of overall firing activity during 7 successive stimulation blocks.**
PSA and LAT were averaged for each train, error bars display standard deviation
.

Figure 3.18: **Lat increases in response to low frequency stimulation.**
Left chart: LAT always increases during stimulation with frequencies above 2.5 Hz.
Right chart: LAT increase can also be observed over the duration of a whole experiment.
Frequency-dependent LAT can reach a plateau or increase continuously until the end of
experiment.

3.4.2   Development of spike productions within stimulus trains

Besides the shown comparison of averaged population spikes per train the development of PSAs within stimulation trains formed a point of interest. The first gives information about the overall firing activity, the second illustrates the immediate response to stimulation, i.e., the response pattern to a stimulation train. Response pattern during stimulation could give hints to short term processes that should be considered as well as causes of BOLD generation.

2.5 Hz stimulation produced a slightly decreasing spiking pattern during 8 s of continuous stimulation, and a slight increase in latency of the firing (Fig 3.19, upper row). But for none of these parameters deviation from the start value (first PSA or LAT) was significant. This resulted in the constant level of ØPSA and ØLAT during the experiment (Fig 3.17, 2.5 Hz).

At 5 Hz stimulation two different spiking patterns could be observed (see Figs 1 in Appendix). PSA values could increase during stimulation forming arching patterns (Figs 3.19, middle row). Start values of firing were constant or decreased slightly in each following train in these cases. The another pattern showed a continuous PSA decrease in response to stimulation. Both patterns could be found in BOLD positive and negative groups, none was accompanying a significant BOLD production.
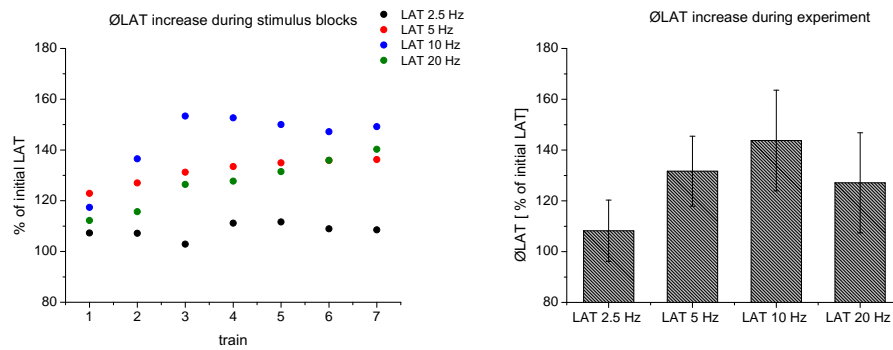LAT always increased during 5 Hz stimulation. There was no perceivable difference in LAT patterns between significant and no BOLD signal groups (Figs 3.19, lower row).

10 Hz stimulation produced ambivalent firing patterns in the course of the experiment. In the first train an initial PSA decrease followed by a sharp increase, forming a V-shaped curve, could always be observed (upper Fig 3.20). The sharp increase of PSA was related to the development of a strong synchronization of firing activity that potentiated spiking (boosted PSA values and shortened LAT) in the end of train 1. This strong synchronization could develop into epilepsy-like activity with additional discharges. Detectable discharges did not always occur. Signal shape changed and PS production usually broke down in or after train 1. After the second train, where signal could drop out entirely or continue on a very low level, spiking showed similar increasing or decreasing arching patterns in response to stimulation as already described for 5 Hz.
Apart from the second half of train 1, were a short phase of potentiation could occur, LAT always increased during 10 Hz stimulation (lower Fig 3.20).
Another common feature of firing during 10 Hz stimulation was oscillation. Successive responses alternated between a high and a low value that could even be zero, resulting in a high standard deviation (Fig 3.20, 10 Hz). Oscillations developed during a stimulation train and often increased in amplitude during stimulation. BOLD generation was independent from this firing pattern.

20 Hz stimulation produced PSA patterns similar to 10 Hz. A real spiking breakdown as observed during 10 Hz stimulation could not be observed during 20 Hz stimulation. Instead firing often dropped out partially within single stimulation trains. A partial drop out could happen in form of an oscillation between zero and a value, or it could be a temporal failure of spike production within a train.

Only in one animal spiking ceased after train 1 without returning for the rest of the experiment. A second animal responded by producing EPSPs but no spikes during the whole experiment. Nevertheless BOLD signals could be observed in both animals.

However, LAT of population spikes developed in an different pattern than LAT in other low frequency experiments. After a short but considerable increase in the beginning of a stimulus train, LAT always decreased during the rest of the stimulation (lower Fig 3.21).

Summary: The observed PSA development within trains is no indicator for significant BOLD signal production. Though response patterns of different stimulation frequencies were rather characteristic, spiking patterns of single animals could never be used to predict the amount of BOLD signal increases or their time courses. No more can an increased LAT guarantee a significant BOLD response.

Although neither response pattern of PSA nor LAT could predict significant BOLD responses or explain their variation, it could yet be observed that significant BOLD responses were always accompanied by a significantly increased LAT during stimulation. The increased LAT points to an increased action of inhibition during that time or, as in the case of 20 Hz stimulation, to more than one interacting process produced by the specific stimulation frequency. For 20 Hz this is a second process, maybe a potentiation, counteracting the arising inhibition during ongoing stimulation.

2.5 Hz   **PSA**   **LAT**

5 Hz   sig BOLD **PSA**   sig BOLD **LAT**

5 Hz   no BOLD **PSA**   no BOLD **LAT**
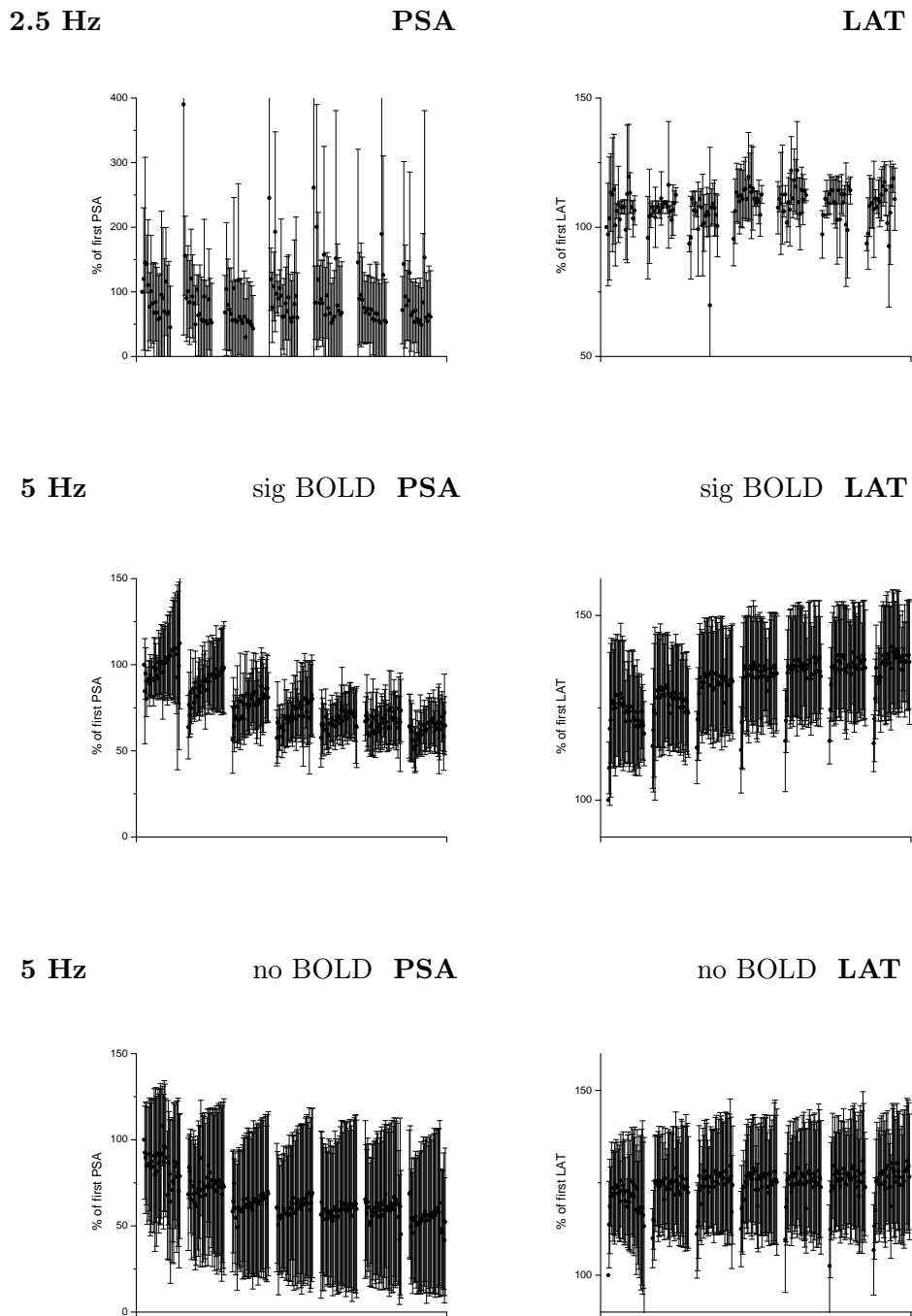
Figure 3.19: **Electrophysiological results: firing activity during stimulation.**
2.5 Hz stimulation tends to produce firing decrease in the course of stimulation (not signif-
icant). 5 and 10 Hz, in contrast, produce augmentation of spike production. LAT always
increases during stimulation.

10 Hz **PSA**
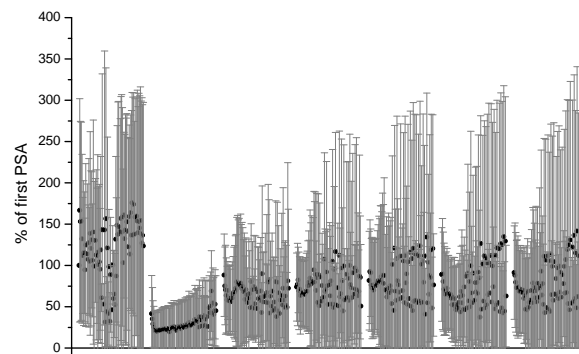
10 Hz **LAT**
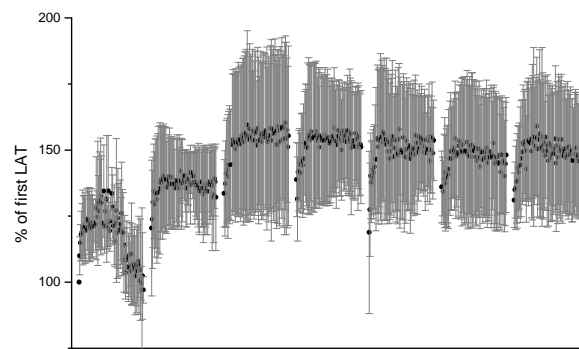
Figure 3.20: **Electrophysiological results: firing activity during stimulation.**
During 10 Hz stimulation PSA augmentation is accompanied by an inhibition canceling out
or interfering with each second response producing a pattern of PSA and LAT oscillation.

20 Hz   **PSA**
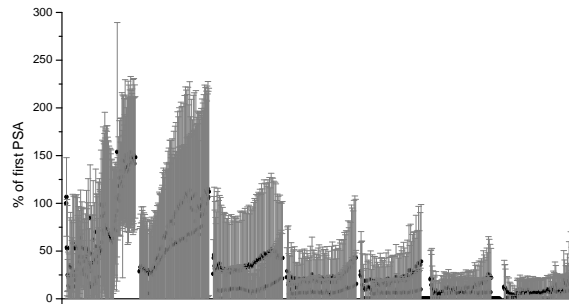
20 Hz   **LAT**
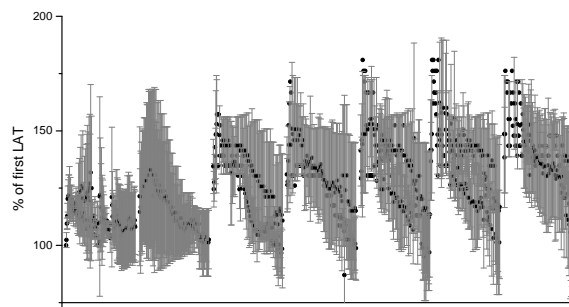
Figure 3.21: **Electrophysiological results: firing activity during stimulation.**
During 20 Hz stimulation PSA augmentation is accompanied by an inhibition canceling out
or interfering with each second response producing a pattern of PSA and LAT oscillation.
Oscillation is even more pronounced that with 10 Hz. Plot displays only average of n = 3
animals, in the rest PSAs dropped during stimulation to zero after the first stimulation
train. Nevertheless EPSPs were observed.

3.5 High frequency protocols - fMRI

Several authors report lower and upper bounds for stimulation frequency ranges generating BOLD responses [81]. In the following experiments high frequency stimulation protocols were applied to test for upper border. To keep the number of delivered stimuli low, continuous low frequency protocols were modified to high frequency burst protocols. Number of stimuli per second remained comparable to low frequency protocols, so duration of stimulus trains was abbreviated (see Methods). Since a longer stimulation had been shown to be adequate, 15 trains were applied instead of seven.

Higher stimulation frequencies turned out to be more suitable for BOLD signal generation than lower. Both, 100 Hz and 200 Hz, always produced significant BOLD responses. BOLD signals increased at least by 2% from the first stimulation train on. No additional discharges appeared on the EEG in response to electrostimulation. Thus no signal collapses occurred as observed in the upper low frequencies. Levels of BOLD signal increase remained fairly constant during the stimulation term of 15 min/15 trains in both frequencies. 100 and 200 Hz produced a baseline shift following the first stimulation train. This decrease remained until the end of the experiment and was more pronounced in 200 Hz (see Figs 3.22 and 3.23, and middle and lower Figs 3.33, in part 3.7 Baseline shift).

100 Hz (20)   ipsilateral hippocampus (n=6)
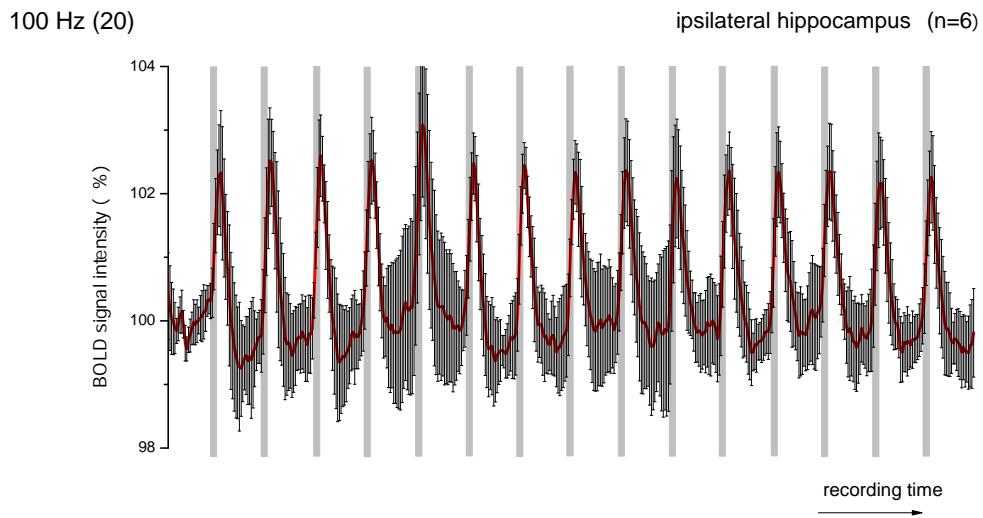
Figure 3.22: **BOLD signal time course in response to 100 Hz electrostimulation** for 15 minutes. Grey bars mark stimulation time of 8 s or 4 frames. Constant BOLD signal production during entire experiment, no signal breakdowns. Baseline shift after train 1. Error bars mark standard deviation.

200 Hz (20)   ipsilateral hippocampus (n=6)
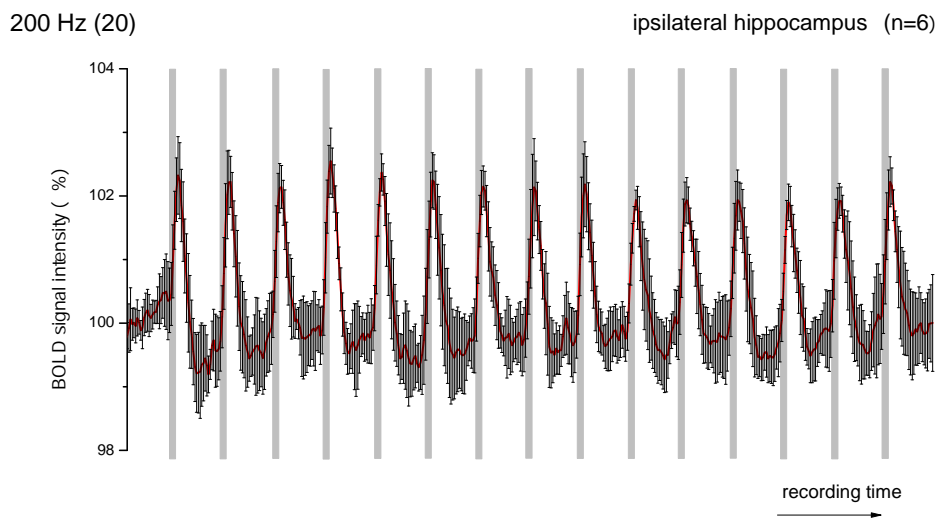
Figure 3.23: **BOLD signal time course in response to 200 Hz electrostimulation** for 15 minutes. Grey bars mark stimulation time of 8 s or 4 frames. Constant BOLD signal production during entire experiment, no signal breakdowns. Baseline shift after train 1. Error bars mark standard deviation.

Reduction of the number of delivered stimuli per second from 20 to 10 per burst did not change the amount of BOLD signal increase. 100 Hz (10) produced an increase by 2% as 100 Hz (20) did (compare Figs 3.24 and 3.22), but BOLD signal time courses were noisier than in 100 Hz (20) data. However, activated area in the ipsilateral dorsal hippcampus differed clearly: 100 Hz (20) activated more voxel than 100 Hz (10) (Mann-Whitney test, $p = 0.018$, $z = -2.373$).

When the same amount of delivered stimuli per second was set as comparison standard, 10 Hz continuous stimulation activated more voxel than 100 Hz (10) (see right Fig 3.26). Yet this difference missed significance narrowly: Mann-Whitney test, $p = 0.053$, $z = -1.931$. But the same amount of stimuli delivered with 50 Hz activated a significantly larger area in the ipsilateral dorsal hippocampus (Mann-Whitney test, $p = 0.012$, $z = -2.503$). It was rather comparable with outcomes produced by stimulation protocols applying 20 stimuli (compare columns in right and left Fig 3.26).

The charts in Fig 3.26 show that activated area might reach a maximum between 20 and 100 Hz, probably around 50 Hz stimulation (Fig 3.26 right side). At 200 Hz extent of activation is already decreasing .

100 Hz (10)   ipsilateral hippocampus (n=6)

Figure 3.24: **BOLD signal time course in response to 100 Hz electrostimulation**
for 15 minutes 10 stimuli per burst. Grey bars mark stimulation time of 8 s or 4 frames.
Constant BOLD signal production during entire experiment, no signal breakdowns. Base-
line shift not perceivable. Error bars mark standard deviation.

50 Hz (10)   ipsilateral hippocampus   (n=7)
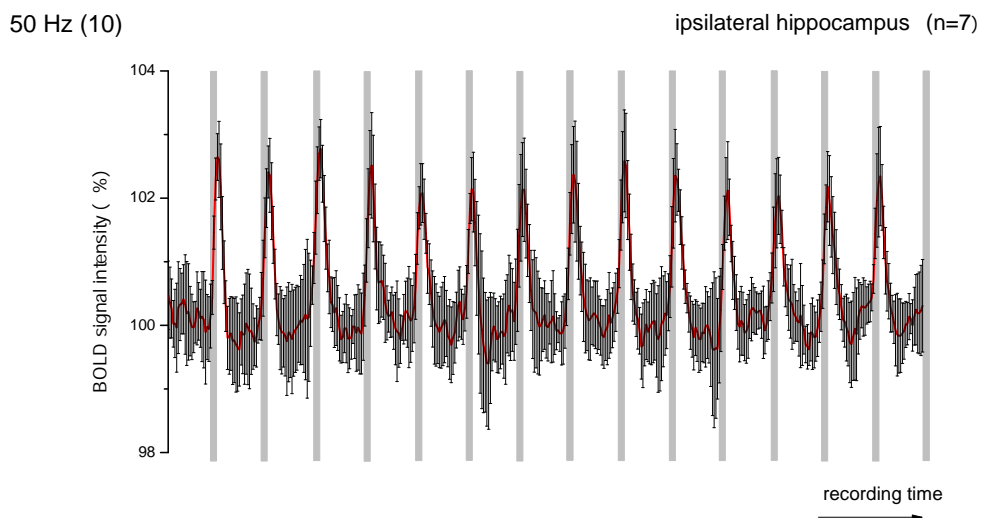
Figure 3.25: **BOLD signal time course in response to 50 Hz electrostimulation**
for 14 minutes 10 stimuli per burst. Grey bars mark stimulation time of 8 s or 4 frames.
Constant BOLD signal production during entire experiment, no signal breakdowns. Base-
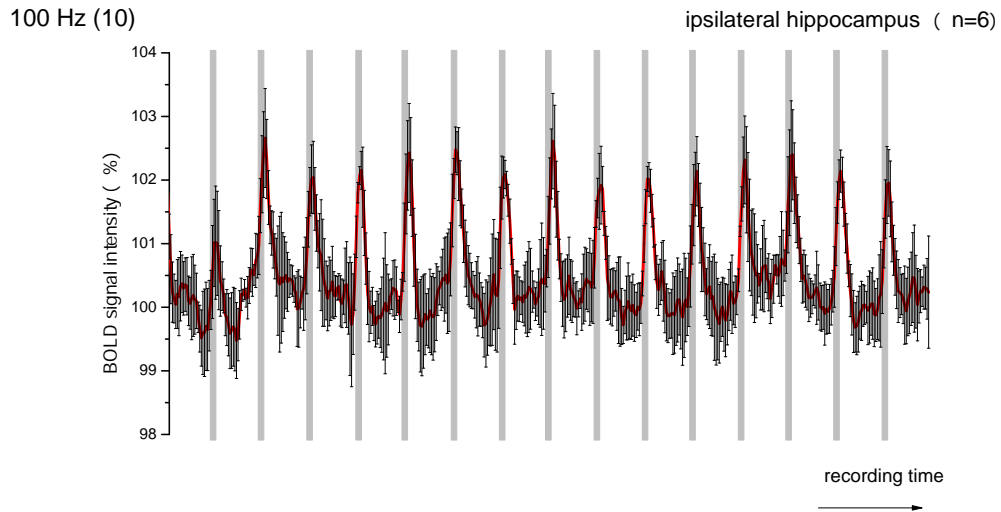line shift not perceivable. Error bars mark standard deviation.
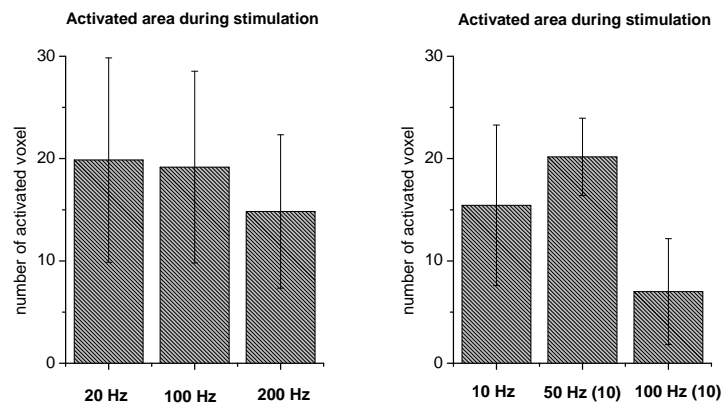
Figure 3.26: **Effect of variation of applied frequency and stimulus number on activated area in ipsilateral dorsal hippocampus.**
Right chart: High frequency protocols applying 20 stimuli per s. Left column displays 20 Hz continuous stimulation results for comparison.
Left chart: High frequency protocols applying 10 stimuli per s. Left column displays 10 Hz continuous stimulation results for comparison.
For a proper comparison between short (7 blocks) and long (15 blocks) protocols only first seven trains were considered for analysis of activation at 50, 100 and 200 Hz. Both plots show that spread of activated area was both frequency and stimulus number dependent. The same amount of stimuli per second produced different spatial spread of BOLD signal.

The dependency between activated area and stimulation frequency could not be evaluated for low frequency stimulation because a different amount of stimuli was applied in each of these experiments. But these data could be used to examine the correlation between the number of applied stimuli during the first 7 trains of an experiment and activated area in the dorsal ipsilateral hippocampus during that time. Fig 3.27 illustrates that number of applied stimuli also influenced spread of activation. But it also indicates, that it was not the only crucial factor. At stimulation frequencies between 2.5 and 20 Hz activated area increased non-linearly with the number of applied stimuli, forming a saturation curve. Higher frequencies triggered amounts of activation that did not prolong or even fit into this curve. Stimulation with 100 Hz and 10 stimuli per s activated a smaller area than the same stimulus amount delivered with 10 Hz. 20 stimuli per s delivered with 20, 100 or 200 Hz each activated different areas. This points to a dependence of activated area from frequency as well as from number of applied stimuli, and maybe also from the pattern of stimulation (burst or continuous).
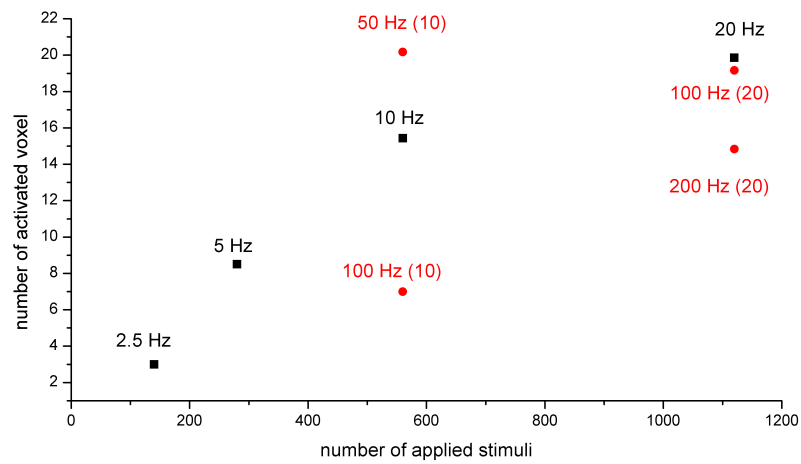
Figure 3.27: **Correlation of activated area in ipsilateral dorsal hippocampus and amount of delivered stimuli during the first 7 trains.**
Activated area depends only partially on the number of applied stimuli. Within low frequencies increase of activated area seems mainly to display increased stimulus number. That frequency itself matters too, can be concluded from the non-linear increase of the curve within the low frequencies pointing to additional frequency-dependent processes. This finding is supported by the data yielded at different stimulation frequencies applying the same amount of stimuli.
For a proper comparison activated area was determined for high frequency experiments by analyzing the first 7 trains only.

3.5.1 Activation patterns

100 Hz stimulation produced BOLD activation in the ipsilateral hippocampus and in the ipsi- and contralateral EC/Sub region. Sometimes adjacent cortex regions as perirhinal and sensory cortices could be activated. A striking feature was a total omission of activation in the contralateral hippocampus.
Ipsi- and contralateral EC/Sub region were comparably activated in 100 Hz experiments.

200 Hz resulted in a variety of BOLD activation patterns. A typical activation comprised ipsilateral hippocampus and the ipsi- and contralateral EC/ Sub region. In 3 of 6 animals activation of other regions could be observed as well (lower Fig 3.28). They appeared not as consistently as the first mentioned but they could be observed too often to be just artefacts. Distribution of these occasional activations was variable and could be found in the striatum, cingulate, medial orbital, pre- and infralimbic cortex.

Activated regions

100 Hz
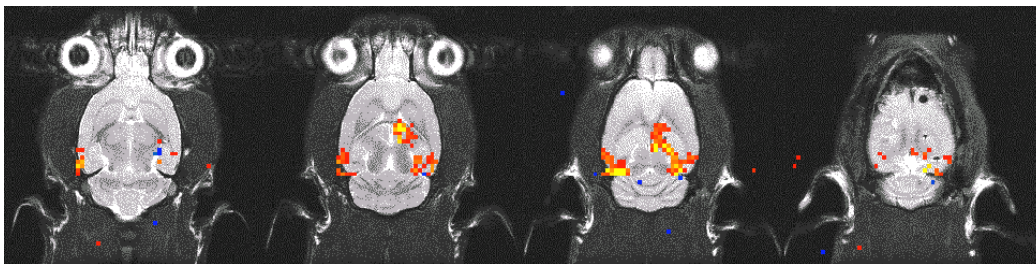
200 Hz
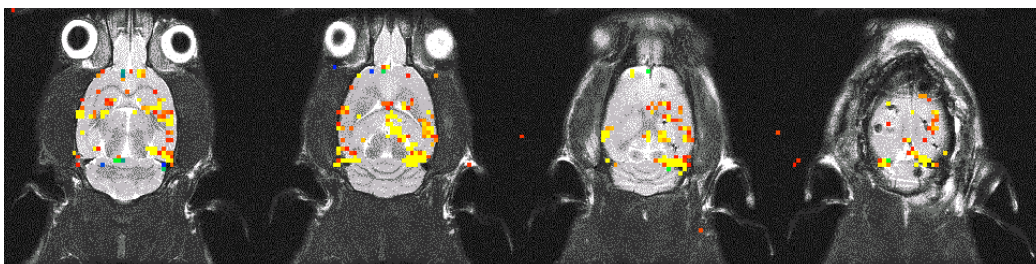
Figure 3.28: **Activation patterns during high frequency stimulation for 15 minutes.** Distribution of significant BOLD responses at a significance level of t: $6 \leq t \leq 8$ evoked during 7 minutes of high frequency stimulation. Figures display single animals as examples of typical activations. 200 Hz activation displays an animal with typical activations of hippocampus and bilateral EC/Sub region, plus activations that could be observed in half of the animals.

3.5.2 Comparison of regional BOLD time courses

In 100 and 200 Hz experiments no clear difference in BOLD signal time courses could be found between hippocampus, ipsi- and contralateral EC/Sub regions. Activation of EC/Sub region was only by trend stronger than activation of ipsilateral hippocampus. Level of activations remained on the same level until the end of experiment. Contralateral EC activation was usually below ipsilateral.
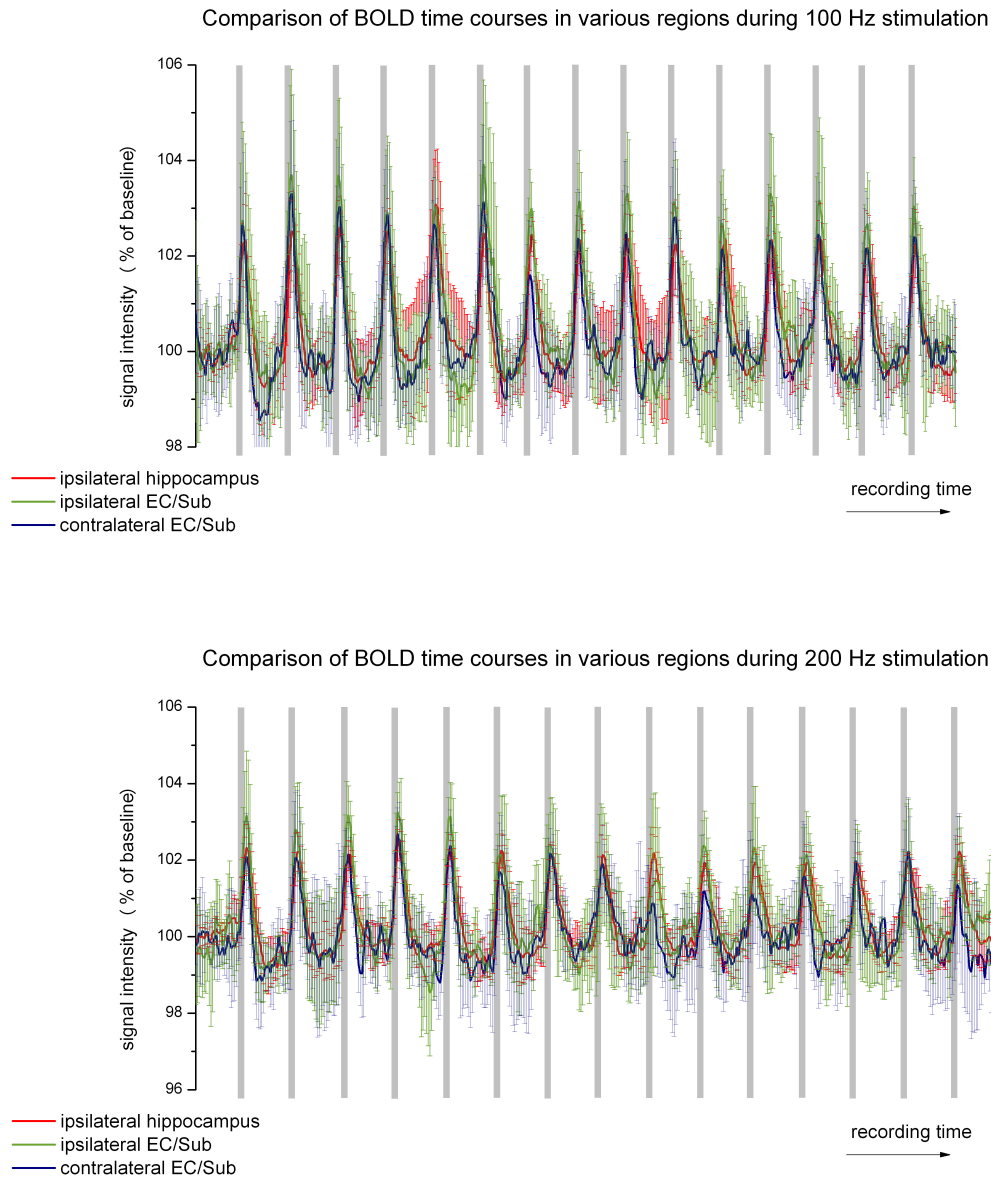
Figure 3.29: **Regional BOLD signal time courses in response to 100 and 200 Hz.** 100 and 200 Hz stimulation was capable to produce significant BOLD signals in in the contralateral EC/ Sub region but not dorsal hippocampus. BOLD signal time courses were comparable in all activated regions.

3.6 High frequency protocols - Electrophysiology

3.6.1 Overall spiking activity

As already done for low frequency protocols electrophysiological result of high frequency experiments were analysed and evaluated for overall spiking activity and response pattern during electrostimulation.

To meet the different response pattern to high frequency stimulation only the first population spikes of a burst were evaluated. In a burst stimulation usually only the first stimulus pulse was capable to evoke a population spike (lower trace in Fig 3.5). All the following responses to stimuli were blocked. So just the first response was used for evaluation.

Firing in response to 200 Hz stimulation could not be quantified reliably because interpulse interval was here 5 ms and population spike latency sometimes increased to the same amount. That means, preceding responses were interrupted and cut off by the next stimulus pulse artefact.

For 100 Hz overall spiking increased slightly during the first four trains, having a maximum in train 2, and decreased continuously from there on. In train 6 level of firing dropped below 100% and stopped decrease at ∼80% and remaining on that level until the end of the experiment. ØLAT decreased during the first four trains to ∼87% and remained on that level for the following 11 trains (Fig 3.30).

100 Hz   ØPSA per train

100 Hz   ØLAT per train
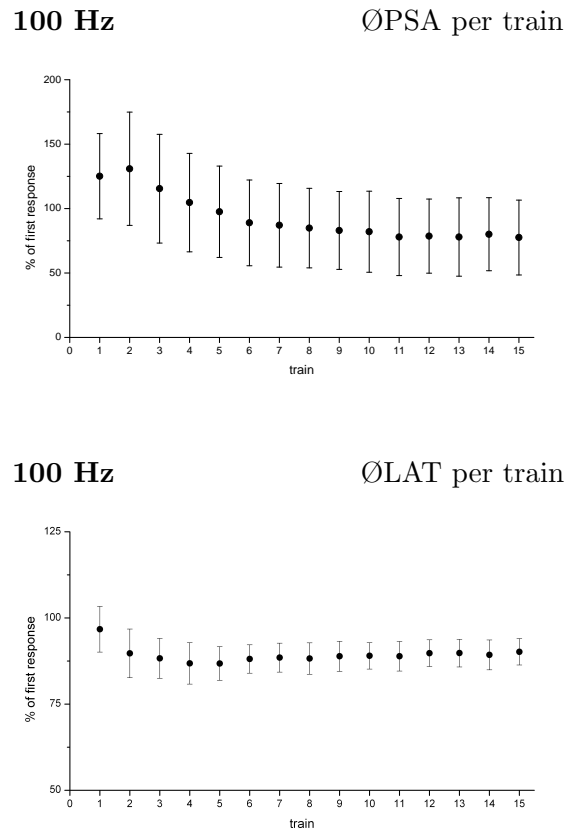
Figure 3.30: **Electrophysiological results: development of overall firing activity during 15 successive 100 Hz burst stimulation blocks.** Overall spiking is increased during the first third, LAT displayed potentiation until the end of experiment. PSA and LAT were averaged for each train, error bars display standard deviation.

3.6.2 Development of spike productions within stimulus trains

First population spikes in successive 100 Hz bursts showed in general augmentation during stimulation. Already the first train produced a short-term potentiation of the PSA. PSA increases of the following train started from an elevated level, though continuously decreasing during the rest of the experiment.

Latency was potentiated during the first two trains, i.e., LAT of population spikes decreased during stimulation. The entire response pattern of LAT seemed to display a basically potentiated LAT, offset by an inhibition that increases LAT during later stimualtion trains.
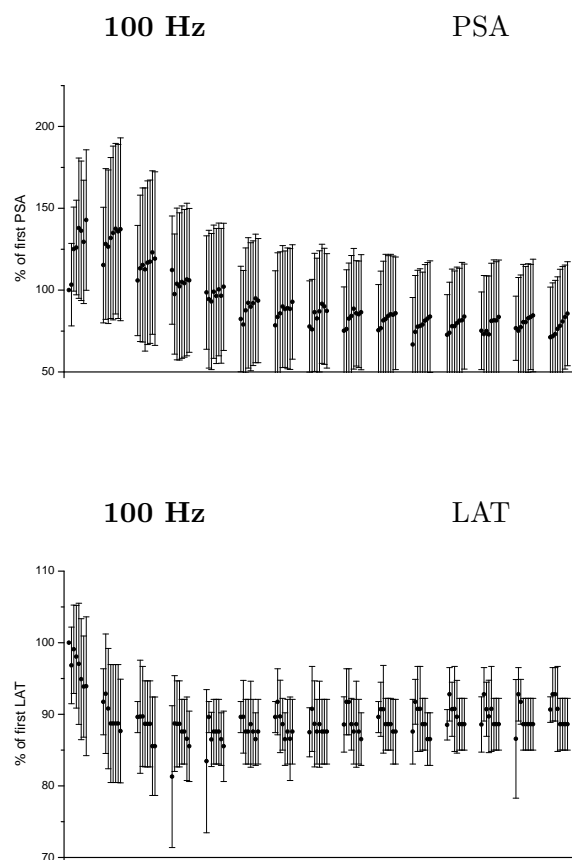
Figure 3.31: Electrophysiological results: firing activity during 100 Hz stimulation.

In spite of a decreasing overall firing, 100 Hz stimulation produced PSA augmentation in the course of inividual stimulation trains. LAT was always potentiated after the first train but showed ambivalent pattern during stimulation. Probably due to an inhibition produced during stimulation.

3.7   BOLD baseline shift

As already mentioned a baseline shift could be observed in the BOLD signal time course of the ipsilateral dorsal hippocampus after the first stimulation train in most experiments using frequencies higher than 10 Hz. In the first, short 10 Hz experiments this became not as clearly noticeable as in later (long lasting) 10 Hz experiments.
In the first 10 Hz experiments significant baseline drop could only be observed constantly in two of seven animals or in 31% of all trains ($p \leq 0.05$, GLM, t-test) (upper Fig 3.32). Maximal drop was about 1%. In later (long) 10 Hz experiments this shift became clearer: all animals except one displayed a significant baseline shift in response to the trains following the first stimulus train ($p \leq 0.01$, GLM, t-test) (upper Fig 3.33). Individual baseline drops were between 0.5 and 3.5%, compared to intitial baseline. Averaged over all trains decrease was between 0.4 and 1.3%.

20 Hz stimulation produced a significant baseline shift in the most animals (5 of 6). 70% of all trains fell below baseline after the first train ($p \leq 0.01$, GLM, t-test). Individual baselines seemed to decline more and more in the course of the experiment (lower Fig 3.32).

BOLD baseline shifts related to high frequency stimulation were moderate compared with low frequency stimulation. After the first 100 Hz stimulation train a significant baseline shift could be observed in only 3 of 6 animals or 53% of the individual trains ($p \leq 0.01$, GLM, t-test). Decrease was around 0.5% (middle Fig 3.33).

200 Hz produced a similar pattern and a stronger baseline shift: clear baseline drops could be observed during the whole experiment in 4 of 6 animals, in the remaining two in most trains. A significant shift could be observed in 88% of individual trains following train 1 ($p \leq 0.01$, GLM, t-test). Baseline drop was moderate around 0.5%, maximally 1% (lower Fig 3.33).

BOLD baseline shifts could also be observed in the BOLD signal time courses of other regions than the ipsilateral hippocampus, but the probability of a significant shift was lower there (see Fig 3.34).

10 Hz 7 min
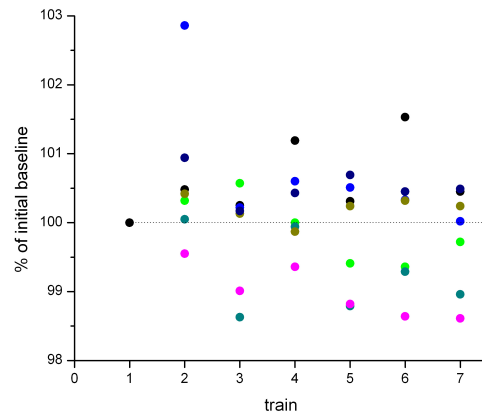
20 Hz 7 min
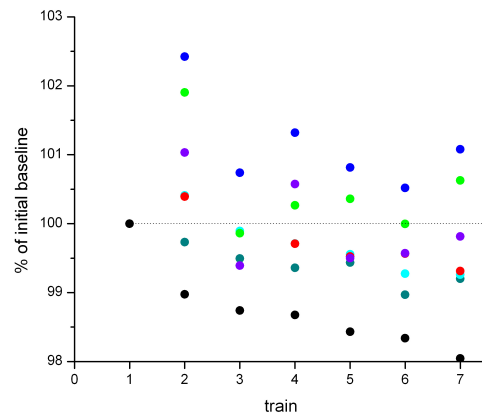
Figure 3.32: **Comparison of averaged individual baselines (train 2-7) with initial baseline (train 1) after 10 and 20 Hz stimulation.** Colors represent $n_{1\,0\text{Hz}} = 7$ and $n_{2\,0\text{Hz}} = 6$ animals. Each point represents the average of the baseline section preceding the respective train. Error bars are not shown in favour of a clear display of the data points. But test results for deviation from initial baseline are discussed in the text.

10 Hz 15 min

100 Hz 15 min

200 Hz 15 min
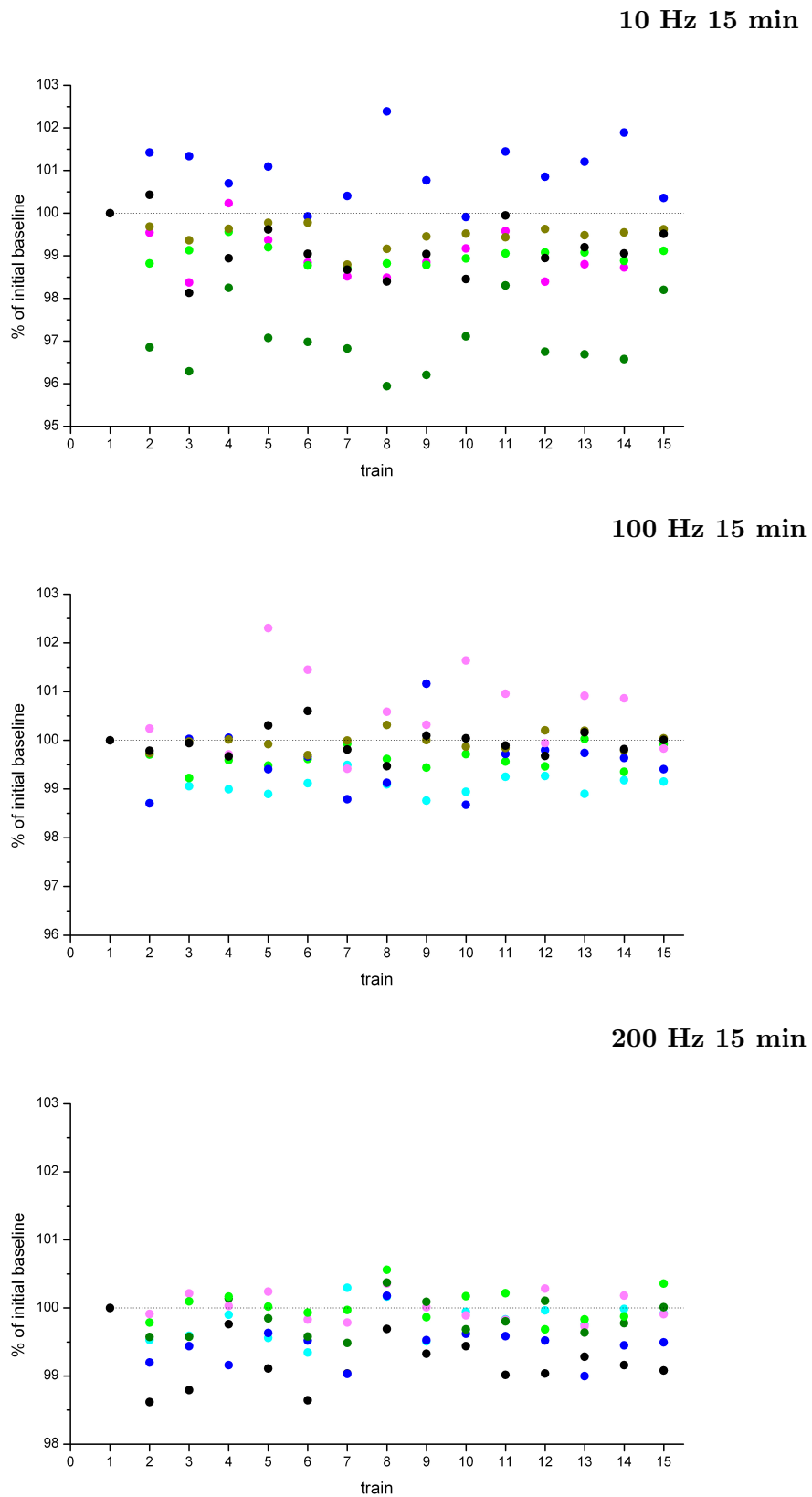
Figure 3.33: **Comparison of averaged individual baselines (train 2-15) with initial baseline (train 1) after 10, 100 and 200 Hz stimulation (15 trains).** Colors always represent n = 6 animals. Each point represents the average of the baseline section preceding the respective train. Error bars are not shown in favour of a clear display of the data points. But test results for deviation from initial baseline are discussed in the text.
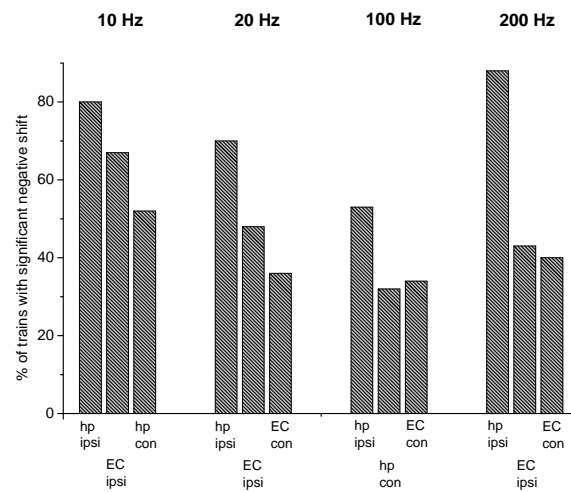
Figure 3.34: **Probability of a significant BOLD baseline shift in various regions**
hp ipsi - ipsilateral dorsal hippocampus, hp con - contralateral dorsal hippocampus, EC
ipsi - ipsilateral EC/Sub region, EC con - contralateral EC/Sub region

3.8   Control I: Anaesthetized animals

In the first control part BOLD generating protocols were examined for longer lasting effects. Since the present stimulation protocols resembled protocols evoking plasticity changes it was necessary to test for plasticity effects of the applied protocols. Cellular processes resulting in longer lasting plasticity changes should as well been taken into account to play a role in BOLD generation as formerly noted short term processes.
Not least, anaesthetized controls should also provide material for a comparison with unanaesthetized controls and allow a determination of the influence of ISO anaesthetization on electrophysiological signal production.

Since control experiments where conducted to complement former fMRI experiments it was checked at first if at least firing during stimulation was comparable in both sets of experiments. There should be no difference, since control experiments where conducted under exactly the same conditions as fMRI experiments, except from recording controls without putting the animal into the scanner.
The electrophysiological parameters PSA and LAT showed similar response patterns during fMRI and ISO control experiments (2.5, 5, 10, 100 Hz). Thus it would be justified to assume that the effect of stimulation was the same during both treatments. Only the variance (homoscedasticity) could differ between fMRI and control experiments.

3.8.1   Baseline changes in consequence to electrostimulation (ISO)

An observation that could very often been made in anaesthetized animals was the tendency of PSA and LAT to increase during the first half hour of baseline recordings (see Fig 3.37, 2.5 Hz or 3.38, 5 Hz), certainly as a result of anaesthetization and body temperature decrease. It is known from experiments on behaving rats that body temperature changes with activity, resulting in changed electrophysiological parameters [8]. Body temperature of animals dropped in the course of the present experiments in spite of heating and showed frequently increasing PSA and LAT, at least during the first 30 min of anaesthetization, as animals reported by Andersen & Moser. The presumably temperature dependent trend of signal development was interrupted and changed by the most electrostimulation protocols.

A control experiment recording electrophysiological signal development over three hours without being interrupted by an electrostimulation protocol should show the effect of anaesthetization alone. Of all experiments these controls did not display the mentioned PSA increase during the baseline recording of 30 min, - only in one of five animals significant signal change could be observed (Fig 3.36). But as mentioned above, this effect could not be observed throughout. It became obvious during the baseline recordings for 2.5, 5 and 100 Hz controls (Figs 3.37, 3.38 or 3.40).
A significant PSA decrease became apparent in almost all animals during the last two hours of recording (four of five animals, $p \leq 0.05$, GLM, t-test). LAT increased during the whole recording time but differed significantly from baseline values only in one of five animals. It can be concluded from these control experiments that the
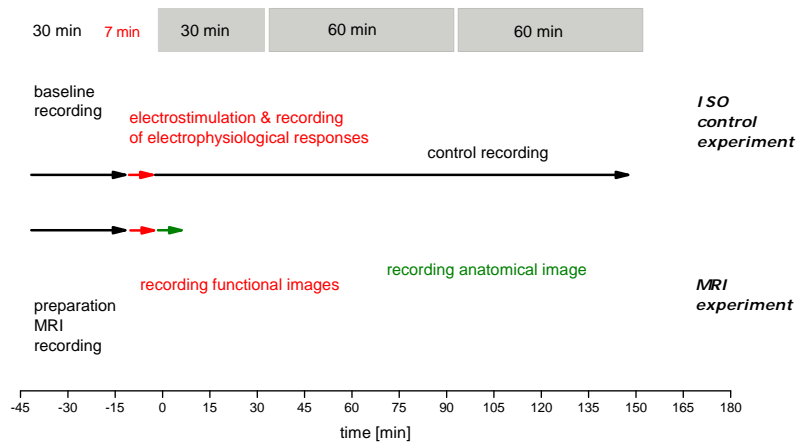
Figure 3.35: **Comparison of MRI experiment timing vs ISO control timing.** Duration of an MRI experiments is between 45 and 60 min. During this time usually no anaesthetization effect impairs electrophysiological signal production

electrophysiological signal degrades during the course of the test pulse recording after one or two hours of anaesthetization, though not in all animals. During the first two hours of anaesthetization signal production occurs rather constant, after that its unreliability increases. This observation should be always taken into account in interpretations of all anaesthetization controls.

ISO control without electrostimulation
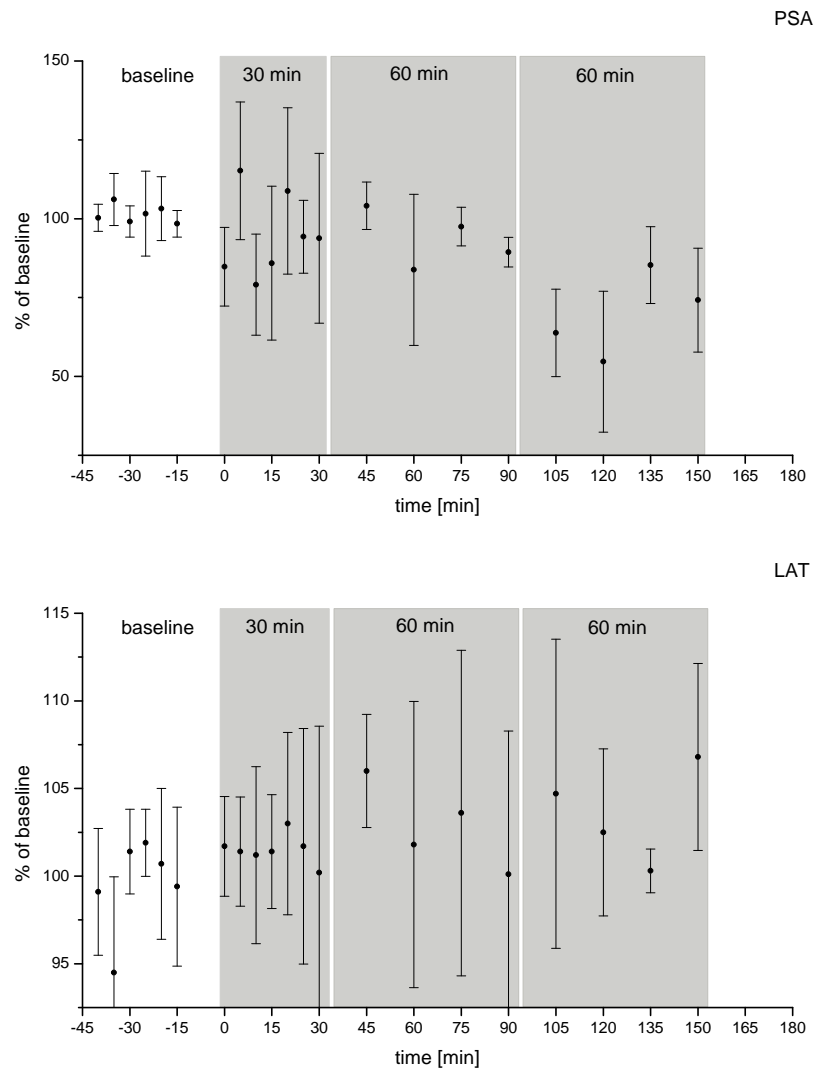
Figure 3.36: **Control for anaesthetization effect alone.** Electrophysiological signal development (PSA, LAT) during baseline recording (white block) and control baseline recording (grey blocks). Responses to single stimulus pulses. n = 5

2.5 Hz electrostimulation produced no consistent long term changes in signal production in the dentate gyrus. One animal of five showed a significant PSA/LAT increase, but that was simply a prolongation of a trend that already developed during the baseline recording. Another animal showed a significant PSA decrease during the first half hour following stimulation. This was probably a signal degradation of the sort that could already be observed during control experiments without electrostimulation.

Electrostimulation seemed to result in a slight change of signal fidelity, i.e., difference in variance, but that could not be proved significant (Levines test)(Fig 3.37).

During 2.5 Hz trains stimulation produced response patterns with heavily fluctuating amplitudes. General pattern of signal development during stimulation was a decreasing spike production and latency increase at the same time. Latency always increased during stimulation but first latency value of every following train started from a level below the end value of the preceding.

The level of PSA and LAT changed significantly from baseline values during stimulation. PSA fell in three animals significantly below baseline and increased in two clearly above baseline ($p \leq 0.05$, GLM, t-test). LAT increased during stimulation in 82% of the trains significantly ($p \leq 0.01$, GLM, t-test).

2.5 Hz ISO

Figure 3.37: **Response pattern during baseline and control recording** (white background) **and 2.5 Hz stimulation** (grey background). **Upper and middle row:** responses averaged for seconds. **Lower row:** responses averaged for trains. n = 5

5 Hz electrostimulation produced a weak but significant firing depression for the first half hour of control baseline recording in three of five animals (p $\leq$ 0.01, GLM, one-side t-test). PSAs decreased to 60-90% and LAT increased to $\sim$104% that is by $\sim$0.2 ms in the first half hour following stimulation. LAT returned to baseline values until the end of experiments. Depression of spike amplitudes remained until the end of the experiment.

Although signal depression was rather obvious after 5 Hz stimulation (see Figs 3.38) significant differences between baseline and control recordings could not always be proved for individual animals because of the low number of compared points (baseline n=6, control n=6), where single deviant data points could spoil the test outcome. However, a longer baseline recording was not possible, since ISO started impairing signal production with longlasting anaesthetization. Hence control experiments had to be kept short under ISO anaesthetization.

The level of PSA production during stimulation decreased stronger during 5 Hz stimulation than during 2.5 Hz (PSA Figs 3.38 and Fig 3.41). LAT deviated during stimulation always significantly from baseline (p $\leq$ 0.01, GLM, one-side t-test). LAT increased in average to 130% of baseline values (LAT Figs 3.38).

As already mentioned in fMRI experiments PSA increase patterns during stimulation could only be observed in a part of animals. The rest showed aberrant patterns. LAT increase patterns differed slightly too. In a part of animals LAT increased constantly during the whole train until stimulation was terminated. In the other part LAT increase turned in the middle of the train to decrease (reflecting a change of inhibition).

5 Hz ISO

Figure 3.38: **Response pattern during baseline and control recording** (white background) **and 5 Hz stimulation** (grey background). **Upper and middle row:** responses averaged for seconds. **Lower row:** responses averaged for trains. n = 5

10 Hz electrostimulation caused a strong and significant depression in firing in four of five animals for the first half hour of control baseline, in several cases even reduced to zero (PSA and LAT: $p \leq 0.01$, GLM, one-side t-test).

Typical area dentate-signal shape was changed too. Besides occurring much delayed, responses to test pulses occurred on the right, falling, instead on the left flank of the area dentata-signal. PSA decreased to 0-70%, LAT increased to 115-160%, that is by about one ms, in response to stimulation.

LAT and PSA depression remained until the end of the experiment (PSA and LAT: $p \leq 0.05$, GLM, one-side t-test) but a beginning recovery to baseline values could be observed within this period (see Fig 3.39).

The common response pattern during 10 Hz stimulation was a V-shaped pattern in the first stimulation train produced by a PSA decrease in the first half followed by a sharp increase in the second half of the train. The sharp increase was produced by population spikes potentiated by the developing synchronization of firing in the stimulated tissue that could develop into additional epilepsy-like discharges. Signal production often started falling apart already in the course of this first train and collapsed in the second (to zero in several cases). After the signal breakdown PSA levels were strongly decreased in train 2, ØLAT was highly elevated at that time. Within stimulation trains LAT was constantly increased forming typical arching pattern. Stimulation responses oscillated typically, especially in the second half of stimulation trains. PSA levels dropped stronger than during 5 Hz stimulation (Fig 3.41), in three animals ØPSA was significantly below baseline. ØLAT increased to train averages up to 150% (PSA and LAT: $p \leq 0.01$, GLM, one-side t-test).
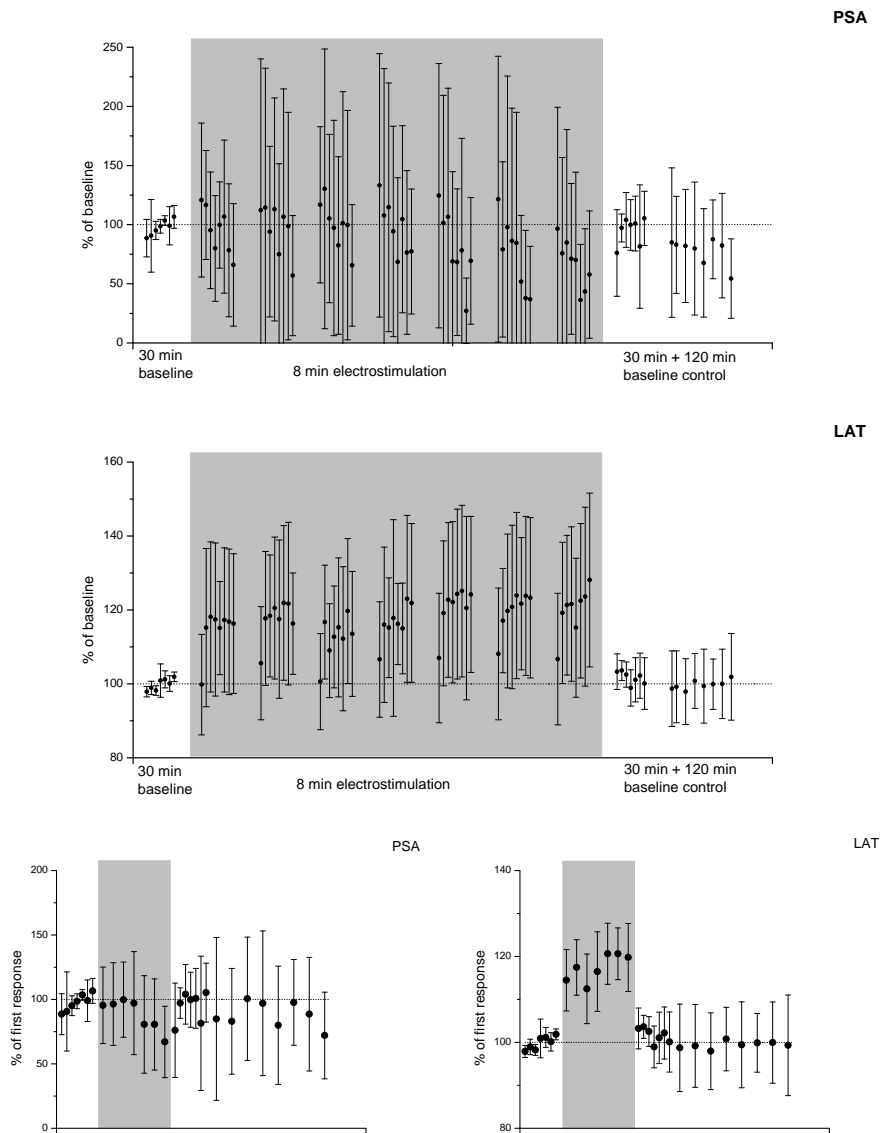
10 Hz ISO

Figure 3.39: **Response pattern during baseline and control recording** (white background) **and 10 Hz stimulation** (grey background). **Upper and middle row:** responses averaged for seconds. **Lower row:** responses averaged for trains. n = 5

While stimulation with low frequencies often caused clear firing depression, **100 Hz electrostimulation** produced an ambivalent signal change. Amplitudes of population spikes clearly decreased during control recordings in five of six animals ($p \leq 0.01$, GLM, one-side t-test). At the same time latency was potentiated, i.e. decreased in four of six animals ($p \leq 0.01$, GLM, one-side t-test). That is, population spikes were depressed, but occurred more rapidly after electrostimulation, in average by 0.5 ms earlier.

Latency and PSAs remained decreased until the end of the control baseline recording time (PSA: $p \leq 0.01$, LAT: $p \leq 0.05$, GLM, one-side t-test).

During 100 Hz stimulation two overlaying processes could be observed: ØPSA decreased in the course of the 15 minutes electrostimulation after being boosted to $\sim$160% in train 1 (PSA Figs 3.40). At the same time a clear patterns of PSA short term potentiation could be observed in response to the stimulation trains (upper Fig 3.40).

In the first stimulation train PSA augmentation produced within trains was strong enough to push the whole train average above baseline. The elevated PSA level decreased then continuously from train to train and dropped below baseline in the course of stimulation ($p \leq 0.05$, GLM, one-side t-test). PSA values remained during the following control baselines on this strongly depressed level. Potentiation within trains was strongest in the first train (steepest rise).

ØLAT decreased in most animals during the first two trains significantly below baseline ($p \leq 0.01$, GLM, one-side t-test). On this decreased, potentiated LAT level a further, inhibitory process could be observed. Each first burst in a train of 8 increased the latency of the following spikes (middle Fig 3.40). This happened probably in consequence to the augmented PSA production (more inhibition produced with more excitation). The overlaying processes produced LAT patterns during stimulation that were not as clear and predictable as in the former, low frequency experiments (2.5 Hz -10 Hz).

After stimulation termination, LAT of control baselines remained on a decreased level and even dropped below to $\sim$90%.
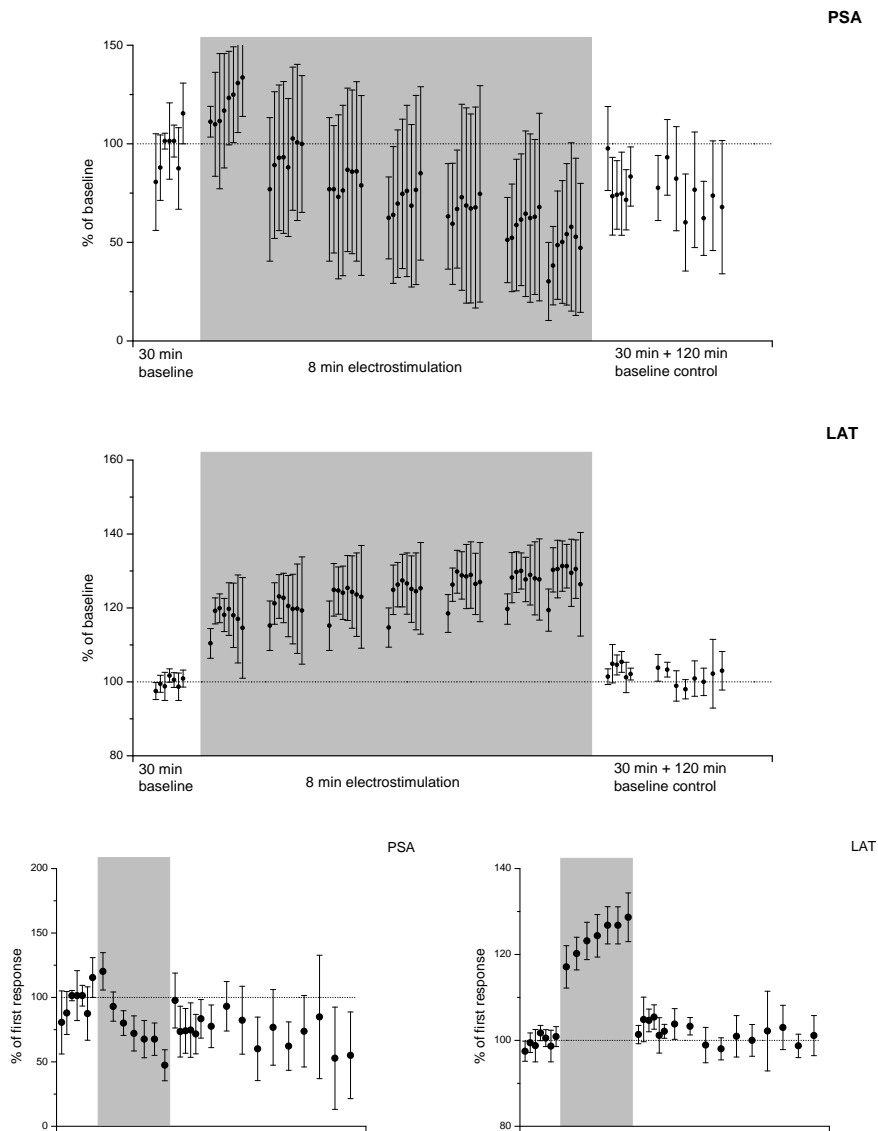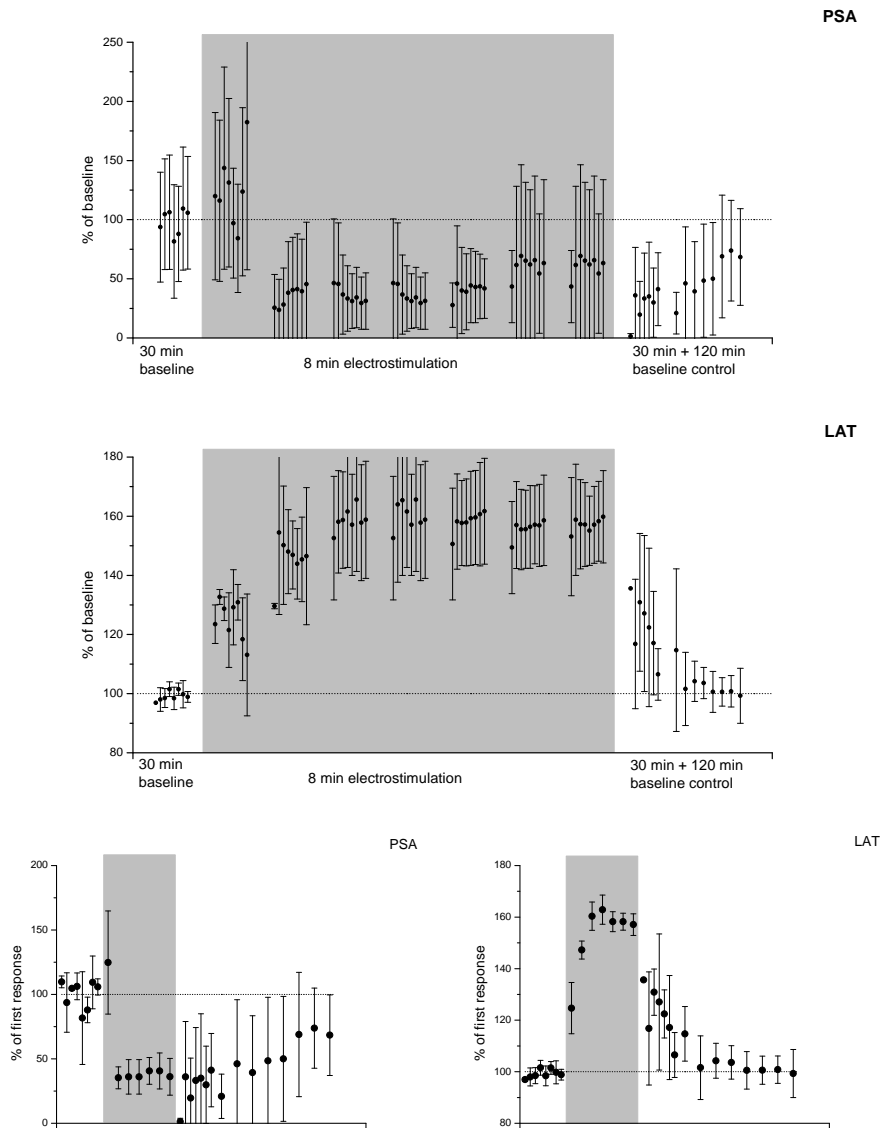
100 Hz ISO
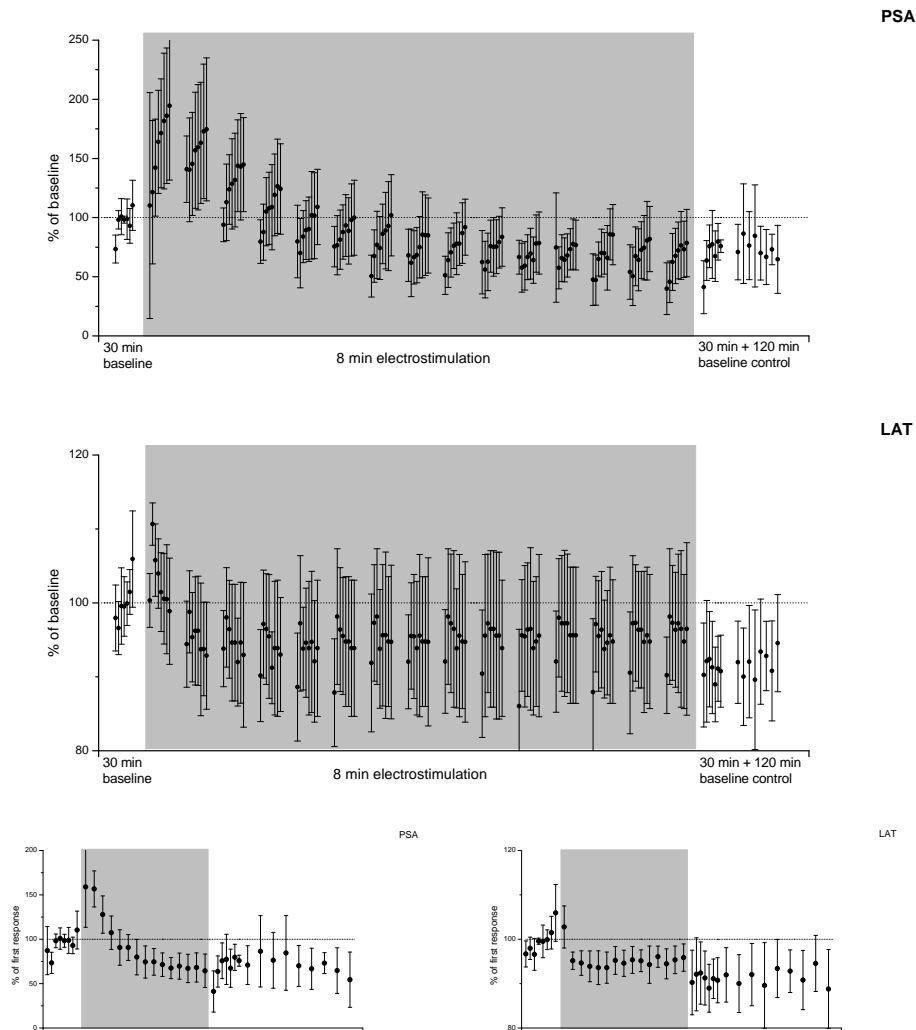
Figure 3.40: **Response pattern during baseline and control recording** (white background) **and 100 Hz stimulation** (grey background). **Upper and middle row:** responses averaged for seconds. Please note the LAT increase between first and second stimulation second in each train. **Lower row:** responses averaged for trains. n = 5

3.8.2 Summary of ISO control experiments

Electrostimulation with frequencies generating significant BOLD responses usually also affected longer lasting signal production in the dentate gyrus. "Longlasting" refers in this case to a time interval of 2.5 h following stimulation and targets to capture effects acting for a longer period than only stimulation duration.
Low and high frequency stimulation produced different outcomes.
Low frequency protocols (5 and 10 Hz) produced signal depression displayed in a reduced and delayed PS production in the dentate gyrus during at least 2.5 hours following stimulation. A tendency for recovery to baseline values could be observed during this time.
High frequency stimulation (100 Hz) resulted in clearly abbreviated response latencies, i.e., decreased LAT or LAT potentiation, but nevertheless depression of PS production.

For low frequencies the amount of signal depression apparent during the first 30 min of control recordings increased with stimulation frequency (Figs 3.41). The amount of signal depression during electrostimulation itself increased also with stimulation frequency within low frequencies (Figs 3.41). I.e., PSA decreased and LAT increased stronger with increasing frequency.

Response patterns during stimulation were heterogeneous. During low frequency stimulation (except at 2.5 Hz) PSAs often showed short term potentiation (STP) but that was not always the case. STP probability was independent from stimulation frequency. Only latency formed a consistent response pattern during stimulation. Signal production during stimulation is characterized by a firing depression, occasionally overlaid by a short term potentiation of PSAs. Signal depression remained often during control baseline recordings for at least 2.5 hours.
100 Hz stimulation produced contradictory results: regular STP during stimulation offsetting an underlying overall spiking depression that was prolonged during control baseline recording. Latency showed potentiation during stimulation but only when per train averaged values were regarded. During stimulation LAT increased slightly, starting on a decreased overall LAT level.

It should be mentioned that the response pattern during stimulation gave no hint about the quality of the following baseline change. Amounts of PSA increase/ LAT change during stimulation could as well not be correlated to stimulation frequency.

Anaesthetization of more than two hours could impair signal production by decreasing population spike amplitudes and increasing latency slightly, but that could only be observed in a part of the examined animals.
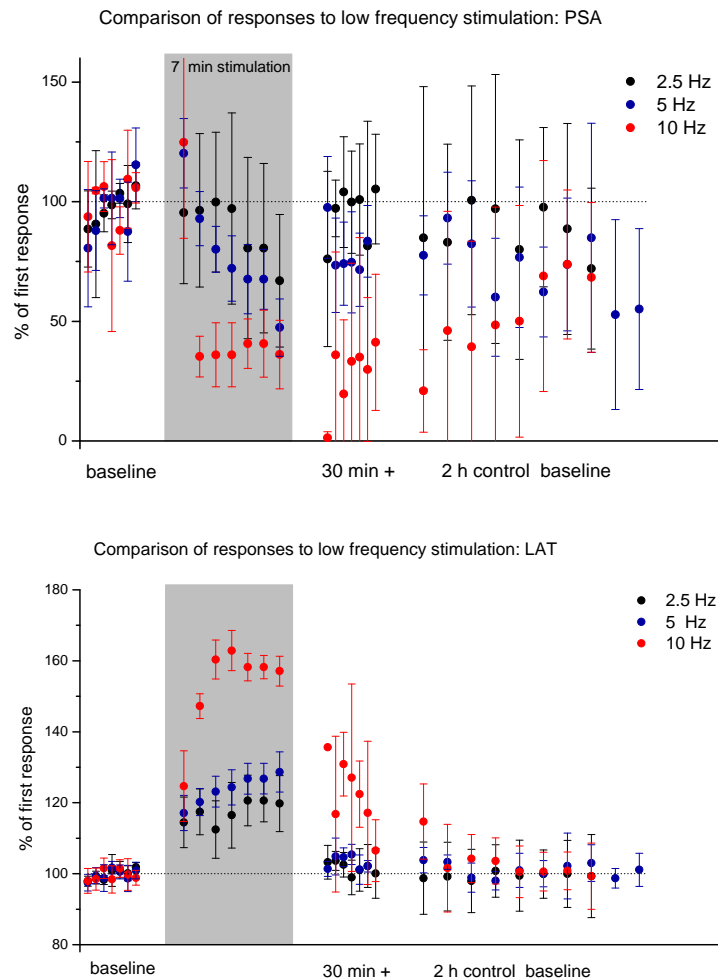
Figure 3.41: **Comparison of spiking activity during and after stimulation with low frequencies**. Single values in the grey box represent spiking activity averaged for individual trains. Baseline values (white background) display responses to single pulses.
Upper plot: Strength of PSA depression during stimulation is frequency dependent. Only in 2.5 Hz experiments deviation from baseline is not significant.
Lower plot: Electrostimulation in increasing spiking delays during stimulation. The increase was frequency dependent. This was not necessarily prolonged during the following control baseline recording. That is, LAT is affected by depression for a shorter time than PSAs.

3.9 Control II: Unanaesthetized animals

The second control part presents results from experiments with unanaesthetized animals. By eliminating the anaesthetic from control experiments the effect of Isoflurane (ISO) on short and long term electrophysiological signal production in the dentate gyrus should be examined. Almost identical experimental setups were applied for control experiments with anaesthetization and without. Only length of unanaesthetized baseline and control recordings differed. Since no regard had to be paid to ISO effects arising from longlasting anaesthetization they could be extended with unanaesthetized animals. Animals were usually resting or sleeping during baseline recordings. It was evident that most protocols produced behavioral changes, they were noted as well.

Baseline changes and response pattern due to electrostimulation/ unanaesthetized

A control experiment checked the stability or fidelity of electrophysiological responses by recording responses to single pulses for five hours. The first hour served as baseline, the following four hours as control. The baseline and first control hour recorded responses to stimulus pulses each five minutes, for the last three hours one response was recorded each 15 min.

During the first half hour of control recording (60 min control) significant PSA change could only be observed in one of five animals. In this animal signal time course showed a continuous PSA increase and LAT decrease during the whole experiment that became apparent in the last three recording hours. In the rest of the animals responses remained constant during the first control hour and degraded in the last three hours. Population spike amplitudes decreased here significantly ($p \leq 0.001$, GLM, t-test). Latencies changed significantly in three of these cases but in different ways: two were decreasing, one increasing.

It can be summerized that even without electrostimulation fidelity of firing obtained in the dentate gyrus degraded when the recording exceeded two hours. The same could be observed in ISO experients. I.e., baseline stability can only be expected during the first two hours of recording. Thus, for the examination of the effects of electrostimulation protocols only the first hour of control baseline could be used for comparisons.

Results of control experiments with unanaesthetized animals equalled ISO controls in many points. General response patterns during stimulation and effects of electrostimuation protocols on electrophysiological baseline were similar. Effects that could already be observed in ISO experiments appeared even more clearly in unanaesthetized controls.

unanaesthetized control without electrostimulation
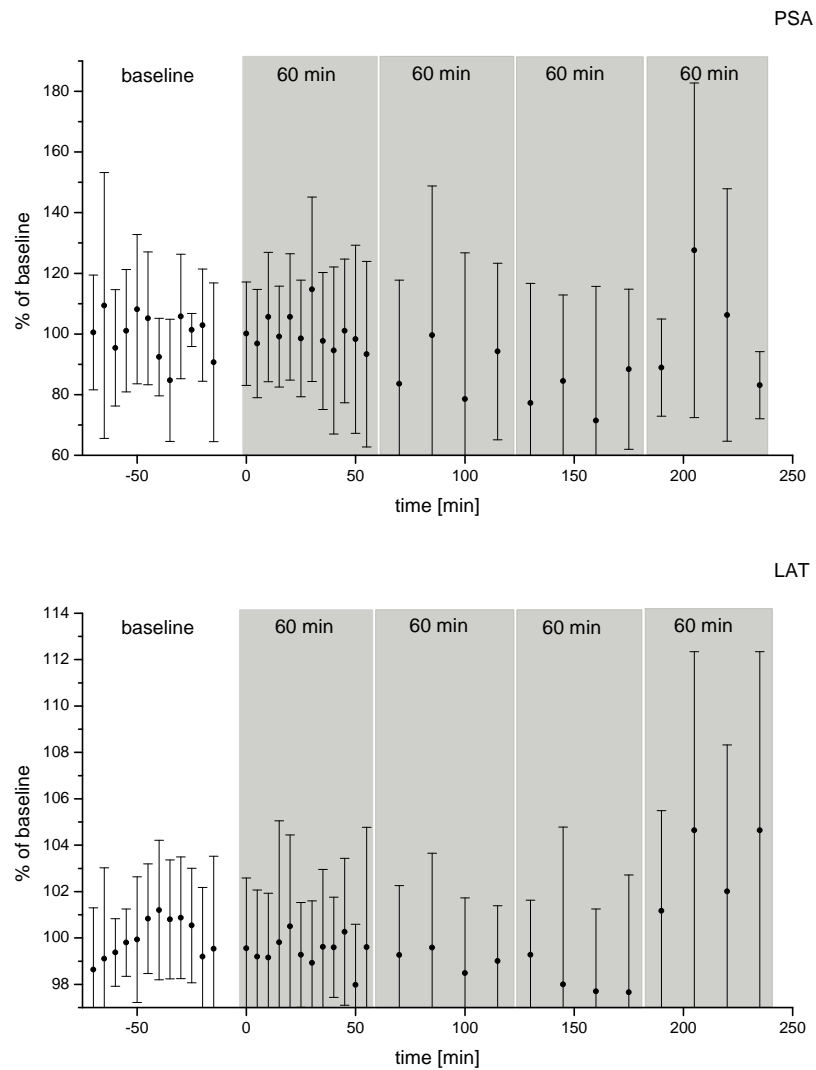
Figure 3.42: **Control unanaesthetized.** Signal development (PSA, LAT) during baseline recording (white block) and control baseline recording (grey blocks). n = 4

2.5 Hz electrostimulation applied to unanaesthetized animals did not change signal production during first hour of control baseline significantly. In two animals PSAs differed significantly from baseline, not in response to stimulation but following a trend developed already during baseline recording. The PSA shifted in those cases gradually during five hours recording time as observed in several animals that did not receive electrostimulation. In one animal PSA increased, in another PSAs decreased ($p \leq 0.05$, GLM, t-test).

2.5 Hz stimulation applied to unanaesthetized animals often produced spiking depression during stimulation: PSAs decreased clearly below baseline during 40% of the trains ($p \leq 0.05$, GLM, t-test) and spiking occurred always significantly delayed during stimulation, i.e., LAT always increased during stimulation ($p \leq 0.01$, GLM, t-test). LAT increases started in each following train from a comparable level. At the end of a stimulus train latency of population spike was delayed by 10-20 % of the baseline value.
Although 2.5 Hz often produced firing depression during stimulation no impairment of signal production in the dentate gyrus could be found during the control recording afterwards.

Behavior: Rats receiving stimulus trains for seven minutes remained in the same resting position they had attained during the first hour of baseline recording. Should there have been a change in, for example, EEG oscillation, it was not sufficient to result in a change of animal behaviour.

2.5 Hz unanaesthetized

Figure 3.43: **Response pattern during one hour baseline and four hours control recording** (white background), **and seven minutes 2.5 Hz electrostimulation** (grey background). **Upper row:** responses during stimulation averaged for seconds to illustrate STP. **Lower row:** responses during stimulation averaged for trains to display overall level of firing in comparison with baseline firing. n = 5

5 Hz electrostimulation resulted in impaired firing during the first hour of control baseline recording. Population spike production was significantly depressed to 30-80 % in four of six animals (PSA: $p \leq 0.01$, GLM, t-test). However, one animal displayed potentiated spike amplitudes (PSA: $p \leq 0.01$, GLM, t-test). LAT increased meanwhile in five of six animals by 1-12%, this is by 0.1 - 0.5 ms (LAT: $p \leq 0.01$, GLM, t-test).
PSAs recovered after the first control hour to baseline values, several even showed an overshoot developing into a weak potentiation (Fig 3.44). LAT remained elevated in the most animals until the end of the recording although a sporadic return to baseline could be observed.
Only one animal did not show any effect, its signal time course resembled a baseline recording.

PSA augmentation could regularly be observed during 5 Hz stimulation of unanaesthetized animals. It could increase PSAs by considerable amounts. In the first train this STP produced a slightly chaotic pattern, in the second spike production could collapse, and if firing occurred, at least augmentation was impaired here. From the third train on strong PSA increases within trains could be observed again in all following trains (upper Fig 3.44, PSA).
In two animals STP increased overall spiking during stimulation significantly above baseline ($p \leq 0.01$, GLM, t-test) (lower left Fig 3.44, PSA). In others STP was weaker resulting in overall spiking that remained on baseline level, or even fell below.
Latency always increased significantly above baseline during the experiment ($p \leq 0.01$, GLM, t-test), in average to a maximum of $\sim$130% (middle Fig 3.44, LAT).

Behaviour: Two of six animals did not show behavioural changes in response to 5 Hz electrostimulation. One remained in a lying, resting position, eyes open, grooming at the end of seven minutes of electrostimulation. The second remained sleeping during the whole application. Stimulation intensity for these animals was in the same range as in the rest, but they did not show additional discharges. However, it is unlikely that discharges triggered the behavioural changes in the other animals. Behavioural responses to stimulation occurred always in a similar pattern. First reactions could be observed with delay to first stimulus train. That is, animals did not change immediately from rest to activity. Typically the switch became apparent 20 seconds or more after the first stimulation train had ceased. Behavioural change started with an elevated alertness displayed by opening the eyes, lifting the head, looking around, and sniffing into the air above. This was followed by an increasing mobilization. Animals were rising, sniffing intensely into the air, at walls, between the metal bars forming the floor and at food pellets, moving perpetually while doing that. Rearing happened, but more often animals straightened up along the walls, standing on two legs, sniffing and "searching" along. The whole behavioural response can be characterized as exploratory behaviour. If additional discharges happened, they started usually in the course of the first train and ceased 25 seconds after stimulation onset. Additional discharges in later trains happened rarely.
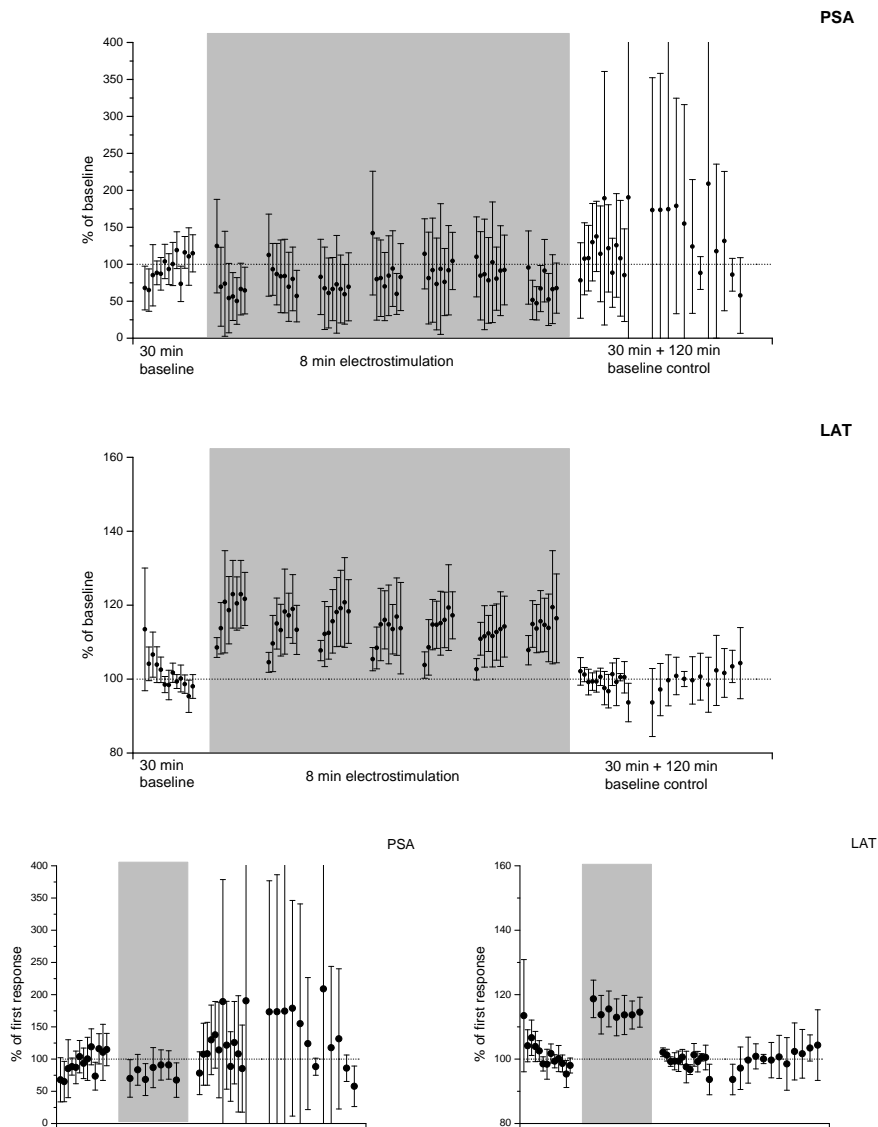
5 Hz unanaesthetized

Figure 3.44: **Response pattern during one hour baseline and four hours control recording** (white background), **and seven minutes 5 Hz electrostimulation** (grey background). **Upper row:** responses during stimulation averaged for seconds to illustrate STP. **Lower row:** responses during stimulation averaged for trains to display overall level of firing in comparison with baseline firing. n = 6

10 Hz electrostimulation produced strong spiking depression, or even break-down, during the following control recordings in all experiments but one, where PSAs remained unchanged (PSA: $p \leq 0.001$, LAT: $p \leq 0.001$, GLM, t-test). PSAs dropped in the first control hour to 0-50%, LAT increased by $\sim$5% for the first hour after stimulation, i.e., by $\sim$0.2 ms. After one hour of control recording most PSAs had not only recovered to baseline values but displayed a significant potentiation ($p \leq 0.001$, GLM, t-test). In four of six animals PSAs increased to 180-260% of baseline values during the last three control hours. The remaining two animals showed clear depression until the end of experiment ($p \leq 0.001$, GLM, t-test). During all that time LAT remained significantly elevated.

10 Hz stimulation in unanaesthetized animals always included the risk to produce additional discharges at least during or after the first train. The first train had the same V-shaped pattern as described in ISO controls. In the second train population spike production collapsed and returned reliably in the third train. STP could be observed during stimulation, but in a rather obscured or distorted form. I.e., PSA increases could be observed during stimulation train application, but in general only in the beginning of the train. After one or two seconds (10-20 stimuli) a further increase seemed to be impaired, population spikes started to oscillate, and firing in response to stimulation got more and more unpredictable. Oscillations could occur from there on around a rising as well as a constant mean. It is impossible to say if STP plays a role at this time point, since STP is a presynaptic mechanism that can only be reflected in (postsynaptic) population spike production under opportune circumstances, i.e., when spike production is not too heavily impaired by concomitant inhibitory events. Yet the observed oscillations reflect a strong inhibitory activity.

Nevertheless a clear increase in the level of spiking activity to $\sim$230% above baseline could be seen during stimulation ($p \leq 0.05$, GLM, t-test) (PSAs in Fig 3.45).

A massive delay in spike production occurred from the first stimulation second on (middle Fig 3.45). LAT increased in average to a maximum level between 160-170%. That means, population spikes occured delayed by up to $\sim$2 ms from train two/three on.

10 Hz stimulation not only changed spiking parameters significantly, the characteristic area dentata-signal also shifted during stimulation gradually into another shape.

Behaviour: Behavioural changes due to 10 Hz stimulation resembled changes described for 5 Hz. Continuously increasing activity, exploration of floor and walls, feeding, drinking, sniffing. Probability of additional discharges was increased with 10 Hz. However, rats without discharges in the EEG displayed the same behavioural response as the rest: a delayed "awakening", sometimes not until the second stimulation train. The behavioural response occurred so much delayed that an electric shock was unlikely be responsible for the activation. One animals even continued sleeping.
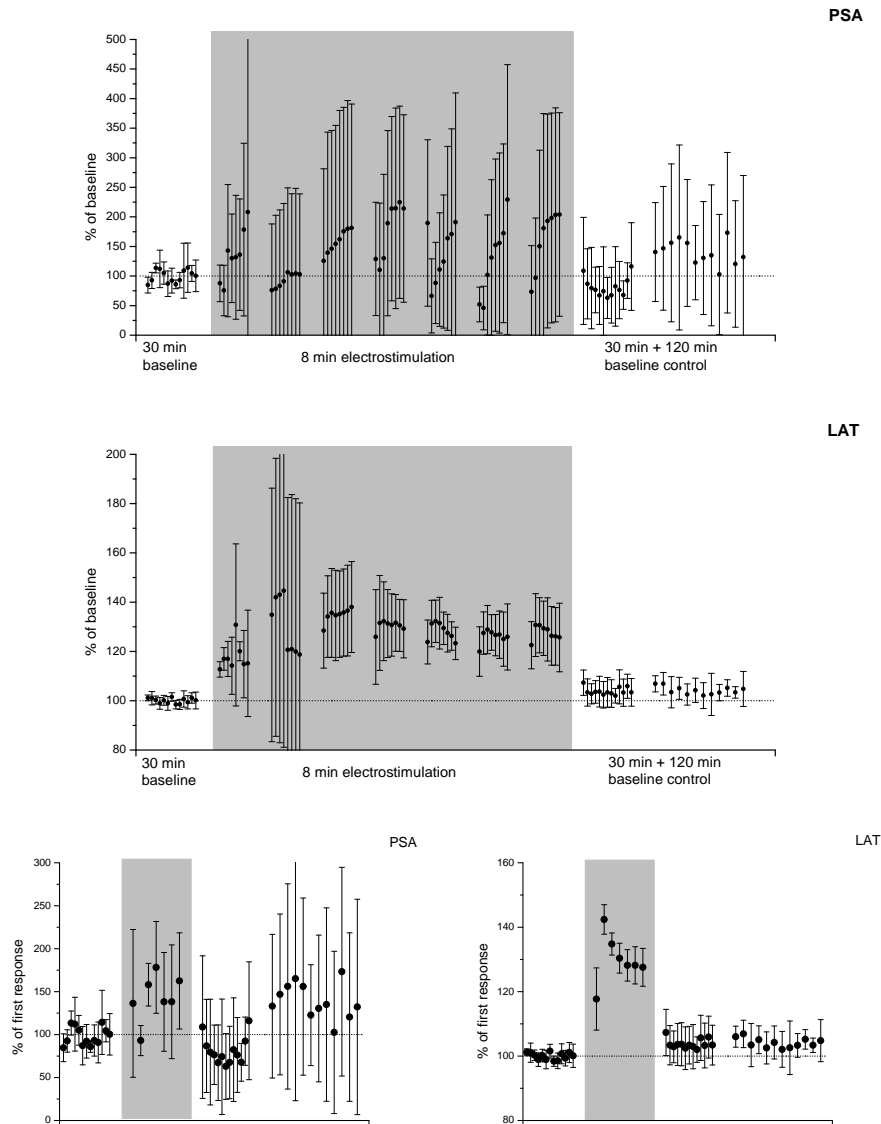
10 Hz unanaesthetized

Figure 3.45: **Response pattern during one hour baseline and four hours control recording** (white background), **and seven minutes 10 Hz electrostimulation** (grey background). **Upper row:** responses during stimulation averaged for seconds to illustrate STP. **Lower row:** responses during stimulation averaged for trains to display overall level of firing in comparison with baseline firing. n = 6

100 Hz burst protocols applied for 15 minutes produced a clear PSA depression to 0-60% in five of six animals during the first hour of the subsequent control baseline recording (p $\leq$ 0.01, GLM, t-test). PSA depression persisted then for three more hours. Recovery to baseline during that time could be observed in one animal.

However, latency did not show depression, instead it was significantly decreased in four of six animals during first hour of control recordings (p $\leq$ 0.05, GLM, t-test). In the last three hours LAT returned to baseline values in two of them.

In one case a clear potentiation could be found after 100 Hz stimulation. PSA and LAT remained potentiated until the end of the control recording.

Additional discharges could be observed after first stimulus train but discharges had no influence on later control baselines or behaviour.

Firing patterns in response to 100 Hz stimulation combined characteristics that could already be found in 5 Hz and 10 Hz data. After an irregular response pattern in train 1 firing failed in most animals in train 2. Recovery in train 3 to at least 100% was typical. From here on PSA augmentation during stimulus train application became apparent (upper Fig 3.46, PSA). The level of averaged spiking activity per train reached its maximum in train 3, certainly due to a high amount of STP, and decreased from there on (Figs 3.46, PSA). Level of firing activity remained above baseline until train 5 in most animals (p $\leq$ 0.05, GLM, t-test). After that in a part of animals PSA remained on an elevated level, a part dropped below 100%. Two ceased firing around train 9. STP was still present during those later trains.

In contrast to experiments on anaesthetized animals latency increased in unanaesthetized animals during stimulation up to ∼125% (LAT Figs 3.46). These increases during stimulation pushed ØLAT in three of six animals significantly above baseline values (p $\leq$ 0.001, GLM, t-test).

Behaviour: Animals displayed increasing exploratory behaviour as seen before, usually until train 5. Around train 7 eagerness of exploration decreased, animals still alert ceased moving as much as before. Activity slowed down, rats started grooming and feeding, some laid down. Stimulus trains following the first seemed to refresh activation triggered by the initial stimulation. This could be observed in all experiments triggering behavioural changes, low frequency protocols included. When stimulation exceeded seven minutes as it was the case in 100 Hz experiments, the "refreshing effect" seemed to be less enduring than the preceeding trains. That is, the effect of stimulation weakened.

100 Hz unanaesthetized

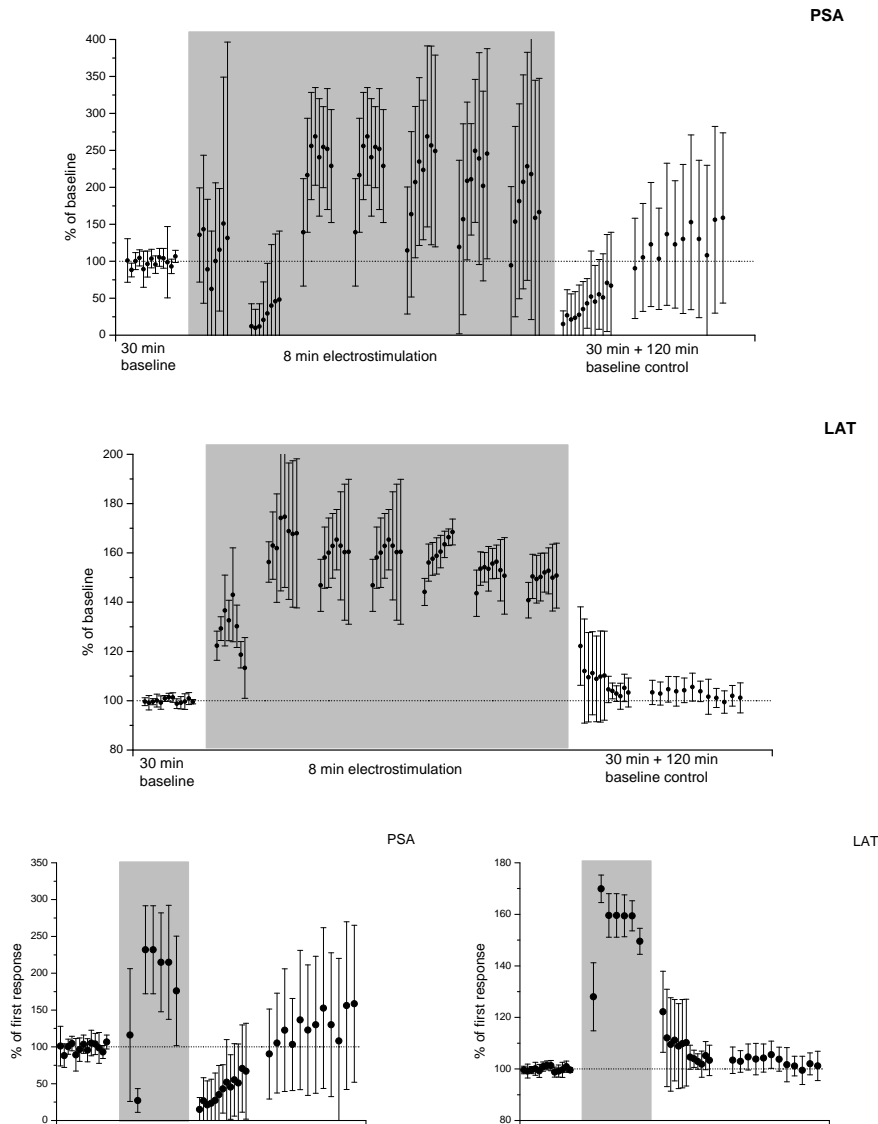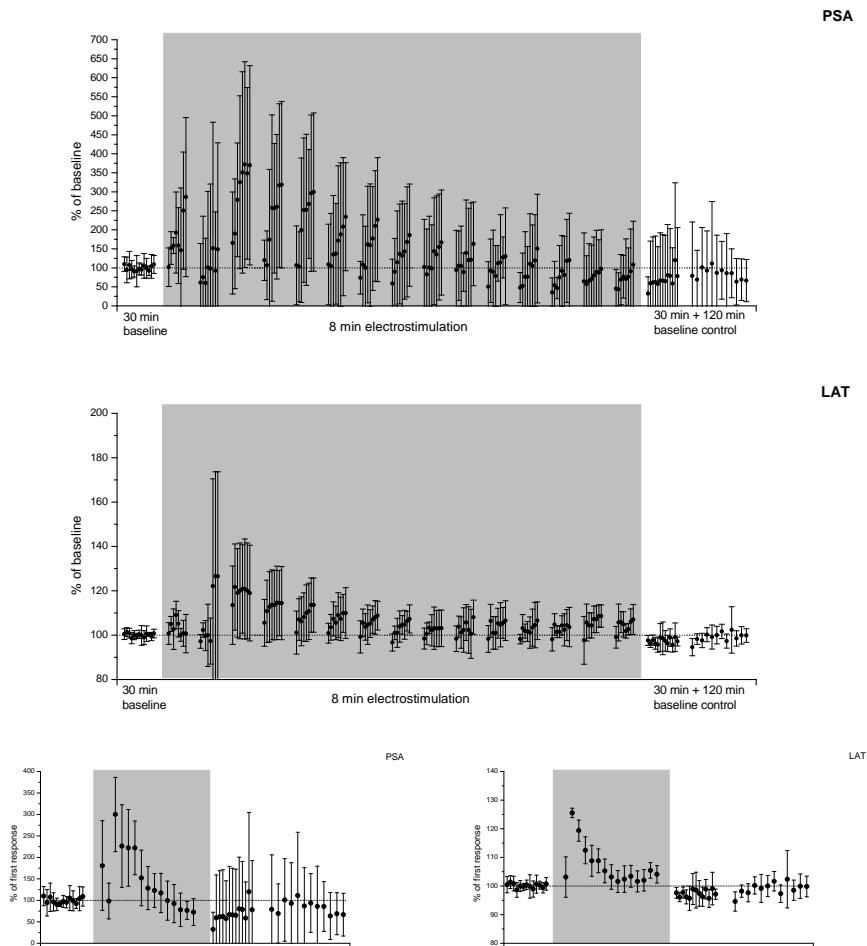Figure 3.46: **Response pattern during one hour baseline and four hours control recording** (white background), **and 15 minutes 100 Hz electrostimulation** (grey background). **Upper row:** responses during stimulation averaged for seconds to illustrate STP. **Lower row:** responses during stimulation averaged for trains to display overall level of firing in comparison with baseline firing. n = 6

Summary of unanaesthetized control experiments

Electrostimulation of unanaesthetized animals with 5, 10 and 100 Hz produced longer lasting effects on firing in the dentate gyrus during the entire time of control baseline recording. 5 and 10 Hz stimulation resulted in PSA and LAT depression, that could turn into a potentiation in the course of the control baseline recording, especially in 10 Hz experiments (upper Fig 3.47). 100 Hz stimulation resulted in impaired population spike production whilst latency showed potentiation.
At low frequencies strength of the subsequent longer lasting PSA and LAT depression seemed to correlate with stimulation frequency, but differences between the groups could not be proved significant.

Short term potentiation during stimulation could be observed regularly in unanaesthetized animals. Usually STP was responsible for significant ØPSA increases above baseline during low and high frequency stimulation. LAT of population spikes always increased significantly during electrostimulation with low frequencies, but that depression did not necessarily continue during the following control recordings. During 100 Hz stimulation LAT also increased significantly and showed a significant potentiation during the following control baseline recordings.

Unanaesthetized animals displayed behavioural changes in response to electrostimulation with 5, 10 and 100 Hz. If a behavioural change occurred, it was a shift from rest to alertness followed by energetic exploratory behaviour. Vigour of activity slowed down when the experiment exceeded seven minutes as it was the case in 100 Hz experiments. Before that each stimulation train seemed to renew the initial behavioural switch. Animals returned to rest 10-15 min after stimulation had ceased.
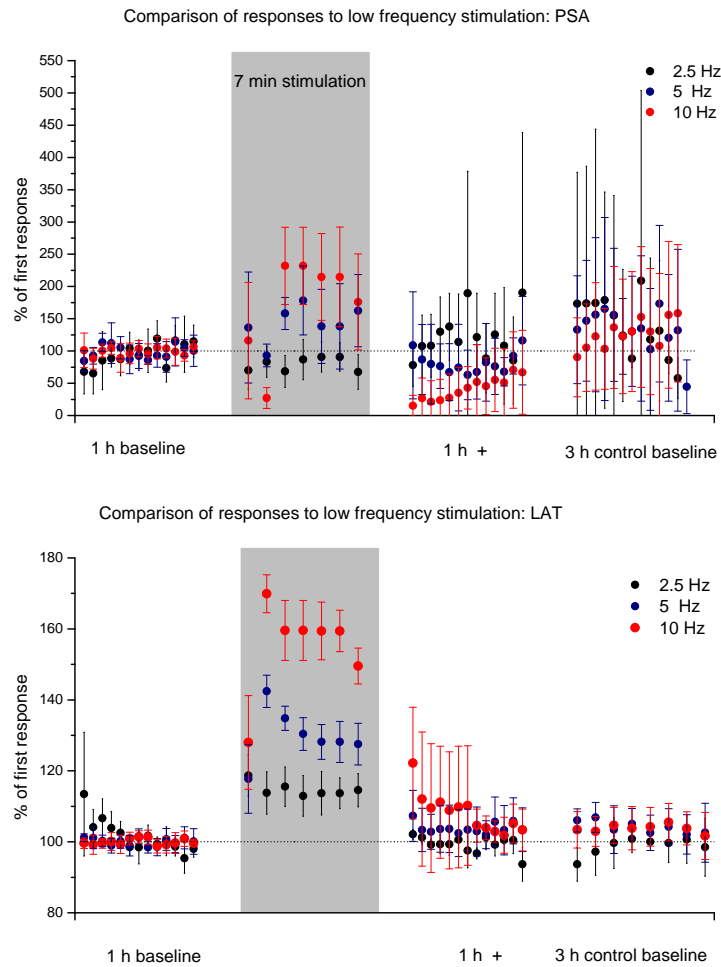
Figure 3.47: **Comparison of spiking activity during and after stimulation with low frequencies**. Values in the grey box represent spiking activity averaged for individual trains. Baseline values (white background) display responses to single pulses.
Upper plot: Strength of PSA depression during stimulation is frequency dependent. Only in 2.5 Hz experiments deviation from baseline is not significant.
Lower plot: Electrostimulation resulted in increasing spiking delays during stimulation. The increase was frequency dependent. After 5 and 10 Hz stimulation it could remain increased during the following control baseline recording.

3.9.1   Comparison between anaesthetized and unanaesthetized animals

Long lasting effect
Effects of electrostimulation on longer lasting signal production were in parts comparable between anaesthetized and unanaesthetized animals. In both groups electrostimulation with 5 and 10 Hz produced firing depression, that is, decreased PSAs and increased LAT during control baseline recordings. However, in unanaesthetized animals the initial depression could recover to baseline values within one hour and develop into a weak potentiation. In anaesthetized animals signal depression usually remained until the end of the experiment. It can be concluded from the data that Isoflurane not only diminishes PSAs on a long term, but also promotes emerging firing depression, probably by inhibiting mechanisms that produce a slow onset potentiation.
Only 100 Hz produced PSA depression but abbreviated, i.e., potentiated LAT in anaesthetized and unanaesthetized animals.

STP
Response patterns during low frequency stimulation were similar in anesthetized and unanaesthetized experiments. Augmentation of PSAs could often be observed while stimulation was applied. In unanaesthetized animals such short term potentiation could be observed more often than in ISO animals. STP was also stronger in unanaesthetized animals but the high standard deviation of the data usually prevented a proof of significance for that (Fig 3.48). STP sometimes pushed PSAs during stimulation to considerable amounts. In response to PSA increases LAT increased during train application too.

This different strength of augmentation during stimulation was responsible for the different ØPSA and ØLAT in ISO and unanaesthetized animals. While overall level of PSA production fell below baseline during stimulation in ISO animals, it was in average above baseline during stimulation in unanaesthetized animals (see left Fig 3.48). In fact, spiking always started at the same values in ISO and unanaesthetized trains, and only the intensity of augmentation created this difference.
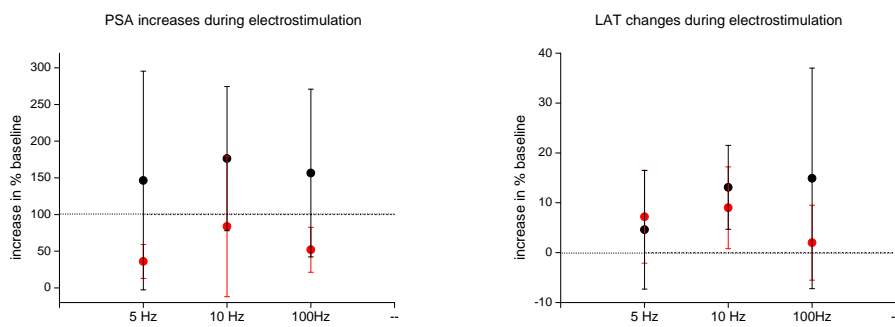
Figure 3.48: **Short term potentiation during electrostimulation in anesthetized and unanesthetized animals.** Although PSA augmentation is stronger in unanaesthetized animals and they tend to display STP more often, a statistical test could not find a difference between anaesthetized (red) and unanaesthetized (black) PSA increments during stimulation.

Chapter 4

Discussion

The results show that significant BOLD response can be induced in the hippocampal formation by electrostimulation of its input, the perforant pathway. BOLD activation can be evoked by low frequency stimulation in the theta (5, 10 Hz) range as well as by high frequency burst stimulation in the low and high gamma range (20 - 200 Hz). Low frequencies are not equally adequate; frequencies from 5 Hz on evoke BOLD responses with an increasing probability.

Events in the dentate gyrus in response to electrostimulation

Frequency specifity of stimulation

What actuate the chosen stimulation frequencies in the hippocampal formation, and in particular the dentate gyrus ?

Already stimulation frequencies between 2.5 and 5 Hz increase synaptic efficacy in the DG and the hippocampus proper, i.e., population spikes (PS) can more easily be produced. Between 5 and 10 Hz this increase reaches a plateau [89, 113]. Stimulation provided from the entorhinal cortex in that frequency range, mainly by monosynaptic inputs, is known to activate hippocampus best [47]. Between 5 and 15 Hz polysynaptic transmission and potentiation of EPSPs and population spikes can be observed in the CA1, CA3 and DG [4, 133]. Under normal circumstances the DG plays a special role in the hippocampal formation. It functions as a control point stopping excessive excitatory activity mainly arriving from the entorhinal cortex, and allowing excitation delivered in an appropriate pattern to pass through. Granule cells in the DG are not easily excitable, neighbouring cells are not interconnected, so activation of granule cells does not potentatiate activity of adjoining cells. Instead, granule cells are part of a network containing strong GABAergic inhibition [31]. Inhibitory neurons of various types can be found throughout the DG: in the hilus, the granular and the molecular cell layer [42, 49, 109]. They are part of a complex circuitry producing a threshold not easy to overcome. However, repetitive stimulation with frequencies in the theta range is able to trespass the gate formed by the DG. Prolonged stimulation can even push activation beyond the limit where the protective function of the DG is broken. The balance between excitation and inhibition gets lost, inhibition lapses, epilepsy-like discharges can be observed.

In the present study an increasing activation of the DG could be observed too when increasing stimulation frequency from 2.5 to 20 Hz. This increase did not become obvious in an elevated population spike production but rather in an elongated latency of these responses, indicating an increased inhibitory action.

As discussed above, a tight network of inhibitory and excitatory circuits controls the output produced in the DG. The extracellular signals obtained here display the postsynaptic summation of inhibitory and excitatory inputs. I.e., a poor population spike can result as well from reduced activity, as from incoming excitation canceled out by a strong inhibition. In the DG a high amount of excitatory activity would usually be met be a likewise counteracting inhibition. It can be reasoned from all this, that the population spike amplitude can not reveal the true amount of participating inhibition and excitation.

The population spike latency seems in this regard to be more informative. Increasing inhibition would delay latency of granule cell responses. Indeed, in the present experiments more and more delayed latencies could be observed during stimulation with increasing stimulation frequencies in the theta range (2 - 10 Hz). This points to an increased inhibition in the DG, and respectively to a net increase of DG activation, since an increased inhibition is derived from an increased excitation.

At 10 and 20 Hz additional discharges could occur during the experiments. Increasing stimulation frequency from 2.5 to 20 Hz increased hippocampal activation up to a maximal dentate activation (MDA) at 10 and 20 Hz. This resulted sometimes in additional discharges at those frequencies, as reported by Stringer and Lothman [113, 114], followed by a signal breakdown. After a short term of depression field potentials and population spikes reappeared showing significantly delayed firing. After this epilepsy-like events inhibition was permanently increased during stimulation. What exactly produced this inhibition can yet not be answered by the given results.

Duration of stimulation

There are not only thresholds for effective stimulation frequencies but also for stimulation duration. Short stimulation durations cause only hyperpolarization in hippocampal principle cells and lead to habituation, i.e. decreasing PS production. Hyperpolarization following an evoked field potential consists of different phases, that is, it has different causations. An early IPSP is produced by inhibitory synaptic activity, i.e. by inhibitory interneurons. The following late IPSP is mainly produced by a change in K^+ conductance [21, 89, 102].

In the DG itself a frequency habituation can be observed during the first seconds of electrostimulation, decreasing population spike amplitudes and EPSPs in the granule cell layer [21, 102]. This is due to an enhanced efficacy of population spike production resulting in increased inhibitory feedback activity. Strength of hyperpolarization increases during this time with increasing stimulation frequency, it is stronger at 10 Hz compared with 2 Hz [89]. Increasing stimulation duration to more than 5 seconds turns frequency habituation into frequency potentiation. Inhibition becomes more and more impaired. Both, early and late inhibition are concerned. Firing of inhibitory neurons attenuates with longer lasting stimulation, increasing population spike amplitudes [89]. Formerly hyperpolarized granule cells in the DG become now depolarized and produce population spikes more easily [21, 102]. Around 5 Hz stimulation brought to the DG can trespass easily and be passed on into the hippocampus.

Most works examining the effect of electrical stimulation of the hippocampal formation usually only picture events during a certain temporal interval or subregion, and use slightly different parameters, what makes it difficult, but not impossible, to speculate about what exactly happens during stimulation with parameters chosen for the present experiments. What probably happens during a stimulation of 8 seconds is, that a succession of activity switches takes place in the DG. Initial net inhibition changes into net excitation that can after some time change into another net inhibition. Those changes of inhibitory and excitatory drive can be based on changes in the intra- and extracellular ion concentrations, or different temporal combinations of inhibitory and excitatory networks during ongoing stimulation of the DG. Different populations of inhibitory interneurons seem to alternate during this time. Interneurons that cease firing after some time may be partially responsible for developing discharges, but it can be assumed that other assemblies of interneurons are more persistent in their activity.

The results of the present experiment show one thing clearly. Electrostimulation with an appropriate frequency and duration moves the system of interacting networks in the DG from one activity mode into another. This change may finally be responsible for the observed BOLD generation.

BOLD production and overall firing activity

Several details of the results prove that amount of BOLD signal obtained in the ipsilateral dorsal hippocampus, or its generation per se, was independent from granule cell firing.

First, although firing was highest in 2.5 Hz experiments it did not produce significant BOLD responses. 10 or 20 Hz stimulation, on the other side produced the least firing but almost always a significant BOLD response.

It could be argued now, that BOLD response and spiking are negatively correlated, but the 5 Hz results point against that. With 5 Hz stimulation probability for BOLD signal generation was 50%. Averaged PSA for the BOLD response group was slightly higher then in the group without significant BOLD response (middle Fig 3.17). Nevertheless, pooled PSAs of single animals overlap so much that BOLD responses could never be predicted from raw data (see Fig 1 in Appendix).

Since averaging alone does not take into account the increasing number of stimulus responses per time interval, going along with increasing frequencies, summed stimulus responses were also examined. But when summed activity is considered instead of averaged values the same conclusion must be drawn. Summed spiking activity during the eight minutes of one experiment does not correlate with BOLD production. Although more stimuli were applied with increasing frequency, and summed firing responses were higher per train (see Fig 2 in Appendix), this had no effect on the amount of BOLD signal increase during the train (see Fig 3 in Appendix).

A further argument against an important role of spiking for BOLD production were cases when firing lapsed for a while. When the electrophysiological response following a strong episode of discharges broke down completely, i.e., population spikes and EPSPs both disappeared, BOLD response was abolished too. But as soon as the EPSP reappeared, a BOLD signal could be observed again. Spiking

was not necessary. That is, a certain amount of synaptic activity seems to be an indispensable precondition, but population spike production can not be linked to BOLD generation. Although an exact quantification of EPSP was not possible for the present data they could at least serve as a monitor for fluctuations of synaptic activity. These results suggest that excitatory postsynaptic activity (EPSPs) but not transmission of action potentials is required for BOLD generation as already found by [24, 76, 91, 101, 121].

Epilepsy-like activity as causation of BOLD responses

As depicted above, several electrostimulation protocols did not only activate the hippocampal formation, they even pushed activation up to a point, where additional discharges emerged. Stimulation with 10 and 20 Hz challenged the capacity of the DG as a control point for epileptic activity most.

Discharges occurred in response to persistent stimulation of the DG that is known to tune the local inhibitory circuit down. That is, a part of interneurons cease to respond to incoming stimulation with firing of action potentials, only EPSPs are produced anymore. Inhibitory neurons discharge with more failures, in result IPSP production in granular cells is impaired [106]. Decline of inhibition in the DG can also be caused by presynaptic receptors, that is down-regulation of GABA release by activation of metabotropic $GABA_B$-receptors. Postsynaptically reduction of GABAergic inhibition can increase NMDA-dependent excitation [87]. Moreover, Ca^{2+}-dependent potassium conductivity increases in response to repetitive activation [13]. Elevated extracellular K^+ moves reversal potential of granule cells to a direction that leaves cells in more depolarized state. This increases the excitability of granule cells and facilitates additional discharges or epilepsy-like discharges. With ongoing stimulation extracellular space in the DG enriches with K^+, while Ca^{2+} concentration decreases [21]. At stimulation frequencies above 10 Hz a critical threshold for extracellular K^+ concentration in the DG is reached [68, 113]. Epilepsy-like behaviour can be elicited that way in the DG, but also in the CA3.

In the present experiments epilepsy-like discharges usually appeared at the end or after the first stimulation train and continued for maximally 20 seconds after stimulation had terminated. They rarely recurred during the rest of the experiment pointing to an elevated threshold for afterdischarges after the first such event [21]. During afterdischarges population spike amplitudes were potentiated for a short period followed by an impaired transmission or complete transmission breakdown. Already this temporally limited occurrence of additional discharges speaks against a basic role in BOLD signal production. Furthermore, BOLD signals could be observed during all stimulation trains and all experiments utilizing frequencies not evoking additional discharges.

Although additional discharges were not the main cause for BOLD production in this study, they could yet account for BOLD activation. Epilepsy-like activity prolonged BOLD production by extending firing activity beyond stimulation duration.

What could be reasons for the cessation of the observed additional discharges is still a matter of discussion, e.g., in the field of epilepsy research. Processes responsible

for a limitation of seizures could be intracellular acidification [130], afterhyperpolarization, receptor desensitization in consequence to a prolonged exposure to glutamate [14,69,116], presynaptic inhibition, and transmitter depletion due to an excessive vesicle use during additional discharges [46,74].

Facilitation and depression during stimulation

If not amount of firing, which other processes active during stimulation could be responsible for BOLD generation? The electrophysiological data of all experiments exposed a couple of overlaying processes when analyzed for the short time interval of the stimulation itself, or for the longer time interval of the entire experiment. During the eight seconds of electrostimulation augmentation of population spike amplitudes could frequently be observed during low and high frequency protocols. This enhancement of population spikes occurred at stimulation frequencies of 5 Hz and above. At higher frequencies, when burst protocols were applied, and only the first population spike of a burst was fired and all successive were depressed, the first population spike in a burst could be augmented in successive bursts. Sometimes a second population spike could appear with ongoing stimulation indicating a reduction in (feedback-)inhibition.
While augmentation of population spikes could not reliably be observed, latency always increased during stimulation. Latency can be used as an indicator of inhibition, latency increases due to increased inhibition. The firing patterns during electrostimulation display contradictory processes. Although firing occurred delayed, i.e., was inhibited, an improvement of spike amplitudes could be observed at the same time. The PSA increase might have different reasons: 1) augmentation, i.e., increased presynaptic efficiency due to repetitive stimulation (STP), 2) increasing number of firing neurons during persistent stimulation and 3) increased efficiency of PS production. What could be behind the observed inhibition can not be cleared by the available data.

Could the observed augmentation of spiking answer for BOLD production? Probably no. Though facilitation indicated an enhanced synaptic efficacy during electrostimulation, it was no obvious prerequisite for significant BOLD responses. What speaks against is that enhanced firing could also be observed in cases where no significant BOLD signal appeared. Nevertheless it can not entirely be excluded that short term plasticity processes do play a role in BOLD generation, but this should be clarified in a future investigation.

Another electrophysiological parameter seemed to relate better to BOLD production: latency of population spikes, and thus inhibition. As shown above, inhibition increased during ongoing stimulation. And also on the longer time scale of a whole experiment an inhibition increase could be observed. Overall firing decreased, spiking occurred more and more delayed.
Already during 2.5 Hz stimulation a weak, but not significant increase in inhibition could be observed. A clearly elevated inhibition became only evident at higher frequencies, when significant BOLD activations emerged too. So, an indispensable minimum amount of inhibition increase seemed to accompany significant BOLD responses. But this correlation is problematic. When 5 Hz experiments were

examined, no segregation into significant and not significant BOLD response groups was possible on the basis of spiking raw data. Overlap of the raw data of both groups was too intense to allow that straightforward interpretation (see Fig 1 in Appendix).

Another point is, that more than one form of inhibition seems to play a role during one experiment. About their origin it can only be speculated. Latency increases during stimulation arise probably from feedback inhibition in response to PSA facilitation. The inhibition increase during the whole experiment is part of a general firing depression, and can only be characterized as an increased intrinsic inhibition of the granule cells. An intrinsic inhibition is not produced by inhibitory interneurons, it can rather be the result of deactivation, desensitization, changed membrane potentials.

The observations made on a short and long term scale could be summerized as follows. Low frequency protocols produced in general firing depression that was only overlaid by by an augmentation of population spikes which developed in immediate response to stimulation trains.

Transmitter depletion

It was shown that overall spiking activity can not explain BOLD generation. Short term plasticity can not be entirely excluded as causation but is not probable. Could transmitter depletion due to persistent firing account for BOLD generation?

Transmitter exhaustion as precondition for BOLD production is quite unlikely. Time constants for reuse (i.e., for a new allocation, not for the faster available ready releasable pool) of transmitter vesicles are between few hundred milliseconds and several seconds [99, 105]. Therefore a pause interval of 52 s between stimulation trains should be sufficient for replenishment. This could be seen especially in longer lasting experiments. Transmitter release was never entirely exhausted during the stimulation, since there was always enough transmitter release to produce EPSPs. EPSPs only lapsed in result of epilepsy-like activity, and in this cases complete transmitter depletion may very well be a reason of discharge termination. However, it can be said, that a minimum of transmitter release was essential for BOLD production.

Yet, when regarding partial transmitter depletion during stimulation, there is no reason why this and the subsequent replenishment mechanisms could not be linked to BOLD generation. But this question can not be cleared in the present study.

Longer lasting stimulation

Longer lasting stimulation protocols of 15 min duration proved that even a maximum of 8 x 20 stimuli per train could not exhaust stimulated axons so much that replenishment of the ready releasable pool could not catch up with transmitter release. Significant BOLD responses occurred throughout all trains and all experiments accompanied by at least EPSPs pointing to an ongoing transmitter release. Of course transmitter release is a necessary but no sufficient precondition for BOLD production. This can be concluded from the fact that transmitter release took place as well in experiments not eliciting BOLD responses.

Correlation between BOLD signal and electrostimulation

It was shown that a significant BOLD response occurred more likely with increasing stimulation frequency. A quantification of particular aspects of the BOLD activation revealed a positive correlation between stimulation frequency and activated area in the ipsilateral dorsal hippocampus (left Fig 3.9), stimulation frequency and maximum BOLD increase (Fig 3.10), but almost no correlation between stimulation frequency and area under the curve of a BOLD signal (right Fig 3.9). The last is probably due to a rather slow responsiveness of the vasculature determining the slow return of the BOLD signal to baseline, convolving events happening on a shorter time scale during a response.

However, event related averages (ERAs) in Fig 3.10 show that BOLD signal time courses differ for the different frequencies, as well as maximum activation, though not significantly. A definite explanation of the variation is hampered by the fact that the resolution of EPI images was 0.625 x 0.625 x 1 mm in functional MR recordings, but adjacent layer in the hippocampal formation are only several 100 μm apart. The pyramidal cell layer of the CA1 and the granule cell layer of the DG below, for example, are between 400 and 600 μm apart. According to this, an activated voxel can and will include not only BOLD signals from the DG but also from adjacent hippocampal regions. Thus the different ERAs could either stem from the effect of different frequencies on one hippocampal subregion, or it could reflect an activation of different combinations of hippocampal regions.

It turns out at this point, that a correlation between the very local electrophysiological and the rather gross BOLD signal is critical. A field potential obtained in the DG does not allow to make conclusions about the electrophysiological activity in other hippocampal regions. Thus it can not be properly correlated to a BOLD signal including the activity of several close hippocampal subregions. All this could explain, why no meaningful correlations were found between electrophysiological activity measured in DG and amount of BOLD generation, and why no BOLD imaging results can be predicted or estimated considering electrophysiological data from the DG.
The problem could be resolved by restricting the field of view to only one layer of the hippocampus, refining the resolution of functional imaging.

The impact of stimulation frequency can never be entirely separated from the amount of delivered stimuli or from stimulation duration. Keeping two of these parameters constant necessarily changes the third. Number of delivered stimuli is correlated to activated area mainly within low frequencies. Correlation is linear between 2.5 and 10 Hz and becomes non-linear between 10 and 20 Hz, pointing to an additional role of stimulation frequency. Probably this is due to the increasing activation of the hippocampus, that depends on a combination of frequency and stimulation duration. At 10 and 20 Hz maximal activation is achieved. Activated area evoked by high frequency stimulation does not exceed this range.

A variation of stimulus parameters demonstrated that train length, or stimulation duration, influenced only the activated area in the hippocampal formation (compare bars in Fig 3.15), but not BOLD signal time course or amount of BOLD

signal increase (Figs 3.13 and 3.14). During a stimulation of 4 s activation could not spread as far as in a train of 8 s in a standard experiment.

Modification of stimulation intensity proved above all, that spiking is not mandatory for BOLD signal production. Averaged BOLD signal increase during stimulation with threshold intensity is not clearly different from the comparison experiment (Figs 3.13), BOLD signal time course even showed in tendency a stronger activation during the first two trains than experiments using higher stimulation intensities (Fig 3.14). The main difference between threshold and standard intensity stimulation is, that other combinations of neurons are activated by threshold intensity. Feedback inhibition is prevented, but not activation of neurons responsible for feedforward inhibition. Hilar interneurons, for instance, are the first to respond to low intensity stimulation, excitatory neurons have a higher threshold for activation.

BOLD activation patterns

A remarkable feature of BOLD responses evoked in the ipsilateral dorsal hippocampus was that activation rose immediately after stimulation onset and fell promptly after stimulation end without reaching a plateau phase during stimulation. It is known from studies on rats that decrease of partial oxygen pressure in the activated neuronal tissue triggers an increase of CBF in less than 2 s [6, 20].

I. BOLD time courses
Only in 10 and 20 Hz experiments bilateral BOLD signal production could be observed in the dorsal hippocampus and the EC/Sub regions. Although activated area differed ipsi- and contralaterally, BOLD time courses were quite similar in homotopic regions. More differences could be found between the hippocampi and the EC/Sub regions. In the ipsi- and contralateral hippocampus BOLD signal attained maximum only in the third train, while it reached maximum already in the first train in both EC/Sub regions.
Not even a BOLD signal collapse looked the same in all hippocampal regions. When strong afterdischarges were followed by an electrophysological and BOLD signal breakdown, the BOLD signal time course of the complimentary dorsal hippocampi displayed a more pronounces signal breakdown than the contralateral EC/Sub region (see Fig 3.12).

Before discussing these different activation patterns, it is necessary to consult the organization of hippocampal projections.
The perforant pathway sends strong associational projections to the DG and CA3 and a weaker projection to the CA1. Moreover, commissural projections branch from the associational fibers targeting mainly the contralateral EC and DG, and also CA1 and the Sub region. The heaviest projection leads to the septal regions [5]. The hilus of the DG and the CA3 send strong commissures to the homotopic contralateral sites [45]. A stimulation of the perforant pathway would thus activate in first line the ipsilateral DG and CA3, and the contralateral EC, DG, CA1, Sub. By all those connections normal ipsilateral activation as well as epilepsy-like activity could be delivered to the contralateral side. But it is more likely,

that epilepsy-like activity observed in the contralateral parts was produced in the ipsilateral hippocampus and conveyed via the commissural CA3 - CA3 connection. The input arriving in the contralateral DG in response to an ipsilateral perforant pathway stimulation is known to produce only 40 - 60% of the EPSP that is produced by the same stimulation in the ipsilateral DG [47]. This decreases the probability to induce epilepsy-like activity by the direct commisural input.

Especially the EC/Sub regions can be activated by multiple routes. Via the trisynaptic DG - CA3 - CA1 loop, the disynaptic CA3 - CA1 loop and by a direct input to the Subiculum. At last, BOLD activation in the ipsilateral EC/Sub region could also be produced by retrograde activation of the perforant pathway. The stimulated angular bundle contains not only projections into the hippocampus but is also wiring back into the deep layers of the entorhinal cortex [84]. That is, an ipsilateral EC/Sub region activation does not require necessarily a DG activation. It can be mainly bypassed by the CA3 that receives an own strong input and forms an alternative loop activating ipsilateral EC/Sub region [128]. As described above, the contralateral EC/Sub region can also be activated by a direct input.

The complex connectivity in the hippocampal formation and the activation of different connections by the same stimulus is reflected in the observed differences of BOLD signal time courses in the EC/Sub region and dorsal hippocampus. The constant level of EC/Sub region activation seems to stem from inputs circumventing the DG. Dorsal hippocampus activation on the other side showed an attenuated BOLD signal during the first two trains, where also an fundamental change of inhibition occurred in the DG. Those two events seem to be linked, but how, remains an open question.

II. Spatial BOLD activation patterns

Spatial BOLD activation patterns in the dorsal hippocampus were in principle similar in all low frequency stimulation experiments (5 - 20 Hz). Increasing frequency enlarged the already known activated area by addition of more activated voxel. The spacial spread of significant BOLD signal into additional regions with increasing stimulation frequency demonstrated that transmission of neural activation to contralateral regions as hippocampus and entorhinal cortex was possible and of sufficient intensity to produce significant BOLD responses. As discussed above, there are several strong projections conveying perforant pathway stimulation to the contralateral side

BOLD signal baseline shift

Another observation could be drawn from BOLD time courses. Stimulation with frequencies above 10 Hz often caused baseline shifts. That is, BOLD signal intensities did not return to initial baseline after the first stimulation train but instead to a new, comparably lowered baseline value.

BOLD baseline shifts occurred as well in experiments producing additional discharges as in experiments not doing so. Therefore, it can be assumed that baseline shifts are not primarily a result of epilepsy-like activity, although baseline shifts can probably be supported by those.

Baseline shifts are not correlated to the amount of BOLD activation following electrostimulation, or summed electrophysiological activity during stimulation. The baseline shift seems in fact to display changes in neuronal population activity that were not captured by the present extracellular recording.

BOLD baseline could change out of two reasons. Level of BOLD signal could drop when blood flow would return to baseline more quickly than neuronal activity. Ongoing oxygen consumption would increase relative CO_2 concentration with the effect that deoxygenated Hb would outweigh oxygenated Hb. Decreasing BOLD signal would be the result. Alternatively reduced neural activity, and by that oxygen consumption, could reduce blood flow to more than only the former baseline level [107]. Czisch and colleagues reported BOLD signal decreases representing true cortical deactivation associated with decreased neuronal firing due to a prolonged hyperpolarization [32].

In the first case measurement of CBF should show the same blood flow before and after electrostimulation. In the second case a reduced CBF would be observed after electrostimulation. Most likely spontaneous firing activity in the observed region decreases during the time interval between stimulation trains.

What can be learned from electrophysiological control experiments

The two series of control experiments served several purposes. They should 1) characterize the stimulation protocols, 2) examine the effect of anaesthetization, and, 3) they could shed some light on the question: What, actually, does the stimulation mean to the animal?

The characterization of the stimulation had the purpose to check the stimulation protocols for effects outreaching the duration of the BOLD signal generating experiment itself. The observed effects can not directly be correlated to a BOLD response since they were conducted separately. Nevertheless they could help to determine if there a more neuronal processes going on during electrostimulation than could be detected during the experiment itself. Electrostimulation with frequencies of more than 5 Hz produced a transmission depression overlaid with a short term potentiation of PSAs. When stimulation was terminated the underlying depression was prolonged during the following control recordings. In unanaesthetized animals this clear PSA and LAT depression remained only for the first half hour following a 5 or 10 Hz electrostimulation. During the four hours following stimulation, PSAs successively developed into a potentiation, latencies normalized to baseline. In anaesthetized animals data only recovered to baseline, without showing such a slow onset potentiation.

A comparison of anaesthetized and unanaesthetized controls showed that anaesthetization itself exerted a depressant effect on electrophysiological signal production, increasing with anaesthetization duration. ISO is already known to inhibit excitatory current flow by reduction of transmitter release. The presynaptic mechanism answers for the largest part of the inhibitory effect produced by ISO [124, 125, 129]. GABA release on the other side is enhanced by ISO, shifting ratio of glutamate and GABA release in favour of GABA [124, 125]. The resulting EPSP depression is about 60% [125]. Isoflurane enhances GABA receptor currents

and inhibits NMDA receptors. In autaptic cultures of rat hippocampal neurons GABA mediated currents were increased by ISO by 70%, NMDA mediated currents were reduced by only 30% [34]. Surprisingly, ISO enhances at the same time synaptic efficacy. *In vivo* measurements in rats showed constant PSAs with decreasing EPSPs during ISO anaesthetization [115]. The mechanisms of action of nitrous oxide, the second anaesthetic in the delivered gaseous mixture, is not as well characterized. It is known to inhibit mainly excitatory transmission at NMDA receptors, enhancing cholinergic and glutamatergic excitatory pathways, but causing only small enhancement of GABA mediated currents [53, 58].

The influence of anaesthetization could be found in many control experiments even before any stimulation was delivered to the perforant pathway. PSA and LAT increased here during the 30 minutes of baseline recording preceding stimulation. Signal depression immediately following electrostimulation was definitely due to stimulation. Yet signal decline after circa 2 hours of anaesthetization was independent from stimulation (see Fig 3.36 and 3.42). Its inhibitory influence could be seen also in the impaired slow onset potentiation (SOP) in anaesthetized animals. The typical progression of an electrophysiological signal under ISO anaesthetization was as follows: In cases PSA increased during the first 30 min, this trend was prolonged for two hours. In the rest of the animals PSA remained on a constant level for the same time. After two hours of anaesthetization electrophysiological signal production degraded. I.e., PSAs and spike latencies became highly irregular and PSAs decreased. LAT of population spikes occurred during the entire experiment much delayed compared with unanaesthetized animals.

The observed phases could be explained by the complex action of anaesthetics described above. During the initial phase PSAs can increase due to inhibition of NMDA receptors on inhibitory neurons. The disinhibition improves spike production but with ongoing anaesthetization that effect may be saturated and the depressant effect on principal cells may overcome disinhibiton. Increased ISO concentrations were shown to inhibit NMDA receptors on principle cells, decreasing by that PSAs [115]. While PSAs displayed more variability, latency delay was a fact intrinsic to the anaesthetization experiments that could not be avoided.

Temperature decrease during MRI experiments could as well be responsible for the observed PSA increase and latency delay during the first 30 minutes of control. Temperature dropped in spite of warming the animals, partially due to the anaesthetic, partially due to immobilization. The moderate cooling did not impair BOLD production. Maybe this is because cooling just delays transmission and attenuates EPSPs and chemical reactions at the synapse but does not prevent them - at least within a physiological range of temperature decrease. The PSA increase linked to cooling can be explained by different temperature sensitivities of potassium and sodium currents. Potassium transport is stronger influenced by temperature decrease, so repolarization is delayed, duration of action potentials increased, and since the membrane moves closer to the sodium equilibrium potential, action potential amplitudes increase too [8]. Critical lower temperatures of 30 ℃ [86] from were on behavioural and spatial learning abilities are impaired were never reached in the present study.

Control experiments with unanaesthetized animals showed that the chosen stim-

ulation protocols had a clear impact on the behaviour of rats. Only stimulation frequencies above 5 Hz were able to trigger behavioural changes. The switch did not occur instantly but during a transition from one behavioural state into another. For the observer it appeared like a 'natural' awakening followed by increasing activation of the animal. The initial state - usually sleep or wakeful rest - changed into a highly activated state that attenuated slightly after several minutes of stimulation. Obviously the provided stimulation resembled or induced an oscillation triggering that behaviour. Frequencies capable of doing so were 5, 10 and 100 Hz. Those are typical frequencies transversing the hippocampus or delivered from EC or extrahippocampal areas to the hippocampus. The hippocampus is intended to respond to exactly the offered frequencies.

Chapter 5

Summary

Functional MRI (fMRI) is a widely used technique measuring hemodynamic changes in response to local changes of neural activity. Those changes are displayed as variation of blood oxygenation level dependent (BOLD) signals. Usually they are interpreted as indirect measurement of neural activity, although the mechanism by which neuronal activity triggers the resulting change in hemodynamics is not clear. The thesis aimed to establish an experimental setup that would allow concurrently to provide a direct, defined stimulation to a rats hippocampus input, the perforant pathway, and to register the evoked neuronal responses in the dentate gyrus, as well as the hemodynamic changes in the same region. A simultaneous recording and correlation of evoked BOLD signals and the underlying neuronal activity were supposed to shed more light on this coupling. After the identification of the technical requirements and the effective stimulation protocols the potential of the combined technique was explored. Correlations between blood oxygenation level dependent (BOLD) and extracellularly obtained neural signals were examined, and checked which effects the applied stimulation protocols exert on the dentate gyrus.

The presented technique was shown to be suitable to evoke significant BOLD signals in the hippocampal formation by an activation of a defined, mainly glutamatergic input to this region. Low and high frequency stimulation protocols were effective to a different amount: High frequency burst protocols (50 - 200 Hz) definitely produced significant BOLD signals, while probability of BOLD signal production increased with frequency for low frequency protocols (2.5 - 20 Hz). The spatial extent of BOLD activations depended of both, stimulation frequency and stimulus number, that is, stimulation pattern played a major role in the generation of the observed BOLD signals.

However, during the fMRI experiments a dissociation between measured neuronal activity and the resulting BOLD signal was observed. Spiking, i.e., postsynaptic activity, could not explain significant BOLD signals or their absence. It is expected, that an evaluation of the synaptic activity (EPSP) would yield the same result, since the extracellularly obtained field potential of the DG is an integrated signal displaying a sum of excitatory and inhibitory components, that can not be quantified in detail.

It can be concluded from this, that the concurrent fMRI + electrostimulation method is feasible and could also be used for a targeted activation of other transmitter systems connected to the hippocampus and examination of their influence on BOLD signal production, e.g., cholinergic inputs coming from the medial septum, serotonergic from the raphe nuclei, or the norandrenergic input from the Locus coeruleus. Concurrent recording of neuronal activity on the other side is

critical, because of the tightly interwoven inhibitory and excitatory signaling that allows no estimation of the true overall neural activity. Of all neuronal parameters only latency was found to be of use as a probable indicator of inhibition.

That inhibition might play a substantial role in BOLD signal production can be concluded from considerably increased population spike latencies during stimulation. Latency increased particularly during the use of stimulation frequencies evoking significant BOLD signals and led to the assumption, that inhibitory activity may be responsible for that.

It was further examined if trains of stimulus pulses could produce short term plasticity (STP) and this STP could explain concurrent BOLD signals. The results were ambivalent. STP could indeed be observed regularly, but not clearly be correlated to significant BOLD signal production. Again the fact that obtained field potentials only show an integrated signal, and could that way obscure existent processes, prevents a final conclusion.

Apart from short term processes changes of signal processing not apparent during stimulation itself were taken into account to play a role in BOLD signal production. To check for long term plasticity effects, control experiments for four stimulation frequencies were conducted paralleling the fMRI experiments.

A further likewise set of control experiments done on unanaesthetized animals examined the influence of Isoflurane anaesthetization on electrophysiological signals. Both sets of controls demonstrated a longlasting depression of spiking when electrostimulation protocols were applied that could also evoke significant BOLD responses in fMRI experiments. In unanaesthetized animals this depression could develop during four hours following stimulation into a potentiation. Of course those parallel experiments cannot prove a correlation between longlasting plasticity and BOLD signal production, but the findings may provide material for further reflexions.

Comparison of anaesthetized and unanaesthetized animals showed that Isoflurane: 1) delayed the population spike latency, but did not change the general response pattern to stimulus pulses, 2) had a destabilizing effect on electrophysiological signal fidelity when used for longer than two hours. It can be taken from this, that fMRI experiments should be kept within a time interval of two hours.

In unanaesthetized animals frequencies potentially producing significant BOLD responses were capable to trigger behavioural changes. Although electrostimulation is assumed only to provide an artificial stimulus, animals responded to it like to a natural impulse. Probably the artificial stimulus resembled a natural activation close enough to be accepted as a carrier of information switching brain oscillation from one to another state, resulting in the observed exploratory behaviour.

A last, surprising observation was a shift of BOLD signal baseline in the dorsal hippocampus that could be observed in experiments applying 10, 100 and 200 Hz. The shift might be related to an decrease of general neural activity in the region triggered by the specific stimulation. Electrophysiological signal depression appeared as 1) increased inhibitory drive displayed as increasing population spike latencies during stimulation 2) spiking depression following stimulation (control experiments).

Interestingly the underlying depression could not prevent an increase of population spike amplitudes during stimulation, showing several concurrent overlying processes during ongoing stimulation. The interesting point in this observation is that within a general depression of neural activity probably only a small group of active neurons might produce the significant BOLD response. Thus, it could be that the quantity of active neurons plays a minor role in BOLD signal production, but the quality of processes at a subset of neurons/synapses is crucial, even if the number of those neurons is comparatively low.

Appendix
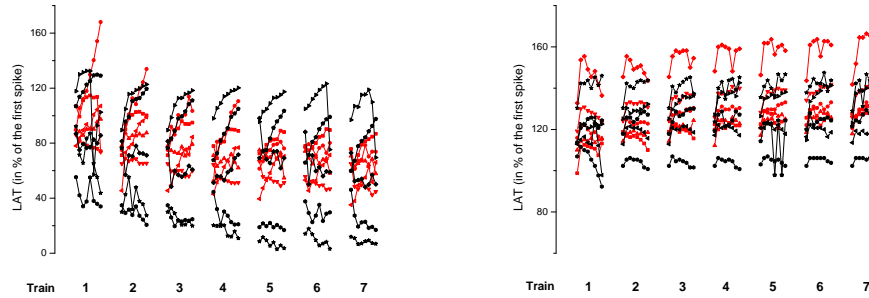
Figure 1: **Electrophysiological raw data of 5 Hz animals**
Response patterns of single animals do not allow a separation into BOLD signal producing (red), or negative (black) groups on the basis of raw data. Data points in this plot signify PSAs and LAT averaged per stimulation second.
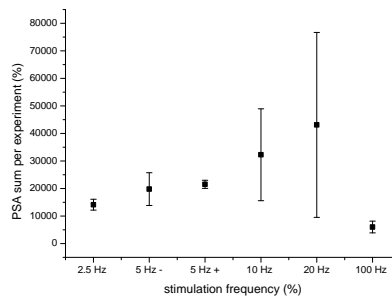
Figure 2: **Correlation between applied frequency and entire amount of firing per experiment**
Summed population spike production in the granule cell layer increased frequency-dependent only at low frequencies. Compared to that, summed firing was low at 100 Hz, although BOLD signal increase was comparable to increases during low frequency stimulation.
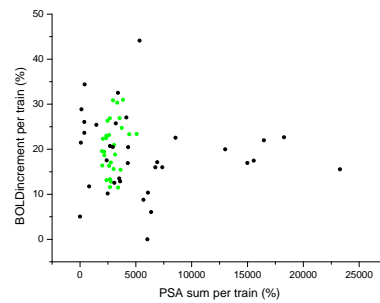
Figure 3: **Correlation between summed PSA and summed BOLD signal**
Data points display BOLD increment within a stimulation block and the corresponding
summed spiking. As well values calculated for 5 Hz (green) as for 10 Hz (black) show
almost no correlation between firing and BOLD signal increase.

List of symbols and abbreviations

100 (10)	100 Hz 10 stimuli per burst
100 (20)	100 Hz 20 stimuli per burst
AA	arachidonic acid
BOLD	blood oxygen level dependent
CBF	cerebral blood flow
CBV	verebral blood volume
CCK	cholecystokinin
CMRO2	cerebral metabolic rate oxygen consumption
COX	cyclooxygenase
DG	dentate gyrus (area dentata)
EC	entorhinal cortex
IPI	inter pulse interval
LAT	latency
LFP	local field potentials
MUA	multi unit activity
NOS	nitrous oxid synthase
NPY	neuropeptide Y
PLA2	phosholipase A2
PSA	population spike amplitude
PV	parvalbumin
SD	standard deviation
SOM	somatostatin
STP	short term potentiation
Sub	subiculum
VDCC	voltage dependant Ca^{2+}-channels
VIP	vasodilatory intestinal protein

Bibliography

[1] R. Abounader and E. Hamel. Associations between neuropeptide Y nerve terminals and intraparenchymal microvessels in rat and human cerebral cortex. *The Journal of Comparative Neurology*, 388(3):444–453, 1997.

[2] W. C. Abraham and T. V. Bliss. An analysis of the increase in granule cell excitability accompanying habituation in the dentate gyrus of the anesthetized rat. *Brain Research*, 331(2):303–313, 1985.

[3] N. Akgoren, M. Fabricius, and M. Lauritzen. Importance of nitric oxide for local increases of blood flow in rat cerebellar cortex during electrical stimulation. *Proceedings of the National Academy of Sciences of the United States of America*, 91(13):5903–7, 1994.

[4] B. E. Alger and T. J. Teyler. Long-term and short-term plasticity in the CA1, CA3, and dentate regions of the rat hippocampal slice. *Brain Research*, 110(3):463–480, 1976.

[5] D. Amaral and P. Lavenex. Hippocampal neuroanatomy. In P. Andersen, R. Morris, D. Amaral, T. Bliss, and J. O'Keefe, editors, *The Hippocampus Book*. Oxford University Press US, 2007.

[6] B. M. Ances, D. G. Buerk, J. H. Greenberg, and J. A. Detre. Temporal dynamics of the partial pressure of brain tissue oxygen during functional forepaw stimulation in rats. *Neuroscience Letter*, 306(1-2):106–10, 2001.

[7] P. Andersen, B. Holmqvist, and P. E. Voorhoeve. Entorhinal activation of dentate granule cells. *Acta Physiologica Scandinavica*, 66(4):448–460, 1966.

[8] P. Andersen and E. I. Moser. Brain temperature and hippocampal function. *Hippocampus*, 5(6):491–8, 1995.

[9] O. J. Arthurs and S. Boniface. How well do we understand the neural origins of the fMRI BOLD signal? *Trends in Neurosciences*, 25(1):27–31, 2002.

[10] D. Attwell and C. Iadecola. The neural basis of functional brain imaging signals. *Trends in Neurosciences*, 25(12):621–625, 2002.

[11] D. Attwell and S. B. Laughlin. An energy budget for signaling in the grey matter of the brain. *Journal of Cerebral Blood Flow and Metabolism*, 21(10):1133–1145, 2001.

[12] A. Aubert and R. Costalat. A model of the coupling between brain electrical activity, metabolism, and hemodynamics: application to the interpretation of functional neuroimaging. *Neuroimage*, 17(3):1162–1181, 2002.

[13] J. Behr. *Interaktion zwischen entorhinalem Kortex und Hippokampus bei der Temporallappenepilepsie*. PhD thesis, Humboldt-Universität zu Berlin, Medizinische Fakultät - Universitätsklinikum Charité, 2003.

[14] J. Behr, U. Heinemann, and I. Mody. Kindling induces transient NMDA receptor-mediated facilitation of high-frequency input in the rat dentate gyrus. *Journal of Neurophysiology*, 85(5):2195–202, 2001.

[15] T. Bliss and T. Lomo. Long lasting potentiation of synaptic transmission in the dentate area of the anaesthetized rabbit following stimulation of the perforant path. *Journal of Physiology*, 232(2):331–356, 1973.

[16] T. Bliss and A. G. Medwin. Long lasting potentiation of synaptic transmission in the dentate area of the unanaesthetized rabbit following stimulation of the perforant path. *Journal of Physiology*, 232(2):357–374, 1973.

[17] C. Bock, H. Krep, G. Brinker, and M. Hoehn-Berlage. Brainmapping of alpha-chloralose anesthetized rats with t2*-weighted imaging: distinction between the representation of the forepaw and hindpaw in the somatosensory cortex. *NMR in Biomedicine*, 11(3):115–119, 1998.

[18] J. E. Brenman, D. S. Chao, S. H. Gee, A. W. McGee, S. E. Craven, D. R. Santillano, Z. Wu, F. Huang, H. Xia, M. F. Peters, S. C. Froehner, and D. S. Bredt. Interaction of nitric oxide synthase with the postsynaptic density protein PSD-95 and alpha1-syntrophin mediated by PDZ domains. *Cell*, 84(5):757–767, 1996.

[19] J. E. Brenman, K. S. Christopherson, S. E. Craven, A. W. McGee, and D. S. Bredt. Cloning and characterization of postsynaptic density 93, a nitric oxide synthase interacting protein. *The Journal of Neuroscience*, 16(23):7407–7415, 1996.

[20] D. G. Buerk, B. M. Ances, J. H. Greenberg, and J. A. Detre. Temporal dynamics of brain tissue nitric oxide during functional forepaw stimulation in rats. *Neuroimage*, 18(1):1–9, 2003.

[21] L. J. Burdette, G. J. Hart, and L. M. Masukawa. Changes in dentate granule cell field potentials during afterdischarge initiation triggered by 5 Hz perforant path stimulation. *Brain Research*, 722(1-2):39–49, 1996.

[22] M. Burke and C. Buhrle. BOLD response during uncoupling of neuronal activity and CBF. *Neuroimage*, 32(1):1–8, 2006.

[23] R. B. Buxton, E. C. Wong, and L. R. Frank. Dynamics of blood flow and oxygenation changes during brain activation: the balloon model. *Magnetic Resonance in Medicine*, 39(6):855–864, 1998.

[24] K. Caesar, K. Thomsen, and M. Lauritzen. Dissociation of spikes, synaptic activity, and activity-dependent increments in rat cerebellar blood flow by tonic synaptic inhibition. *Proceedings of the National Academy of Sciences of the United States of America*, 100(26):16000–16005, 2003.

[25] N. V. Camp, M. Verhoye, C. I. D. Zeeuw, and A. V. der Linden. Light stimulus frequency dependence of activity in the rat visual system as studied with high resolution BOLD fMRI. *Journal of Neurophysiology*, 2006.

[26] B. Cauli, X. Tong, A. Rancillac, N. Serluca, B. Lambolez, J. Rossier, and E. Hamel. Cortical GABA interneurons in neurovascular coupling: relays for subcortical vasoactive pathways. *The Journal of Neuroscience*, 24(41):8940–8949, 2004.

[27] A. Chedotal, C. Cozzari, M. P. Faure, B. K. Hartman, and E. Hamel. Distinct choline acetyltransferase (ChAT) and vasoactive intestinal polypeptide (VIP) bipolar neurons project to local blood vessels in the rat cerebral cortex. *Brain Research*, 646(2):181–193, 1994.

[28] A. Chedotal, D. Umbriaco, L. Descarries, B. K. Hartman, and E. Hamel. Light and electron microscopic immunocytochemical analysis of the neurovascular relationships of choline acetyltransferase and vasoactive intestinal polypeptide nerve terminals in the rat cerebral cortex. *The Journal of Comparative Neurology*, 343(1):57–71, 1994.

[29] N. Cholet, G. Bonvento, and J. Seylaz. Effect of neuronal NO synthase inhibition on the cerebral vasodilatory response to somatosensory stimulation. *Brain Research*, 708(1-2):197–200, 1996.

[30] Z. Cohen, G. Bonvento, P. Lacombe, and E. Hamel. Serotonin in the regulation of brain microcirculation. *Progress in Neurobiology*, 50(4):335–362, 1996.

[31] D. A. Coulter and G. C. Carlson. Functional regulation of the dentate gyrus by GABA-mediated inhibition. *Progress in Brain Research*, 163:235–43, 2007.

[32] M. Czisch, R. Wehrle, C. Kaufmann, T. C. Wetter, F. Holsboer, T. Pollmächer, and D. P. Auer. Functional MRI during sleep: BOLD signal decreases and their electrophysiological correlates. *The European Journal of Neuroscience*, 20(2):566–574, 2004.

[33] T. Davis, K. Kwong, R. Weisskoff, and B. Rosen. Calibrated functional MRI: mapping the dynamics of oxidative metabolism. *Proceedings of the National Academy of Sciences of the United States of America*, 95(4):1834–1839, 1998.

[34] S. L. de Sousa, R. Dickinson, W. R. Lieb, and N. P. Franks. Contrasting synaptic actions of the inhalational general anesthetics isoflurane and xenon. *Anesthesiology*, 92(4):1055–1066, 2000.

[35] U. Dirnagl, K. Niwa, U. Lindauer, and A. Villringer. Coupling of cerebral blood flow to neuronal activation: Role of adenosine and nitric oxide. *American Journal of Physiology - Heart and Circulatory Physiology*, 267(H296-H301), 1994.

[36] R. M. Douglas and G. V. Goddard. Long-term potentiation of the perforant path-granule cell synapse in the rat hippocampus. *Brain Research*, 86(2):205–215, 1975.

[37] J. P. Dreier, K. Kärner, A. Gärner, U. Lindauer, M. Weih, A. Villringer, and U. Dirnagl. Nitric oxide modulates the CBF response to increased extracellular potassium. *Journal of Cerebral Blood Flow and Metabolism*, 15(6):914–919, 1995.

[38] K. M. Dunn and M. T. Nelson. Potassium channels and neurovascular coupling. *Circulation Journal*, 74(4):608–616, 2010.

[39] P. Enager, H. Piilgaard, N. Offenhauser, A. Kocharyan, P. Fernandes, E. Hamel, and M. Lauritzen. Pathway-specific variations in neurovascular and neurometabolic coupling in rat primary somatosensory cortex. *Journal of Cerebral Blood Flow and Metabolism*, 29(5):976–986, 2009.

[40] A. Fergus and K. S. Lee. GABAergic regulation of cerebral microvascular tone in the rat. *Journal of Cerebral Blood Flow and Metabolism*, 17(9):992–1003, 1997.

[41] J. A. Filosa and V. M. Blanco. Neurovascular coupling in the mammalian brain. *Experimental Physiology*, 92(4):641–646, 2007.

[42] T. F. Freund and G. Buzsaki. Interneurons of the hippocampus. *Hippocampus*, 6(4):347–470, 1996.

[43] S. Frey and J. U. Frey". Synaptic plasticity and the analysis of the field-EPSP as well as the population spike using separate recording electrodes in the dentate gyrus in freely moving rats. *Journal of Neuroscience Methods*, 184(1):79 – 87, 2009.

[44] K. J. Friston, A. Mechelli, R. Turner, and C. J. Price. Nonlinear responses in fMRI: the balloon model, volterra kernels, and other hemodynamics. *Neuroimage*, 12(4):466–477, 2000.

[45] M. Frotscher and L. Seress. Morphological development of the hippocampus. In P. Andersen, R. Morris, D. Amaral, T. Bliss, and J. O'Keefe, editors, *The Hippocampus book*, pages 115–128. Oxford University Press US, 2007.

[46] M. Galarreta and S. Hestrin. Frequency-dependent synaptic depression and the balance of excitation and inhibition in the neocortex. *Nature Neuroscience*, 1(7):587–594, 1998.

[47] G. Golarai and T. P. Sutula. Bilateral organization of parallel and serial pathways in the dentate gyrus demonstrated by current-source density analysis in the rat. *Journal of Neurophysiology*, 75(1):329–342, 1996.

[48] J. Gotoh, T. Y. Kuang, Y. Nakao, D. M. Cohen, P. Melzer, Y. Itoh, H. Pak, K. Pettigrew, and L. Sokoloff. Regional differences in mechanisms of cerebral circulatory response to neuronal activation. *American Journal of Physiology - Heart and Circulatory Physiology*, 280(2):H821–829, 2001.

[49] K. Halasy and P. Somogyi. Subdivisions in the multiple GABAergic innervation of granule cells in the dentate gyrus of the rat hippocampus. *The European Journal of Neuroscience*, 5(5):411–429, 1993.

[50] E. Hamel. Cholinergic modulation of the cortical microvascular bed. *Progress in Brain Research*, 145:171–178, 2004.

[51] D. J. Heeger, A. C. Huk, W. S. Geisler, and D. G. Albrecht. Spikes versus BOLD: what does neuroimaging tell us about neuronal activity? *Nature Neuroscience*, 3(7):631–3, 2000.

[52] N. Hewson-Stoate, M. Jones, J. Martindale, J. Berwick, and J. Mayhew. Further nonlinearities in neurovascular coupling in rodent barrel cortex. *Neuroimage*, 24(2):565–74, 2005.

[53] K. Hirota. Special cases: ketamine, nitrous oxide and xenon. *Best Practice & Research. Clinical Anaesthesiology*, 20(1):69–79, 2006.

[54] R. D. Hoge, J. Atkinson, B. Gill, G. R. Crelier, S. Marrett, and G. B. Pike. Investigation of BOLD signal dependence on cerebral blood flow and oxygen consumption: the deoxyhemoglobin dilution model. *Magnetic Resonance in Medicine*, 42(5):849–863, 1999.

[55] T. Horiuchi, H. H. Dietrich, K. Hongo, T. Goto, and R. G. Dacey. Role of endothelial nitric oxide and smooth muscle potassium channels in cerebral arteriolar dilation in response to acidosis. *Stroke*, 33(3):844–849, 2002.

[56] J. K. Huttunen, O. Grohn, and M. Penttonen. Coupling between simultaneously recorded BOLD response and neuronal activity in the rat somatosensory cortex. *Neuroimage*, 39(2):775–85, 2008.

[57] C. Iadecola and R. P. Kraig. Focal elevations in neocortical interstitial K^+ produced by stimulation of the fastigial nucleus in rat. *Brain research*, 563(1-2):273–277, 1991.

[58] V. Jevtovic-Todorovic, S. M. Todorovic, S. Mennerick, S. Powell, K. Dikranian, N. Benshoff, C. F. Zorumski, and J. W. Olney. Nitrous oxide (laughing gas) is an NMDA antagonist, neuroprotectant and neurotoxin. *Nature Medicine*, 4(4):460–463, 1998.

[59] M. Jones, N. Hewson-Stoate, J. Martindale, P. Redgrave, and J. Mayhew. Nonlinear coupling of neural activity and CBF in rodent barrel cortex. *Neuroimage*, 22(2):956–965, 2004.

[60] M. Kadekaro, A. M. Crane, and L. Sokoloff. Differential effects of electrical stimulation of sciatic nerve on metabolic activity in spinal cord and dorsal root ganglion in the rat. *Proceedings of the National Academy of Sciences of the United States of America*, 82(17):6010–6013, 1985.

[61] C. Kayser, M. Kim, K. Ugurbil, D. Kim, and P. Knig. A comparison of hemodynamic and neural responses in cat visual cortex using complex stimuli. *Cerebral Cortex*, 14(8):881–891, 2004.

[62] C. M. Kerskens, M. Hoehn-Berlage, B. Schmitz, E. Busch, C. Bock, M. L. Gyngell, and K. A. Hossmann. Ultrafast perfusion-weighted MRI of functional brain activation in rats during forepaw stimulation: comparison with t2 -weighted MRI. *NMR in Biomedicine*, 9(1):20–23, 1996.

[63] D. Kim, I. Ronen, C. Olman, S. Kim, K. Ugurbil, and L. J. Toth. Spatial relationship between neuronal activity and BOLD functional MRI. *Neuroimage*, 21(3):876–885, 2004.

[64] H. J. Knot, P. A. Zimmermann, and M. T. Nelson. Extracellular K^+ -induced hyperpolarizations and dilatations of rat coronary and cerebral arteries involve inward rectifier K^+ channels. *The Journal of Physiology*, 492(2):419–430, 1996.

[65] A. Kocharyan, P. Fernandes, X. Tong, E. Vaucher, and E. Hamel. Specific subtypes of cortical GABA interneurons contribute to the neurovascular coupling response to basal forebrain stimulation. *Journal of Cerebral Blood Flow and Metabolism*, 28(2):221–231, 2008.

[66] R. C. Koehler, R. J. Roman, and D. R. Harder. Astrocytes and the regulation of cerebral blood flow. *Trends in Neurosciences*, 32(3):160–169, 2009.

[67] L. S. Krimer, E. C. Muly, G. V. Williams, and P. S. Goldman-Rakic. Dopaminergic regulation of cerebral cortical microcirculation. *Nature Neuroscience*, 1(4):286–289, 1998.

[68] K. Krnjevic, M. Morris, and R. Reiffenstein. Stimulation-evoked changes in extracellular K^+ and Ca^{2+} in pyramidal layers of the rat's hippocampus. *Canadian Journal of Physiology and Pharmacology*, 60(12):1643–1657, 1982.

[69] A. U. Larkman, J. J. Jack, and K. J. Stratford. Quantal analysis of excitatory synapses in rat hippocampal CA1 in vitro during low-frequency depression. *The Journal of Physiology*, 505 (Pt 2):457–471, 1997.

[70] M. Lauritzen. Reading vascular changes in brain imaging: is dendritic calcium the key? *Nature Reviews Neuroscience*, 6(1):77–85, 2005.

[71] M. Lauritzen and L. Gold. Brain function and neurophysiological correlates of signals used in functional neuroimaging. *The Journal of Neuroscience*, 23(10):3972–3980, 2003.

[72] U. Lindauer, A. Kunz, S. Schuh-Hofer, J. Vogt, J. P. Dreier, and U. Dirnagl. Nitric oxide from perivascular nerves modulates cerebral arterial pH reactivity. *American Journal of Physiology - Heart and Circulatory Physiology*, 281(3):H1353–63, 2001.

[73] U. Lindauer, J. Vogt, S. Schuh-Hofer, J. P. Dreier, and U. Dirnagl. Cerebrovascular vasodilation to extraluminal acidosis occurs via combined activation of ATP-sensitive and Ca^{2+} -activated potassium channels. *Journal of Cerebral Blood Flow and Metabolism*, 23(10):1227–1238, 2003.

[74] G. Liu and R. W. Tsien. Properties of synaptic transmission at single hippocampal synaptic boutons. *Nature*, 375(6530):404–408, 1995.

[75] N. K. Logothetis. The neural basis of the blood-oxygen-level-dependent functional magnetic resonance imaging signal. *Philosophical Transactions of the Royal Society of London. Series B, Biological Sciences*, 357(1424):1003–1037, 2002.

[76] N. K. Logothetis, J. Pauls, M. Augath, T. Trinath, and A. Oeltermann. Neurophysiological investigation of the basis of the fMRI signal. *Nature*, 412(6843):150–157, 2001.

[77] N. K. Logothetis and B. A. Wandell. Interpreting the BOLD signal. *Annual Review of Physiology*, 66:735–769, 2004.

[78] T. Lomo. Patterns of activation in a monosynaptic cortical pathway: the perforant path input to the dentate area of the hippocampal formation. *Experimental Brain Research*, 12(1):18–45, 1971.

[79] T. Lomo. Potentiation of monosynaptic EPSPs in the perforant path-dentate granule cell synapse. *Experimental Brain Research*, 12(1):46–63, 1971.

[80] P. J. Magistretti and L. Pellerin. Cellular mechanisms of brain energy metabolism and their relevance to functional brain imaging. *Philosophical Transactions of the Royal Society of London. Series B, Biological Sciences*, 354(1387):1155–1163, 1999.

[81] K. Masamoto, T. Kim, M. Fukuda, P. Wang, and S. G. Kim. Relationship between neural, vascular, and BOLD signals in isoflurane-anesthetized rat somatosensory cortex. *Cerebral Cortex*, 17(4):942–50, 2007.

[82] C. Mathiesen, K. Caesar, and M. Lauritzen. Temporal coupling between neuronal activity and blood flow in rat cerebellar cortex as indicated by field potential analysis. *The Journal of Physiology*, 523:235–246, 2000.

[83] J. G. McCarron and W. Halpern. Potassium dilates rat cerebral arteries by two independent mechanisms. *The American Journal of Physiology*, 259(3):H902–908, 1990.

[84] B. L. McNaughton and C. A. Barnes. Physiological identification and analysis of dentate granule cell responses to stimulation of the medial and lateral perforant pathways in the rat. *The Journal of Comparative Neurology*, 175(4):439–54, 1977.

[85] M. A. Mintun, B. N. Lundstrom, A. Z. Snyder, A. G. Vlassenko, G. L. Shulman, and M. E. Raichle. Blood flow and oxygen delivery to human brain during functional activity: theoretical modeling and experimental data. *Proceedings of the National Academy of Sciences of the United States of America*, 98(12):6859–6864, 2001.

[86] E. I. Moser, M. B. Moser, and P. Andersen. Potentiation of dentate synapses initiated by exploratory learning in rats: dissociation from brain temperature, motor activity, and arousal. *Learning & Memory*, 1(1):55–73, 1994.

[87] D. D. Mott and D. V. Lewis. Facilitation of the induction of long-term potentiation by GABAB receptors. *Science*, 252(5013):1718–1720, 1991.

[88] R. Mukamel, H. Gelbard, A. Arieli, U. Hasson, I. Fried, and R. Malach. Coupling between neuronal firing, field potentials, and FMRI in human auditory cortex. *Science*, 309(5736):951–4, 2005.

[89] M. D. Munoz, A. Nunez, and E. Garcia-Austt. Frequency potentiation in granule cells in vivo at theta frequency perforant path stimulation. *Experimental Neurology*, 113(1):74–8, 1991.

[90] A. N. Nielsen and M. Lauritzen. Coupling and uncoupling of activity-dependent increases of neuronal activity and blood flow in rat somatosensory cortex. *The Journal of Physiology*, 533(3):773–785, 2001.

[91] J. Niessing, B. Ebisch, K. E. Schmidt, M. Niessing, W. Singer, and R. A. Galuske. Hemodynamic signals correlate tightly with synchronized gamma oscillations. *Science*, 309(5736):948–51, 2005.

[92] K. Niwa, E. Araki, S. Morham, M. Ross, and C. Iadecola. Cyclooxygenase-2 contributes to functional hyperemia in whisker-barrel cortex. *Journal of Neuroscience*, 20(2):763–770, 2000.

[93] R. J. Nudo and R. B. Masterton. Stimulation-induced [14C]2-deoxyglucose labeling of synaptic activity in the central auditory system. *The Journal of Comparative Neurology*, 245(4):553–565, 1986.

[94] S. Ogawa, T. M. Lee, A. R. Kay, and D. W. Tank. Brain magnetic resonance imaging with contrast dependent on blood oxygenation. *Proceedings of the National Academy of Sciences of the United States of America*, 87(24):9868–9872, 1990.

[95] L. Park, E. Gallo, J. Anrather, G. Wang, E. Norris, J. Paul, S. Strickland, and C. Iadecola. Key role of tissue plasminogen activator in neurovascular coupling. *Proceedings of the National Academy of Sciences of the United States of America*, 105(3):1073–1078, 2008.

[96] C. D. Paspalas and G. C. Papadopoulos. Ultrastructural evidence for combined action of noradrenaline and vasoactive intestinal polypeptide upon neurons, astrocytes, and blood vessels of the rat cerebral cortex. *Brain Research Bulletin*, 45(3):247–259, 1998.

[97] G. Paxinos and C. A. K. Watson. *The rat Brain in stereotaxic coordinates.* Academic Press, 4th edition, 1998.

[98] G. Petzold, D. Albeanu, T. Sato, and V. Murthy. Coupling of neural activity to blood flow in olfactory glomeruli is mediated by astrocytic pathways. *Neuron*, 58(6):897–910, 2008.

[99] J. L. Pyle, E. T. Kavalali, E. S. Piedras-Renteria, and R. W. Tsien. Rapid reuse of readily releasable pool vesicles at hippocampal synapses. *Neuron*, 28(1):221–31, 2000.

[100] A. Rancillac, J. Rossier, M. Guille, X. Tong, H. Geoffroy, C. Amatore, S. Arbault, E. Hamel, and B. Cauli. Glutamatergic control of microvascular tone by distinct GABA neurons in the cerebellum. *The Journal of Neuroscience*, 26(26):6997–7006, 2006.

[101] A. Rauch, G. Rainer, and N. K. Logothetis. The effect of a serotonin-induced dissociation between spiking and perisynaptic activity on BOLD functional MRI. *Proceedings of the National Academy of Sciences of the United States of America*, 105(18):6759–64, 2008.

[102] G. Rausche, J. M. Sarvey, and U. Heinemann. Slow synaptic inhibition in relation to frequency habituation in dentate granule cells of rat hippocampal slices. *Experimental Brain Research*, 78(2):233–242, 1989.

[103] G. Rees, K. Friston, and C. Koch. A direct quantitative relationship between the functional properties of human and macaque V5. *Nature Neuroscience*, 3(7):716–723, 2000.

[104] R. J. D. Rocco, G. H. Kageyama, and M. T. Wong-Riley. The relationship between CNS metabolism and cytoarchitecture: a review of 14C-deoxyglucose studies with correlation to cytochrome oxidase histochemistry. *Computerized Medical Imaging and Graphics*, 13(1):81–92, 1989.

[105] T. Sakaba. Two Ca^{2+} -dependent steps controlling synaptic vesicle fusion and replenishment at the cerebellar basket cell terminal. *Neuron*, 57(3):406–19, 2008.

[106] H. Scharfman and P. Schwartzkroin. Responses of cells of the rat fascia dentata to prolonged stimulation of the perforant path: Sensitivity of hilar cells and changes in granule cell excitability. *Neuroscience*, 35(3):491–504, 1990.

[107] M. L. Schroeter, T. Kupka, T. Mildner, K. Uluda, and D. Y. von Cramon. Investigating the post-stimulus undershoot of the BOLD signal–a simultaneous fMRI and fNIRS study. *NeuroImage*, 30(2):349–358, Apr. 2006.

[108] W. J. Schwartz, C. B. Smith, L. Davidsen, H. Savaki, L. Sokoloff, M. Mata, D. J. Fink, and H. Gainer. Metabolic mapping of functional activity in the hypothalamo-neurohypophysial system of the rat. *Science*, 205(4407):723–725, 1979.

[109] L. Seress and C. Ribak. GABAergic cells in the dentate gyrus appear to be local circuit and projection neurons. *Experimental Brain Research*, 50(2-3):173–182, 1983.

[110] A. C. Silva and A. P. Koretsky. Laminar specificity of functional MRI onset times during somatosensory stimulation in rat. *Proceedings of the National*

Academy of Sciences of the United States of America, 99(23):15182–15187, 2002.

[111] A. C. Silva, S. P. Lee, G. Yang, C. Iadecola, and S. G. Kim. Simultaneous blood oxygenation level-dependent and cerebral blood flow functional magnetic resonance imaging during forepaw stimulation in the rat. *Journal of Cerebral Blood Flow and Metabolism*, 19(8):871–879, 1999.

[112] A. J. Smith, H. Blumenfeld, K. L. Behar, D. L. Rothman, R. G. Shulman, and F. Hyder. Cerebral energetics and spiking frequency: the neurophysiological basis of fMRI. *Proceedings of the National Academy of Sciences of the United States of America*, 99(16):10765–70, 2002.

[113] J. Stringer, J. Williamson, and E. Lothman. Induction of paroxysmal discharges in the dentate gyrus: Frequency dependence and relationship to afterdischarge production. *Journal of Neurophysiology*, 62(1):126–135, 1989.

[114] J. L. Stringer and E. W. Lothman. Reverberatory seizure discharges in hippocampal-parahippocampal circuits. *Experimental Neurology*, 116(2):198–203, 1992.

[115] K. Tachibana, K. Takita, T. Hashimoto, M. Matsumoto, M. Yoshioka, and Y. Morimoto. Isoflurane bidirectionally modulates the paired-pulse responses in the rat hippocampal CA1 field in vivo. *Anesthesia & Analgesia*, 105(4):1006–11, table of contents, 2007.

[116] M. Takahashi, Y. Kovalchuk, and D. Attwell. Pre- and postsynaptic determinants of EPSC waveform at cerebellar climbing fiber and parallel fiber to purkinje cell synapses. *The Journal of Neuroscience*, 15(8):5693–5702, 1995.

[117] K. Thomsen, N. Offenhauser, and M. Lauritzen. Principal neuron spiking: neither necessary nor sufficient for cerebral blood flow in rat cerebellum. *The Journal of Physiology*, 560(1):181–189, 2004.

[118] A. S. Tolias, F. Sultan, M. Augath, A. Oeltermann, E. J. Tehovnik, P. H. Schiller, and N. K. Logothetis. Mapping cortical activity elicited with electrical microstimulation using FMRI in the macaque. *Neuron*, 48(6):901–911, 2005.

[119] X. K. Tong and E. Hamel. Basal forebrain nitric oxide synthase (NOS)-containing neurons project to microvessels and NOS neurons in the rat neocortex: cellular basis for cortical blood flow regulation. *The European Journal of Neuroscience*, 12(8):2769–2780, 2000.

[120] M. Ureshi, T. Matsuura, and I. Kanno. Stimulus frequency dependence of the linear relationship between local cerebral blood flow and field potential evoked by activation of rat somatosensory cortex. *Neuroscience Research*, 48(2):147–53, 2004.

[121] A. Viswanathan and R. D. Freeman. Neurometabolic coupling in cerebral cortex reflects synaptic more than spiking activity. *Nature Neuroscience*, 10(10):1308–1312, 2007.

[122] S. Waldbaum and F. E. Dudek. Single and repetitive paired-pulse suppression: A parametric analysis and assessment of usefulness in epilepsy research. *Epilepsia*, 50(4):904–916, 2009.

[123] R. Weber, P. Ramos-Cabrer, D. Wiedermann, N. van Camp, and M. Hoehn. A fully noninvasive and robust experimental protocol for longitudinal fMRI studies in the rat. *Neuroimage*, 29(4):1303–10, 2006.

[124] R. I. Westphalen and H. C. Hemmings. Volatile anesthetic effects on glutamate versus GABA release from isolated rat cortical nerve terminals: basal release. *Journal of Pharmacology and Experimental Therapeutics*, 316(1):208–15, 2006.

[125] B. D. Winegar and M. B. MacIver. Isoflurane depresses hippocampal CA1 glutamate nerve terminals without inhibiting fiber volleys. *BMC Neuroscience*, 7:5, 2006.

[126] M. P. Witter and D. Amaral. Hippocampal formation. In G. Paxinos, editor, *The rat nervous system*. Gulf Professional Publishing, 2004.

[127] A. Wree and A. Schleicher. The determination of the local cerebral glucose utilization with the 2-deoxyglucose method. *Histochemistry*, 90(2):109–121, 1988.

[128] K. Wu and L. S. Leung. Monosynaptic activation of CA3 by the medial perforant path. *Brain Research*, 797(1):35–41, 1998.

[129] X. S. Wu, J. Y. Sun, A. S. Evers, M. Crowder, and L. G. Wu. Isoflurane inhibits transmitter release and the presynaptic action potential. *Anesthesiology*, 100(3):663–70, 2004.

[130] Z. Xiong, P. Saggau, and J. L. Stringer. Activity-Dependent intracellular acidification correlates with the duration of seizure activity. *Journal of Neuroscience.*, 20(4):1290–1296, 2000.

[131] G. Yang and C. Iadecola. Obligatory role of NO in glutamate-dependent hyperemia evoked from cerebellar parallel fibers. *The American Journal of Physiology*, 272(4):R1155–1161, 1997.

[132] G. Yang, Y. Zhang, M. E. Ross, and C. Iadecola. Attenuation of activity-induced increases in cerebellar blood flow in mice lacking neuronal nitric oxide synthase. *American Journal of Physiology - Heart and Circulatory Physiology*, 285(1):H298–304, 2003.

[133] M. F. Yeckel and T. W. Berger. Feedforward excitation of the hippocampus by afferents from the entorhinal cortex: redefinition of the role of the trisynaptic pathway. *Proceedings of the National Academy of Sciences of the United States of America*, 87(15):5832–5836, 1990.

[134] F. Zhao, T. Jin, P. Wang, and S. Kim. Improved spatial localization of post-stimulus BOLD undershoot relative to positive BOLD. *Neuroimage*, 34(3):1084–1092, 2007.